Decoding the Information Content of Fish Sounds and How Fishes Extract Information from Sounds: Insights from the Plainfin Midshipman and Beyond

Sujay Balebail

A dissertation

submitted in partial fulfillment of the

requirements for the degree of

Doctor of Philosophy

University of Washington

2024

Reading Committee:

Joseph A. Sisneros, Chair

Andrew Brown

Adam P. Summers

Program Authorized to Offer Degree:

Biology

University of Washington

Abstract

Decoding the Information Content of Fish Sounds and How Fishes Extract Information from Sounds: Insights from the Plainfin Midshipman and Beyond

Sujay Balebail

Chair of the Supervisory Committee:
Dr. Joseph A. Sisneros
Department of Psychology

Many species have evolved the ability to produce sound for communication. One of the most common types of sounds produced by animals is advertisement calls made by males to attract females for mating. These calls often contain information about morphometric parameters that indicate the quality or reproductive potential of the male. Acoustic communication is commonly observed in ray-finned fishes. While most sonic fish species produce short-duration advertisement calls (~1s or less), the plainfin midshipman fish (*Porichthys notatus*) produces calls averaging ~10 minutes and up to 2 hours, making them some of the longest vocalizations in the animal kingdom. Despite its long-standing role as a model organism for neuroethology research on acoustic communication and social behaviors, it was unclear if the long-duration hums produced by type I (singing) males contain information about male quality. In Chapter 1, I demonstrate that the acoustic features of the hums produced by type I males are correlated with morphometric parameters indicative of quality, such as body size and condition. This suggests that these hums contain information that females could potentially use in mate-choice decisions. Female midshipman are effective at localizing these hums, following local particle motion cues to find the source.

However, there is a 180-degree ambiguity in determining sound direction from particle motion. It has been proposed that gas-filled swim bladders, which detect acoustic pressure, help resolve this ambiguity. Yet, how the swim bladder affects the motion of the fish's inner ears remains unclear. In Chapter 2, I used the finite element method to predict how the swim bladder affects the motion of the otoliths in the inner ear of the midshipman for sounds incident from various directions. I showed that the swim bladder likely resolves the 180-degree ambiguity in directional hearing at behaviorally relevant frequencies for the plainfin midshipman. These predictions can be tested using advanced experimental methods. Many fish do not actively produce sounds but can hear, suggesting that fish hearing may have originally evolved to extract information useful for survival and reproduction from ambient environmental sounds. However, most bioacoustic studies on fishes have focused on communication sounds. In Chapter 3, I review cases where natural ambient sounds serve as sources of information for fishes. I highlight various sources of ambient sound in aquatic environments and hypothesize how they could act as beneficial cues. I also found evidence of natural sounds functioning as noise, disrupting the detection of important signals. This review aims to encourage more studies on ambient sounds and their impact on fish, which is crucial for understanding the effects of underwater noise pollution. Fishes are attracted to sounds such as conspecific advertisement calls. In Chapter 4, I developed Sound-bait, an acoustic trapping method to selectively capture fish species using species-specific attractive sounds. This low-cost method has implications for reducing bycatch in fishing and determining the biological function of fish sounds. In summary, my dissertation provides insights into fundamental questions about fish hearing and acoustic communication, and offers practical applications of this knowledge to aid wildlife conservation.

TABLE OF CONTENTS

ACKNOWLEDGEMENTS

I would like to express my deepest gratitude to my advisor, Joseph Sisneros, for being a fantastic mentor, always having my best interests at heart, and playing a pivotal role in my growth as a scientist. My sincere thanks also go to my committee members, Thomas Daniel, Andrew Brown, Adam Summers, and Yi Shen, for their invaluable support throughout my Ph.D. journey.

I am grateful to the current and past members of the Sisneros lab, including Nicholas Lozier, Ruiyu Zeng, Loranzie Rogers, Sofia Gray, Brooke Vetter, and Julian L. Davis. Without their help, this dissertation would not have been possible. Additionally, I extend my thanks to all my undergraduate field assistants: Jiho Li, Sandra Yang, Anton Reicherter, Cassie Kim, Andy Kim, Arion Norris Chao, and John Han. Their time and effort in fieldwork were pivotal in completing Chapter 4 of my dissertation.

Special thanks to my collaborators, Vaibhav Chhaya and Johannes Veith, who played an important role in Chapter 2 of my dissertation. I would also like to thank Louiza Van Zeeland and Sam McKennoch for helping fund part of my field research for Chapter 4 through Vulcan Inc. I am grateful to the Department of Biology at the University of Washington for their support through various grants and fellowships throughout my Ph.D.

I would like to thank my family: my father, B.G. Dharmanand, my mother, Usha Dharmanand, and my sister, Balebail Sanjana Acharya, for always supporting my passion and career choices, even from the other side of the planet. My heartfelt thanks go to my partner, Alissa Evelyn Palmer, for her unwavering support and wonderful company during the final, hectic stages of my Ph.D.

Lastly, I would like to thank my friends, Vaibhav Thakur, Varun Srivastava, Kesav Krishnan, Maria Kuruvilla, Oscar Sprumont, David Alonso-Villalobos Chaves, Ellie Dawson, Pascal Sturmfels, Nicole Baram, and Aoi Hunsaker, for being great friends and making life outside my Ph.D. better.

Chapter 1: Long duration advertisement calls of nesting male plainfin midshipman fish are honest indicators of size and condition

Published in the journal of experimental biology
Balebail, S. and Sisneros, J. A. (2022). Long duration advertisement calls of nesting male plainfin midshipman fish are honest indicators of size and condition. Journal of Experimental Biology 225, jeb243889.

Abstract

The plainfin midshipman fish (*Porichthys notatus*) has long served as a model organism for neuroethology research on acoustic communication and related social behaviors. Type I or 'singing' males produce highly stereotyped, periodic advertisement calls that are the longest known uninterrupted vertebrate vocalizations. Despite the extensive literature on the acoustic behaviour of this species, it remains unclear whether reproductive males signal their quality via their highly energetic, multiharmonic advertisement calls. Here, we recorded the advertisement calls of 22 reproductive type I males at night in a controlled laboratory setting in which males were housed in aquaria maintained at a constant temperature (13.9±0.3°C). The duration of the advertisement calls from type I males was observed to increase from the first call of the night to the middle call after which call duration remained steady until the early morning hours and first light. A strong positive correlation was observed between loudness (sound pressure level and maximum sound pressure level) of the advertisement call and body size (mass and standard length; r_s>0.8). In addition, an asymptotic relationship was observed between the harmonic frequencies (f_0–f_{10}) of the advertisement calls and male body condition, with harmonic frequencies initially increasing with body condition indices, but then plateauing when body condition measures were high. Taken together, our results suggest that type I male advertisement calls provide reliable honest information about male quality regarding size and body condition. Such condition-dependent information of calling males could potentially be used by receptive females to help facilitate mate choice decisions.

Introduction

Animal signals provide information from one animal to another and often convey information that is the result of natural selection on the sender to help the receiver make a decision, which usually benefits both parties (Bradbury and Vehrencamp, 2011; Smith and Harper, 2003). The use of acoustic signals to convey social information is widely used by animals during reproductive and social behaviours. Acoustic signals can provide a variety of sender information to the receiver, including species identification, sex, individual identity, sexual receptivity, motivation and condition-dependent information used in sexual selection such as age, body size and condition (Bradbury and Vehrencamp, 2011). In the context of reproductive behaviours, acoustic signals are often used as advertisement signals to attract mates (Amorim et al., 2015; Brillet and Paillette, 1991; Catchpole and Slater, 2003; Charlton et al., 2007; Gerhardt and Huber, 2002; Ryan, 1985). Most commonly, advertisement signals are produced by males to attract receptive conspecific females for solicitation, courtship, mating, copulation/gamete release and post-mating announcements (Bradbury and Vehrencamp, 2011).

Acoustic advertisement calls can be physiologically expensive to produce. Increased calling activity has been known to decrease lipid content and growth rate in frogs (Given, 1988) and to increase oxygen consumption in frogs (Given, 1988) and crickets (Prestwich and Walker, 1981). The energy efficiency of call production can be extremely low, ranging from 0.05 to 3.4% in insects (Kavanagh, 1987; Nally and Young, 1981), 0.05–1.2% in frogs (Ryan, 1985) and is at around 2% in birds (Brackenbury, 1980), making them good candidates as 'honest signals' that can convey condition- dependent information about the sender. The calling effort (percentage of time spent calling relative to the total calling period) of acoustic advertisement calls is known to directly reflect a sender's energy expenditure in diverse taxa such as frogs (Bucher et al., 1982; Taigen and Wells, 1985), birds (Eberhardt, 1994) and insects (Nally and Young, 1981). Higher calling effort is associated with senders that are in better condition or have greater energy reserves in several vertebrate clades such as fishes (Amorim et al., 2010; Pedroso et al., 2013),

birds (Reid, 1987) and frogs (Ziegler et al., 2016). Calling effort can be enhanced by increasing either calling rate, call duration, or both. Other signal characteristics of advertisement calls that are condition dependent include the amplitude or loudness of the signal and its spectral properties such as the fundamental frequency and associated harmonics. Loudness of advertisement calls has been associated with body size in certain fishes (Amorim et al., 2013; Lindström and Lugli, 2000), birds (Cardoso, 2010) and insects (Gray, 1997). In addition, larger individuals produce calls with lower fundamental frequencies and harmonics in fishes (Amorim et al., 2013; Myrberg et al., 1993), frogs (Davies and Halliday, 1978; Robertson, 1986), birds (Mager et al., 2007; Marcolin et al., 2022) and mammals (Reby and McComb, 2003; Vannoni and McElligott, 2008). In general, larger animals tend to possess larger sound-producing organs that generate louder calls containing lower fundamental frequencies and harmonics.

Fish likely represent the largest taxon of sound-producing vertebrates and the production of acoustic advertisement signals is an important component of mating behaviour in at least 800 species (Ladich, 2015; Radford et al., 2014). Teleost fishes have evolved a diversity of sound-producing organs and can generate sound by plucking enhanced tendons (Kratochvil, 1978; Ladich, 2004), rubbing bony elements such as teeth or enhanced fin rays (Fine and Parmentier, 2015), stridulating the entire pectoral girdle or other hard skeleton parts (Bertucci et al., 2014; Colleye et al., 2012; Parmentier et al., 2007) or by vibrating the swim bladder with specialized sonic muscles (Bass and McKibben, 2003; Fine and Parmentier, 2015; Fine et al., 2001). One sound-producing fish that has become a good model organism for investigating the neural mechanisms of vocal production and auditory reception shared by all vertebrates is the plainfin midshipman, *Porichthys notatus*, which is a vocal marine teleost that uses social acoustic signals for communication during reproductive and social behaviours (Bass and McKibben, 2003; Bass et al., 1999; Fay and Simmons, 1999; Forlano et al., 2015). The midshipman is nocturnally active and produces a relatively simple repertoire of social acoustic signals that include ‘grunts’, ‘growls’ and ‘hums’ by using sonic muscles to vibrate their swim bladders (Bass et al., 1999; Sisneros, 2009). All three adult midshipman sexual phenotypes (females and males: types I and II) are capable of producing short-duration, broadband agonistic grunts, but only type I nesting males can produce trains of grunts, long duration agonistic growls, and the multi-harmonic advertisement calls or ‘hums’ (Brantley and Bass, 1994; McKibben and Bass, 1998; Sisneros, 2009). The advertisement calls of midshipman are unique among vertebrates in that they are continuous, highly stereotyped and long in duration, ranging from 1 min to a couple of hours (Bass et al., 1999). Females rely on their auditory sense to detect and locate ‘singing’ males that produce the multi-harmonic advertisement calls during the breeding season. Reproductive females become adaptively tuned to detect the dominant harmonic components of male advertisement calls owing to seasonal increases in estrogen levels prior to the breeding season (Sisneros and Bass, 2003; Sisneros et al., 2004a, b). This seasonal enhancement in auditory sensitivity to the higher dominant harmonics of the advertisement call may be important for conspecific detection and localization in shallow water acoustic environments and for the perception of auditory information used in mate choice decisions. Despite this seasonal shift in auditory tuning in females, making them better able to detect male vocalizations, it remains unknown whether the male advertisement call contains condition-dependent information about the sender that could potentially be used in decisions of mate choice.

The primary goal of this study was to characterize the bioacoustics of male advertisement calls and determine if there are any relationships between spectro-temporal features in the advertisement calls and condition dependent morphometrics of calling type I males. We hypothesize that the multiharmonic advertisement calls of type I males are honest indicators of morphometric parameters which reflect male quality, such as size and body condition. Based on previous bioacoustics studies, we predict a positive correlation between calling effort and body condition (Pedroso et al., 2013). We also expect a negative correlation between harmonic frequencies and body size, and a positive relation between loudness and body size (Amorim et al., 2013). Additionally, we investigate if there are temporal rhythms/ patterns in male calling behaviour. We interpret our findings as they relate to the possible use of condition-dependent information in midshipman acoustic communication during social and reproductive behaviours.

Methods

Animals

Type I male plainfin midshipman (*Porichthys notatus* Girard 1854) were captured during periods of low tide when male nests were exposed at Seal Rock, Brinnon, WA, USA in the late spring–summer breeding seasons (April–July) of 2019 and 2020. Animals were transported to the University of Washington and housed in artificial saltwater tanks maintained at a salinity of 26–28 parts per thousand (ppt) and a controlled temperature of 13.9±0.3°C (mean±s.d.) using aquarium chillers. The fish were acclimatized to a 14 h:10 h light:dark cycle by turning the lights off at 20:00 h and turning them on at 06:00 h, approximating the ambient day–night cycle during the nesting period in the wild. Males were fed small pieces of thawed frozen shrimp twice per week.

Experimental setup and acoustic recordings

Two artificial nest chambers were constructed by placing terracotta pot plant saucers (diameter=25 cm, height=3.5 cm) over two bricks (5.7×5.7×22 cm^3), in two separate 50-gallon (230 liter) tanks (121×32×43 cm^3). A brick was placed on top of the pot plant saucer to prevent it rattling when the male vocalized (Fig. 1). The nest chambers were filled with sand to entice the males to excavate and build their own nests. Three to five type I males were added to each tank with the nest chambers. We waited 2–3 days for the nest to be occupied. If no male occupied the nest during these days, either more males were added to the tank or the males residing in the tank were replaced with new individuals. We observed that a strong indicator of the propensity to produce advertisement calls during a given night was the tendency of the resident nesting male to float up against the pot plant saucer (ceiling of nest chamber), presumably due to the increase in swim bladder volume. As soon as this floating behaviour was observed, non-nesting males were removed from the tank to ensure that any recorded call was generated by the nesting male. Floating behaviour generally continued even after a night of calling. An HTI-99-HF hydrophone (Sensitivity: −204 dB re. 1 V µPa−1; Frequency response: 2 Hz–125 kHz) (High Tech Inc., Long Beach, MS, USA) was positioned above the center of the nest (Fig. 1). The hydrophone was connected to a recorder (Zoom H2 digital recorder, Zoom, Hauppauge, NY, USA). Calls were recorded overnight onto an SD card at a sampling frequency of 44.1 kHz and a bit depth of 16. Calls were recorded from a total of 22 type I males, 8 males recorded during the summer of 2019, and 14 males recorded during the summer of 2020. The hydrophone was positioned a fixed distance of 1 cm above the center of the artificial nest in the recordings conducted in 2020 (*N*=14), whereas in 2019 the hydrophone was positioned at a variable distance of ~1–10 cm above the nest (*N*=8) (Fig. 1A). Additionally in 2020, the hydrophone recorders were calibrated using a pistonphone (Type 42AC, G.R.A.S. Sound & Vibration, Holte, Denmark). Background noise in the tanks was primarily due to an aquarium chiller, which turned on and off periodically, and a submersible water pump that stayed on throughout the course of the recording period. Background noise level was 122 dB re. 1 µPa RMS with the chiller on and 113 dB re. 1 µPa RMS with the chiller off.

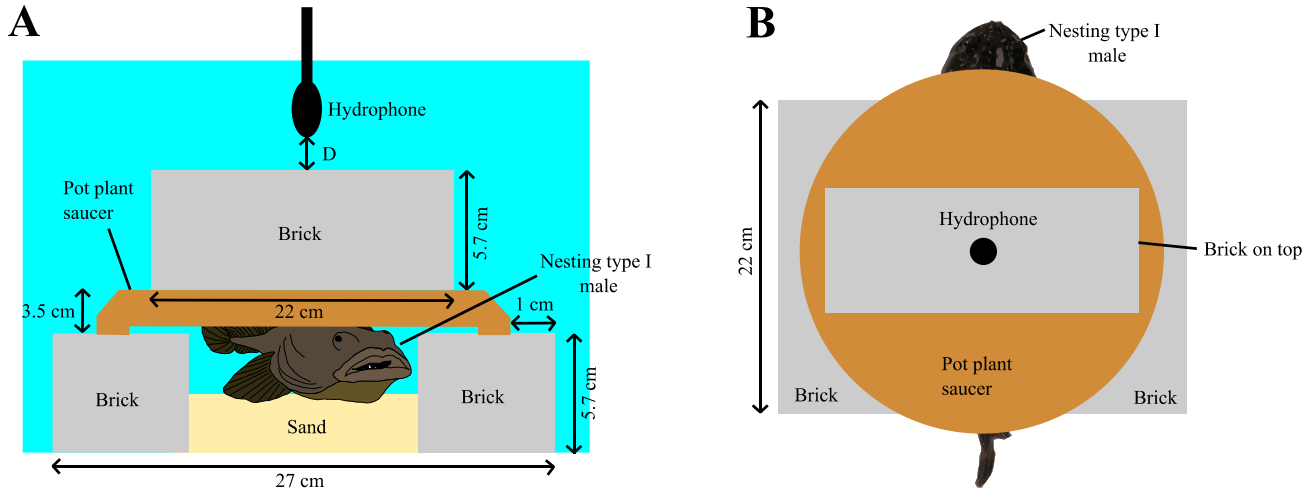

Figure 1. Illustrations depicting (A) frontal view and (B) top view of the artificial nest used to record the

overnight advertisement calls of type I males. During the acoustic recordings conducted in 2020 (N = 14), the hydrophone was placed at a fixed distance (D) = 1 cm on top of the artificial nest, approximately at the center. In 2019 (N = 8), the hydrophone was placed above the nest, but its position was more variable (~1-10 cm above the nest).

Morphometric parameters

After a single night of calling, males were euthanized in a saltwater bath containing excess 10% benzocaine. In 2019 (*N*=8 males), swim bladders were extracted from calling type I males for an alternate set of experiments. Body mass measured to the nearest 0.1 g did not include the mass of the swim bladder (but did include the sonic muscles). Body mass without the swim bladder is highly correlated to total body mass ($R^2 \approx 1$; data from 2020, *N*=14 males; Fig. S1). To maintain consistency between the two summers, all subsequent references to body mass excludes the mass of the swim bladder. We measured standard length to the nearest 0.1 cm. The sonic muscles were carefully removed from the attached swim bladder using scissors and forceps and their mass was measured. In 2020 (*N*=14 males), we also measured the mass of the swim bladder from calling type I males. The swim bladder comprised 1.91±0.3% (mean±s.d.) of the total body mass (*N*=14; data from 2020). Mass of the gonads were measured and used to calculate the gonadosomatic index (GSI), the ratio of gonad mass to somatic mass expressed as a percentage computed by the formula 100×[mass of gonads/(body mass−mass of gonads)].

Body condition was estimated using two indices, the residuals of the regression between the common logarithm (log) of body mass (in g) versus log of standard length (in cm) (COND), and Fulton's condition factor (K) which was computed using the formula 100×(body mass/standard length^3). Both COND and K are indirect measures of energy reserves in fish (Chellappa et al., 1995; Sutton et al., 2000) and have been used to assess body condition in the plainfin midshipman (Bose et al., 2018; Sisneros et al., 2009) and related toadfish (Amorim et al., 2010, 2016). In 2020 (*N*=14 males), we measured the mass of the liver and used it to compute the hepatosomatic index, the ratio of liver mass to somatic mass expressed as a percentage computed by the formula 100×[mass of liver/(body mass−mass of gonads)]. The hepatosomatic index also reflects energy reserves in some fish species (Chellappa et al., 1995).

Spectro-temporal features of the advertisement call

Type I males produce long-duration, multi-harmonic advertisement calls that are highly periodic with a fundamental frequency of around 80–100 Hz and contain harmonics up to 1000 Hz (Fig. 2). For every advertisement call, the duration was measured using Raven pro v.1.5 (Center for Conservation Bioacoustics, Cornell lab of Ornithology, Ithaca, NY, USA). Type I males produced advertisement calls almost exclusively during the night phase of the photoperiod between 20:00 h and 06:00 h, when the lights were turned off. Calling rate was defined as the number of calls per hour. For each male, calling rate was computed as the ratio of the total number of calls produced overnight to the number of hours present in the dark photoperiod (10 h). Calling effort for each individual (percentage of time spent calling) was computed by calculating the ratio of the total time spent calling (in hours) to the total number of hours present in the dark photoperiod (10 h) and multiplying the ratio by 100.

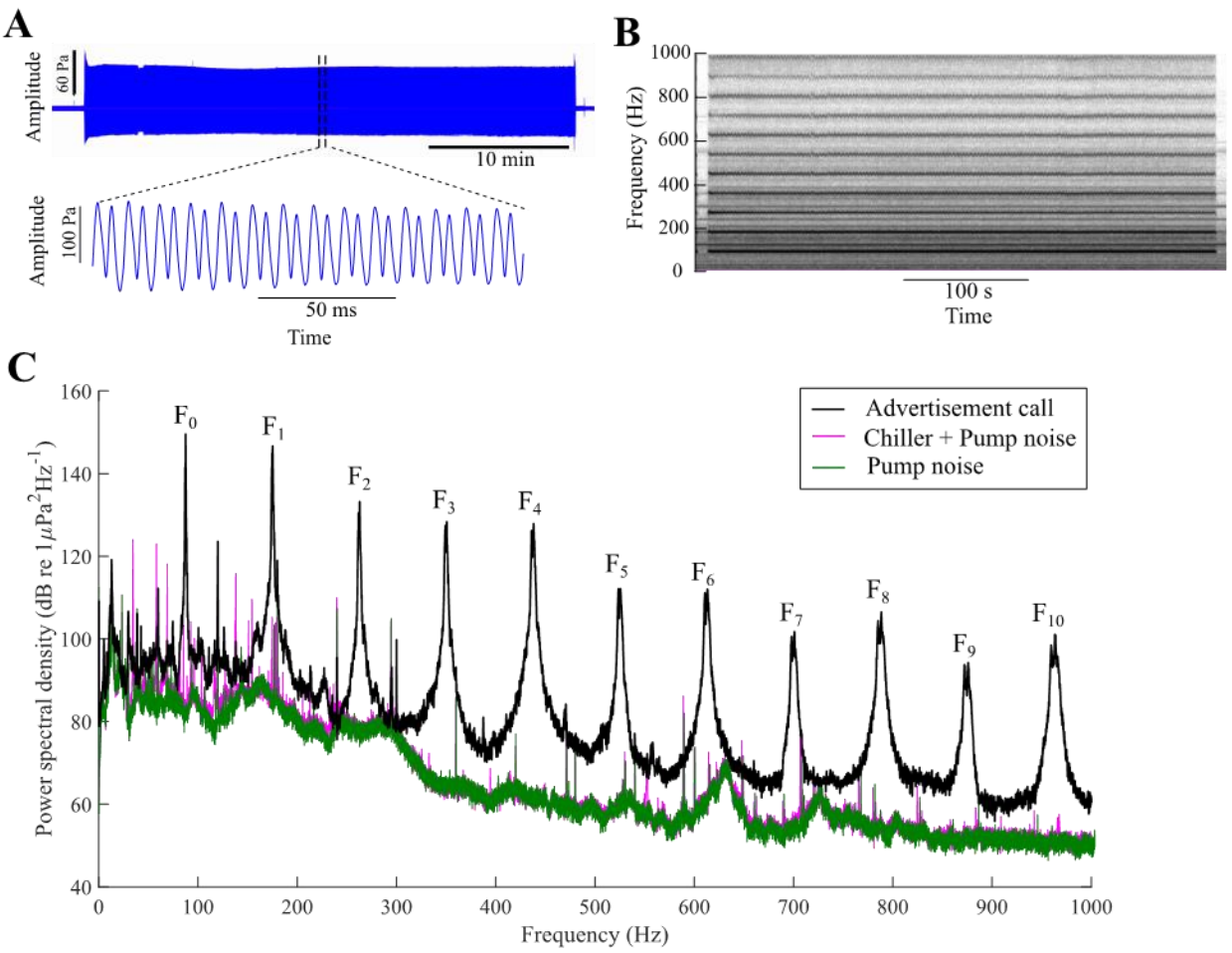

Figure 2. Advertisement calls of type I male plainfin midshipman. (A) Top- Oscillogram of a representative advertisement call which is ~35 minutes in duration; bottom- zooming into a small segment of the call demonstrates that the waveform is highly periodic in nature (B) Spectrogram and (C) Black- Power spectral density plot of a representative advertisement call demonstrates that sound energy is distributed among the fundamental frequency (F_0) and higher harmonics ($F_{1\text{-}10}$). Background noise in the tanks was caused by an aquarium chiller which turned on and off periodically and a water pump, which ran continuously. Pink- Power spectral density curve of the combined sound from the chiller and pump. Green- Power spectral density curve of the sound emanating from the pump when the chiller was in the off phase. The spectrogram in (B) was generated in Raven Pro v1.5 with the following settings, a Hann window with 13606 samples and a 3 dB filter bandwidth of 4.66 Hz, a hop size of 6803 samples with 50% overlap, frequency grid with grid spacing 2.69 Hz and DFT size 16384. For the individual in (B and C), F_0 was close to 90 Hz, with the higher harmonics being integral multiples of F_0.

Each advertisement call contained an initial transient phase at the beginning of the call that was marked by a sharp rise and fall in amplitude. After the initial transient phase of the call, the amplitude becomes relatively stable for the remainder of the advertisement call (Fig. 3). The transient phase of the call was the segment that contained the largest amplitude of the signal. Recordings from calling type I males in 2020 (*N*=14) were calibrated using a pistonphone. For every call recorded in 2020 we selected ~1s duration call segments of the transient phase where the amplitude was greatest using Raven pro v.1.5 (Fig. 3). The root mean square (RMS) amplitude of this transient phase segment was computed to estimate the maximum amplitude produced during the call. The RMS amplitude of the remaining stable portion of the advertisement call was also computed. Sound pressure level (SPL) in dB was computed from the rms pressure amplitude using the following equation:

$$\text{SPL (dB)} = 20^{*} \log_{10}\left(\frac{p}{p_{ref}}\right) \quad (1)$$

where p=RMS pressure amplitude and p_{ref}=1 µPa. Sound pressure level of both the maximum amplitude of the call during the transient phase (henceforth called maximum SPL) and the stable portion (henceforth referred to as just SPL) of the advertisement call was computed for each call produced by the calling type I males. SPL and maximum SPL reflect the loudness of the advertisement call.

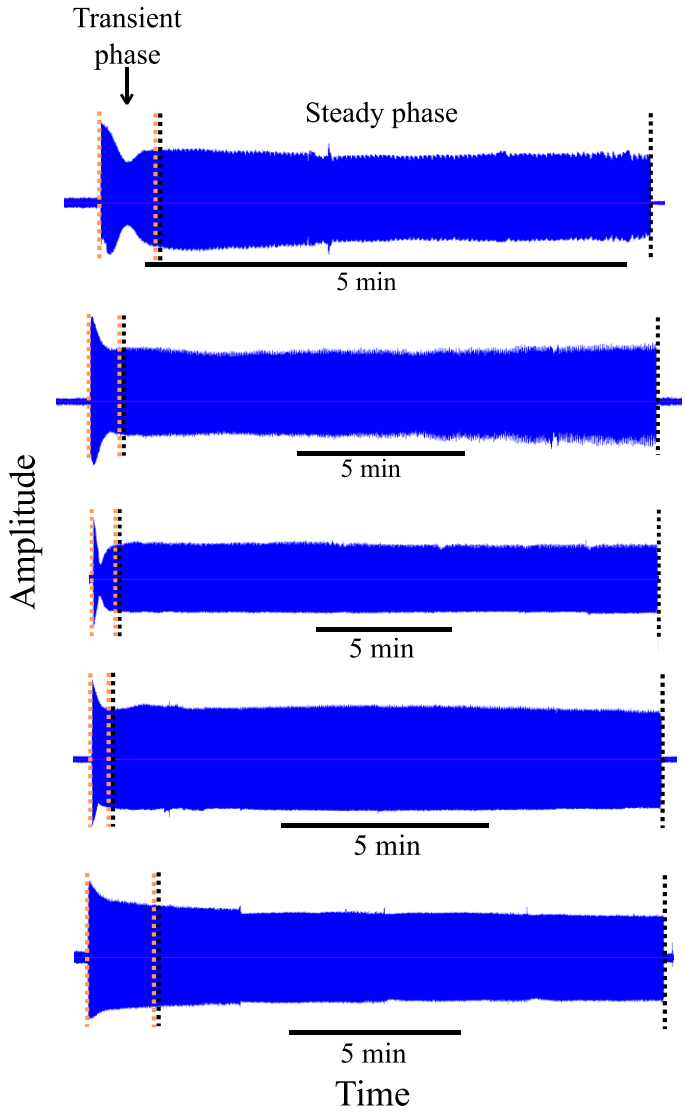

Figure 3. Oscillograms of five representative advertisement calls reveal that the call has an initial transient phase marked by a sharp rise and fall in pressure amplitude, followed by a steady phase where there is little change in pressure amplitude. Pressure amplitude is plotted in voltage units of the Zoom H2 digital recorder used to record the advertisement calls produced by calling type I males.

We extracted 1 min audio clips from the stable portion of the advertisement signal for each call. These 1 min segments were used in the analysis of the following features: the first 11 harmonics (f_0–f_{10}), harmonic decay rate and aggregate entropy. Harmonics, ranging from the fundamental frequency (f_0) to the eleventh harmonic (f_{10}), were estimated by manually marking the peaks in the power spectrum, which was generated using custom code in MATLAB (MathWorks, Natick, MA, USA). The amplitude of each harmonic tends to decrease exponentially with harmonic number (Fig. S2). Exponential functions of the

form $y=a\times e^{-bx}$ were fit to a plot of amplitude versus harmonic number (0–10) in MATLAB, where a and b are positive constants (Fig. S2). The parameter b represents the rate of decline in harmonic amplitude with increase in harmonic number, with larger values representing a steeper decline in the amplitude of higher harmonics relative to the fundamental frequency. We term the parameter *b* as 'harmonic decay rate'. An alternative way to measure how evenly acoustic energy is distributed among harmonic frequencies is through aggregate entropy (*H*) (Charif et al., 2010). *H* was computed using the following equation:

$$H=\sum_{f=f1}^{f2}\frac{E_{bin}}{E}*\log_2\left(\frac{E_{bin}}{E}\right) \quad (2)$$

where, f_1 and f_2 are lower and upper frequency bounds on the spectrogram, E_{bin} is the energy in each bin, and *E* is the total energy summed over each bin. Aggregate entropy was computed for each advertisement call from spectrograms using Raven pro v.1.5. The following settings were used to generate the spectrogram of the call: a Hann window with 65,525 samples and a 3 dB filter bandwidth of 0.968 Hz, a hop size of 32,763 samples with 50% overlap, frequency grid with grid spacing 0.673 Hz and DFT size 65,536. A signal dominated by the fundamental frequency will have low aggregate entropy whereas a signal with more even energy distribution among all the harmonic frequencies will have higher aggregate entropy. To determine if call duration changes during the night, we used a Friedman test to compare the durations of the first, middle, and final calls produced during the night. Conover *post hoc* tests with Bonferroni corrections were used to test for pairwise differences. The criterion for significance α was set to 0.05. If the total number of calls produced by an individual (*n*) was an odd number, then the [(*n*+1)/2]th call was considered as the middle call and its duration was noted. If the individual produced an even number of calls, the middle calls comprised both the (*n*/2)th call and the [(*n*/2)+1]th calls. The duration of the 'middle' call was then computed as the average of the durations of the (*n*/2)th and the [(*n*/2)+1]th calls. Mean call duration was highly variable across animals. To facilitate comparison of temporal patterns in duration across animals, call duration was normalized for each animal by dividing the duration of each call by the length of the longest call produced by that animal. A non-parametric test was used for pairwise comparisons because the assumption of normality was violated for the distribution of duration of the first call (Shapiro–Wilk test; W=0.84; P<0.01). One individual was excluded from the analysis comparing the durations of the first, middle, and final calls as it produced two calls during the recording period.

Correlating morphometrics with spectro-temporal features of the advertisement calls

We measured pairwise Spearman's rank correlation coefficients (r_s) between morphometric parameters and spectro-temporal call features. A *t*-test was used to determine if r_s was significantly different from zero (α= 0.05) (Zar, 1972). The morphometric parameters are mass, standard length, body condition measures (COND and K), sonic muscle mass, swim bladder mass, liver mass, and hepatosomatic index. Call features computed were calling rate, calling effort, and the means of duration, sound pressure level, maximum sound pressure level, fundamental frequency (f_0), harmonic decay rate (*b*) and aggregate entropy (*H*).

Results

Advertisement calling activity and temporal patterns of call duration

The calling type I males had a size range of 18.1–27.2 cm standard length (SL) with mean SL of 23.1±3.4 cm, body mass (BM), 173.5±74.5 g; COND, 0.00±0.05; Fulton's condition factor (K), 1.32±0.15 g cm^{-3}; gonadosomatic index, 2.15±0.76; swim bladder mass, 3.60±1.41 g; sonic muscle mass, 2.53±0.93 g; liver mass, 3.29±1.25 g; and hepatosomatic index, 1.85±0.40 g (all means±s.d.). A total of 408 calls were recorded from 22 type I males. The time to start calling after the onset of the dark photoperiod was variable, ranging from ∼15 min to almost 8 h (mean=1 h 46 min; s.d.=1 h 59 min). One male began calling approximately half an hour before the onset of the dark photoperiod. The number of calls produced

overnight ranged from 2 calls to 80 calls (mean number of calls per night=19±18). The calling rate (calls per hour) varied among the type I males that ranged from 0.2 calls per hour to 8 calls h^{-1} (1.9±1.8 calls h^{-1}, mean±s.d.). Call duration ranged from 6.5 s to 1 h 34 min (9 min 46 s±10 min 40 s). Calling effort ranged from ~2% of the dark photoperiod (20 min) to ~65% (6 h 30 min) with mean calling of 31±20% which equates to 3 h 6 min±2 h spent calling each night on average. The duration of the transient phase ranged from 1.0 s to 109.5 s, with mean duration 28.1±17.4 s. For the calls recorded from males in 2020 (*N*=14), SPL of the transient phase exceeded the SPL of the steady phase by 1.9±1.7 dB.

The duration of the calls produced by vocally active type I males increased over the course of the night and then remained roughly consistent until the early morning hours (Fig. 4A–D, also see Fig. S3). There was a significant main effect of call position (first, middle or final) on call duration (Friedman test: x^2=26.95, Kendall's *W*=0.58, *N*=21, *P*<0.001). Duration of the middle call and final calls were significantly greater than the duration of the first call (Conover *post hoc* test: *N*=21, *P*<0.001 for both comparisons; Fig. 4E). Thus, our data show that type I males, on average, initially produce calls that are shorter in duration at the beginning of the night and as the night progressed call duration increased and remained steady until the males stopped calling in the early hours of the morning.

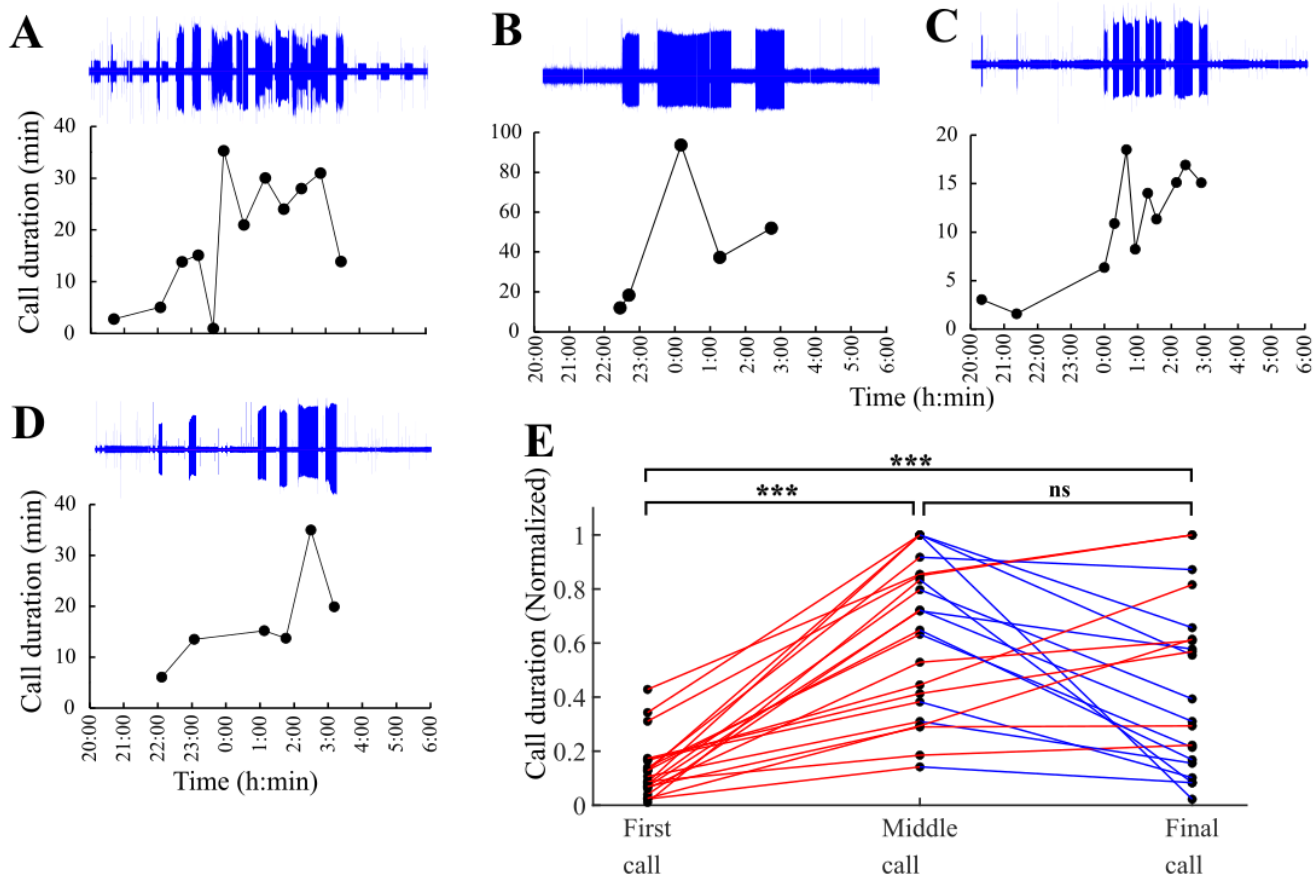

*Figure 4. Temporal trends in call duration. (A-D) Oscillogram (Top), duration (Bottom) of the advertisement call as a function of time of the night for 5 representative individuals. Time on the x-axis represents the instantaneous time at the midpoint of each advertisement call. (E) Normalized duration of the first, middle, and final advertisement call produced by the type I male over the course of a single night. There was a significant main effect of call position (first, middle, or final) on call duration ($\chi^2(2)$ = 26.95, P < 0.001, Kendall's W = 0.58, N = 21). Pairwise comparisons between the first, middle, and final calls were performed using Conover post-hoc tests with Bonferroni corrections Wilcoxon signed-ranks test, with Bonferroni corrections for multiple comparisons (N = 21). *, **, and *** represent P < 0.05, P < 0.01, and P < 0.001. Red and blue lines represent increments and decrements, respectively.*

Spectro-temporal characteristics of advertisement calls predict male morphometrics

We observed strong positive correlations between body size measures and loudness of the advertisement calls. SPL was positively correlated with BM (r_s=0.81, N=14, P<0.001; Fig. 5A) and SL (r_s=0.83, N=14, P<0.001; Fig. 5B) (Table 1). Maximum SPL was also positively correlated with BM (r_s=0.81, N=14, P<0.001; Fig. 5C) and SL (r_s=0.84, N=14, P<0.001; Fig. 5D) (Table 1). Thus, advertisement call loudness was a strong predictor of body size for the calling type I males. The measures of advertisement call loudness (SPL and maximum SPL) were also positively correlated with swim bladder mass, sonic muscle mass, and liver mass (r_s=0.56–0.85, N=14, P<0.05) (Table 1).

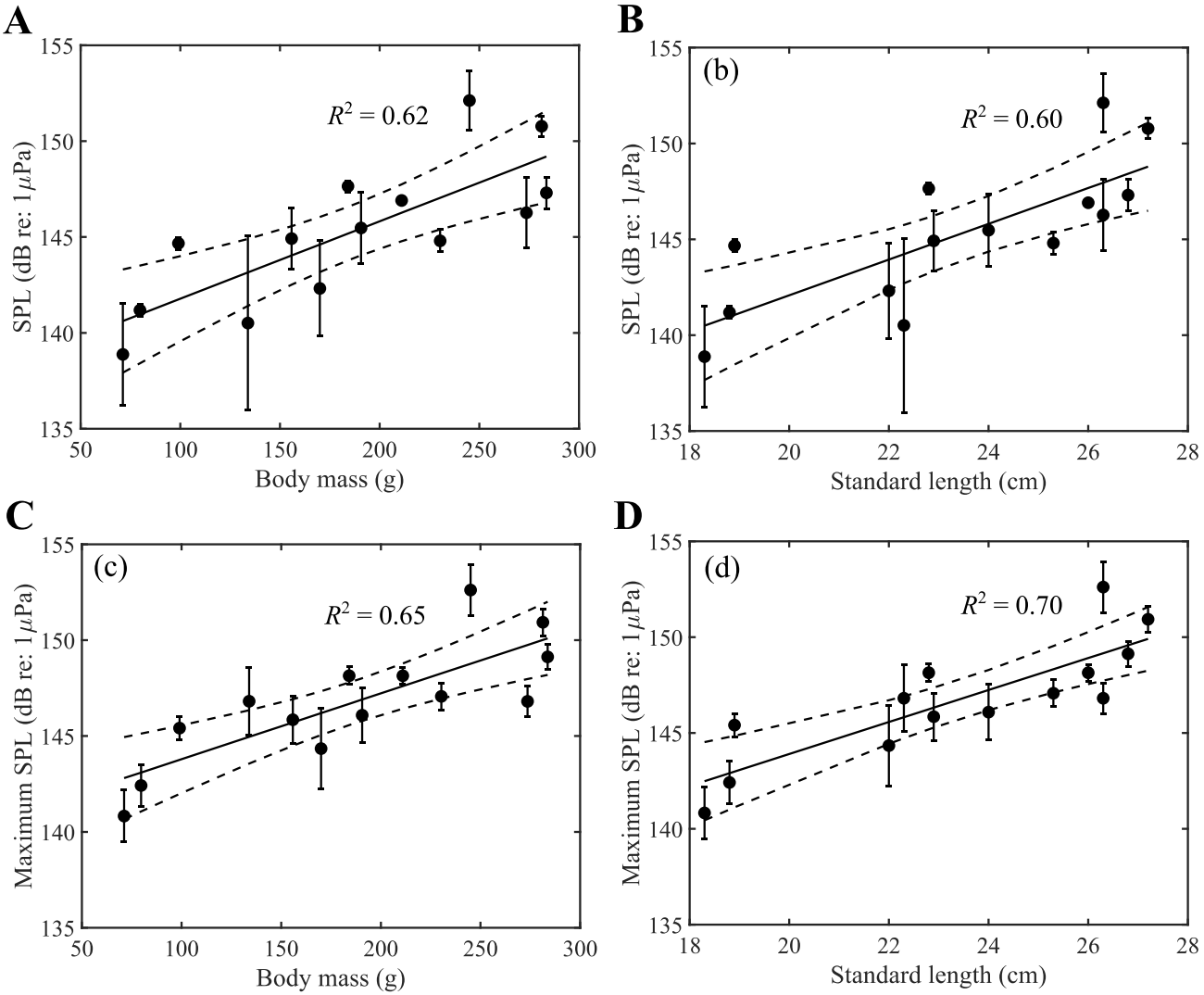

Figure 5. Loudness of the advertisement call reflects body size. Sound pressure level (SPL) is strongly positively correlated with (A) body mass (r_s = 0.81, P < 0.001) and (B) standard length (r_s = 0.83, P < 0.001). Maximum SPL is also strongly positively correlated with (C) body mass (r_s = 0.81, P < 0.001) and (D) standard length (r_s = 0.84, P < 0.001). N = 14 for all correlations. Best fit lines, 95% confidence interval bands, and R^2 values of the best fit lines are shown on the plots. Error bars represent mean value ± standard deviation in this figure and all subsequent figures.

	SPL	Maximum SPL	F_0
Body mass	r_s = 0.81*** *N* = 14	r_s = 0.81*** *N* = 14	r_s = 0.28 *N* = 22
Standard length	r_s = 0.83*** *N* = 14	r_s = 0.84*** *N* = 14	r_s = 0.22 *N* = 22
COND	r_s = 0.23 *N* = 14	r_s = 0.07 *N* = 14	r_s = 0.42 *N* = 22
K	r_s = 0.36 *N* = 14	r_s = 0.25 *N* = 14	r_s = 0.48* *N* = 22
Swim bladder mass	r_s = 0.75** *N* = 14	r_s = 0.85*** *N* = 14	r_s = 0.37 *N* = 14
Sonic muscle mass	r_s = 0.63* *N* = 14	r_s = 0.75** *N* = 14	r_s = 0.09 *N* = 22
Liver mass	r_s = 0.64* *N* = 14	r_s = 0.58* *N* = 14	r_s = 0.47 *N* = 14
Hepatosomatic index	r_s = -0.24 *N* = 14	r_s = -0.41 *N* = 14	r_s = 0.29 *N* = 14

*Table 1. Spearman's rank correlation coefficients (r_s) between morphometric parameters and acoustic features, namely sound pressure level (SPL), maximum SPL and fundamental frequency (F_0). See METHODS for more details. *, **, and *** represent P < 0.05, P < 0.01, and P < 0.001*

The fundamental frequency and higher harmonics (f_0–f_{10}) of the advertisement call increased initially with increasing body condition but then plateaued at higher body condition of calling type I males (Fig. 6). Approximately 50% of the variation in the plots of call harmonics versus body condition can be explained by fitting an asymptotic regression model of the form $y=f_{AS}-(f_{AS}-I)\times e^{-kx}$, where y=harmonic frequency (f_0–f_{10}), x=body condition (COND or K), f_{AS} is the asymptotic frequency at higher body condition, I is the intercept and k represents the rate of exponential decay (Fig. 6, Table 2). An asymptote in the relationship between the harmonic frequencies with body condition occurred at a threshold body condition of approximately 0 (COND) and 1.3 g cm^{-3} (K) (Fig. 6). f_0 was also significantly positively correlated with K (r_s=0.48, P<0.05) but not COND (Table 1). Thus, the harmonic frequencies of the advertisement call serve as a predictor of body condition, with males above a threshold body condition being able to produce calls with higher harmonic frequencies.

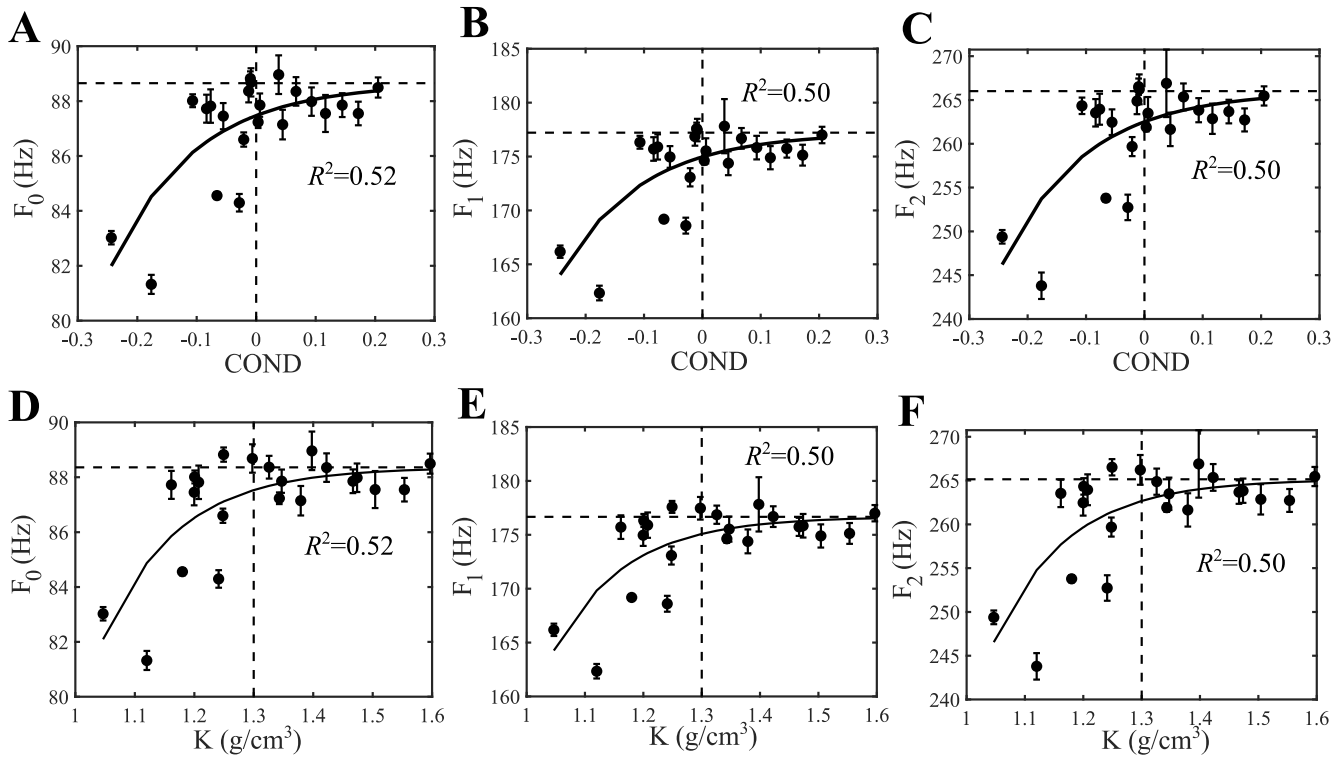

Figure 6. Harmonic frequencies ($F_{0\text{-}10}$) reflect body condition. (A-F) Harmonics (F_0-F_2) plotted against two measures of body condition, (A-C) residuals of the regression between logln body mass and logln standard length (COND), and (D-F) Fulton's condition factor (K) for N = 22 type I males. Black curves represent the best fit asymptotic regression models of the form $y = F_{AS} - (F_{AS} - I)*e^{-kx}$ where y= Harmonic frequency ($F_{0\text{-}2}$), x= Body condition (COND or K), F_{AS} is the asymptotic frequency at higher body conditions, I is the intercept, and k represents the rate of exponential decay. R^2 values of the best fit lines are shown on the plots. Dashed horizontal lines represent the asymptotic frequency (F_{AS}) and dashed vertical lines represent the approximate inflection point where harmonic frequency plateaus with increasing body condition (COND or K).

Harmonic frequency	R^2 (COND)	R^2 (K)
F_0	0.52	0.52
F_1	0.50	0.50
F_2	0.50	0.50
F_3	0.50	0.49
F_4	0.49	0.49
F_5	0.50	0.50
F_6	0.50	0.50
F_7	0.49	0.50

F_8	0.50	0.50
F_9	0.49	0.49
F_{10}	0.49	0.49

Table 2. R^2 values of the best fit asymptotic regression models to explain the relationship between harmonic frequencies ($F_{0\text{-}10}$) and two body condition measures (COND and K). The regression model was of the form $y = F_{AS} - (F_{AS} - I)*e^{-kx}$ where y= Harmonic frequency ($F_{0\text{-}10}$), x= Body condition (COND or K), F_{AS} is the asymptotic frequency at higher body conditions, I is the intercept, and k represents the rate of exponential decay.

There was no correlation between measures of calling activity such as calling rate, call duration and calling effort, and the morphometric parameters examined. Since we demonstrated temporal patterns in call duration, only calls produced after the middle call were used to compute mean call duration to avoid the potential confounding effects of the temporal patterns in call durations as duration increased from initial to middle calls. Therefore, *n*/2 or (*n*+1)/2 calls were included in the computation of mean call duration if the total number of calls produced by the type I male (*n*) was even or odd respectively. Features measuring the energy distribution among harmonic frequencies, aggregate entropy (*H*) and harmonic decay rate (*b*) also showed no correlation with any of the morphometric parameters examined (Table 3).

	Calling rate	Calling effort	Call duration	H	b
Body mass	r_s = -0.21 *N* = 22	r_s = -0.29 *N* = 22	r_s = -0.14 *N* = 22	r_s = -0.01 *N* = 22	r_s = 0.25 *N* = 22
Standard length	r_s = -0.23 *N* = 22	r_s = -0.26 *N* = 22	r_s = -0.08 *N* = 22	r_s = -0.11 *N* = 22	r_s = 0.21 *N* = 22
COND	r_s = 0.00 *N* = 22	r_s = -0.21 *N* = 22	r_s = -0.25 *N* = 22	r_s = -0.39 *N* = 22	r_s = 0.30 *N* = 22
K	r_s = -0.04 *N* = 22	r_s = -0.25 *N* = 22	r_s = -0.28 *N* = 22	r_s = -0.38 *N* = 22	r_s = 0.33 *N* = 22
Swim bladder mass	r_s = -0.24 *N* = 14	r_s = -0.18 *N* = 14	r_s = 0.19 *N* = 14	r_s = -0.10 *N* = 14	r_s = 0.26 *N* = 14
Sonic muscle mass	r_s = -0.09 *N* = 22	r_s = -0.16 *N* = 22	r_s = -0.13 *N* = 22	r_s = 0.10 *N* = 22	r_s = 0.12 *N* = 22
Liver mass	r_s = -0.23 *N* = 14	r_s = -0.35 *N* = 14	r_s = -0.09 *N* = 14	r_s = -0.44 *N* = 14	r_s = 0.51 *N* = 14
Hepatosomatic index	r_s = 0.02 *N* = 14	r_s = -0.13 *N* = 14	r_s = 0.10 *N* = 14	r_s = -0.16 *N* = 14	r_s = 0.24 *N* = 14

Table 3. Spearman's rank correlation coefficients (r_s) between morphometric parameters and acoustic features measuring calling activity (calling rate, calling effort, and call duration), and energy distribution

among harmonic frequencies, namely aggregate entropy (H) and harmonic decay rate (b). See METHODS for more details.

Discussion

The primary goal of this study was to characterize the advertisement calls of reproductive type I male midshipman and determine whether these calls contain condition-dependent information about the sender that could potentially be used in mate choice decisions. In this discussion, we consider how the vocal activity patterns of type I males, the observed correlation between loudness of the advertisement calls and body size, and the asymptotic relation between harmonic frequencies and body condition may influence mate choice decisions in female plainfin midshipman.

Advertisement calling activity and temporal patterns of advertisement call duration

Despite occupying artificial nests in a laboratory setting, type I males called for an average period of 3 h during the dark photoperiod. Mean call duration was approximately 10 min. The average calling period and call duration is consistent with previous studies on captive type I male midshipman (Brantley and Bass, 1994; Feng and Bass, 2016; Ibara et al., 1983). Measures of vocal activity such as call duration, rate and effort did not correlate with the morphometrics of mass, standard length or body condition. This is in contrast to other studied fishes such as the painted goby where calling rate reflects body condition (amount of energy reserves) (Amorim et al., 2013) and the Lusitanian toadfish, where both calling rate and calling effort positively correlate with body condition (amount of energy reserves) (Amorim et al., 2010). In these species, the advertisement calls are quite short in duration being ~0.05 s in the painted goby and ~0.6 s in the Lusitanian toadfish and therefore it is likely that females can directly assess these quantities. However, calling rate and effort cannot be directly assessed by female midshipman as call duration is of the order of minutes or hours and therefore these features may play a limited role in female midshipman mate choice decisions. An increase in calling activity over the course of the night could confer fitness benefits to the type I male by increasing the probability of detection by females. However, we did not observe any correlation between morphometric indicators of reproductive potential such as body condition and size, and any measures of vocal activity. It is possible that the artificial captive conditions in the laboratory may have affected the natural calling activity of nesting type I males. It should also be noted calling activity was recorded over the course of a single night. Monitoring calling activity over a longer duration such as weeks or even the course of the entire breeding season could still reveal a correlation between measures of calling activity and morphometric parameters. However, calling activity appears to be inconsistent across nights, at least in captive conditions (see fig. 3 in Feng and Bass, 2016), strengthening the argument that there is no correlation between measures of calling activity such as call duration and effort and morphometric parameters predicting fitness or reproductive potential. Future studies that characterize the vocal activity of type I males in the natural nesting environment may provide helpful insight into whether the calling activity observed in the laboratory reflects the natural calling activity of nesting males in the wild.

We observed that type I males almost exclusively called during the dark photoperiod. In a previous study, Feng and Bass (2016) demonstrated that type I males primarily produced advertisement calls during the dark photoperiod and that they maintain a 24 h circadian rhythm in calling activity, regulated by the hormone melatonin. Our study is consistent with their results, but we also show that there are temporal trends in calling activity during the night with call duration initially increasing and then remaining stable after the middle call of the night into the early morning hours. We should also note that other acoustic features (SPL, maximum SPL, f_0, H and b) of the initial calls did not differ from that of the middle or final calls (Table 3), indicating a lack of temporal patterns for these features.

Spectro-temporal characteristics of advertisement calls predict male morphometrics

We observed that larger males produced advertisement calls with greater amplitude. This observed increase in loudness with size is likely due, in part, to larger males having larger sonic muscles and larger

swim bladders as shown here in the current study. Larger sonic muscles are capable of producing greater contraction forces to produce louder vocalizations, while larger swim bladders are better for transferring acoustic energy to the surrounding tissues and water. Thus, loudness of the advertisement call provides condition dependent information about the size of the caller. Previous work by McKibben and Bass (1998) revealed that female midshipman preferred louder calls when presented with two calls containing the same fundamental frequency. Females also preferred to spawn in the nests of the larger males, when allowed to choose between two males differing in body size (Bose et al., 2018). Furthermore, type I males with greater body size are known to father more offspring in the wild (Bose et al., 2018; Brown et al., 2021; DeMartini, 1988; Sisneros et al., 2009). Our study provides a positive link between body size and loudness, indicating that female preference for louder calls may also lead them into the nests of larger males. Nest takeovers are a common occurrence in the wild, with the winner likely feeding on the offspring of the displaced male (Cogliati et al., 2013). Therefore, choosing a large male for mating would likely improve female fitness, as larger males would be more likely to fend off smaller competitors and retain nests throughout the course of the breeding season.

The results from our study demonstrate that advertisement call loudness is related to the size of calling males, but call loudness decreases as a function of distance from the calling male. How might females use call loudness to access potential mates? One possibility would be to assess loudness at or in the nest, when females are very close or in physical contact with type I males. In a previous study, Brantley and Bass (1994) showed that approximately 47% of the females that entered a type I male's nest left without spawning. One hypothesis for these results is that the loudness of the advertisement call produced by these type I males did not meet a loudness threshold required by females for mate selection and spawning. Further studies are required to test if the advertisement calls of type I males need to cross a loudness threshold in order to be selected by females for mating. The perception of advertisement call loudness by females in the natural environment may also be influenced by environmental factors such as ambient sound levels and the distribution and attenuation of male advertisement calls in the rocky substrate environment where type I males 'sing' and nest. Future studies that examine vocal signal propagation and loudness in the natural environment will be useful in determining the role of call loudness in mate selection and mate choice decisions by female midshipman.

Loudness or amplitude of the advertisement call maybe an important call attribute that females use in mate choice decisions to access large males as suitable fathers because type I males are the only providers of parental care after spawning. Sisneros et al. (2009) showed that larger nesting type I males (both greater in size and body mass) had a greater number of offspring in their nest at end of the nesting cycle, which suggests that larger males have greater spawning success, a greater capacity to care for more offspring and the potential of having greater fitness. Similarly, Bose et al. (2018) showed in the field that male size and nest size were important correlates of reproductive success, but nest size was found to impose a limit on reproductive success regardless of male nest owner quality. Moreover, Bose et al. (2018) also showed in laboratory mate-choice experiments that females prefer larger males when nest size was held constant, while females showed no preference for larger nests when male size was held constant. Future studies that examine whether female preference for louder advertisement calls and larger males results in greater spawning success and fitness of calling type I males will be needed to determine if call loudness is important in female mate choice decisions.

Although the harmonic frequencies of the type I male advertisement calls were not found to be related to body size, we did find that the harmonics of the advertisement call were related to the body condition of the calling males. This relationship was best explained by an asymptotic regression model that showed that the harmonic frequencies of the advertisement call increased with body condition values up to a threshold of approximately 0 (COND) and 1.3 g cm^{-3} (K) but not at higher body condition values where the harmonic frequencies plateaued (see Fig. 6). This inflection point (at ~COND=0 and K=1.3 g cm^{-3}) in the relationship between the call's harmonic frequencies and body condition may represent a threshold for body condition which if crossed are indicative of high body condition or high quality of nesting type I males. Alternatively, this relationship may represent a threshold for body condition used by females to

evaluate and avoid selecting mates that are in relatively poor body condition. Not surprisingly, Sisneros et al. (2009) reported that type I males with nests containing only fresh eggs from recent spawning (likely within 24 h) had a minimum K value of 1.3 g cm^{-3} and maximum K value of 1.9 g cm^{-3} [mean K=1.5±0.2 g cm^{-3} s.d.; see Table I in Sisneros et al. (2009)]. This body condition threshold or minimum K value of 1.3 g cm^{-3} observed in successfully mated males may correlate with the production of an upper harmonic frequency limit of the male advertisement call at a given temperature and function to identify type I males that are in relatively high body condition. Body condition is an important morphometric and indicator of energy reserves for nesting type I males during breeding season when males are actively calling to attract mates but are slowly starving due to lack of food while in the nest. The data from our current study support the hypothesis that body condition may be an important criterion used by females and can be obtained from the information in the harmonics of the male advertisement call. We should also note that body condition is also likely not the only criterion used by females for mate choice decisions. Brantley and Bass (1994) noted that type I males often stop calling shortly after females enter a male's nest during courtship. This suggests that other non-auditory sensory cues could be used by females to evaluate males such as the 'fin quivers' or hydrodynamic fin movements produce by courting males that can be detected by the lateral line, or the olfactory signals produced by nesting males, and even perhaps the odors of eggs in the nest, which could potentially provide cues of mating success. Future studies that examine the attractiveness of different advertisement calls based on the harmonic frequency content related to body condition in behavioral two-choice playback experiments and whether other sensory cues are used during mating will be extremely useful in determining what information females use in mate choice decisions.

One critical factor that is important in determining the relationship between advertisement call harmonic frequencies and body condition is temperature. Previously, it has been demonstrated that the fundamental frequency and corresponding harmonics of the advertisement call vary linearly with temperature (Brantley and Bass, 1994; Halliday et al., 2018; McIver et al., 2014) and this is likely due to a temperature-coupling mechanism of sender and receiver in the vocal communication system of the plainfin midshipman. Such temperature coupling mechanisms are known to occur in the vocal-acoustic systems of other vertebrates and in invertebrates (Brenowitz et al., 1985; Ladich, 2018; Pires and Hoy, 1992). McIver et al. (2014) showed that the fundamental frequency of the advertisement call varies linearly with temperature such that an increase of 1°C corresponds to a 5 Hz increase in fundamental frequency. Because the fundamental frequency and advertisement call harmonics vary with temperature, it was important to control and maintain a constant temperature in this study to reduce frequency variation in call's harmonics due to temperature. Midshipman research labs (including the Sisneros lab) have previously examined the potential relationship of the advertisement call harmonics with type I male morphometrics (e.g. size, body condition, etc.) but failed to find any significant relationships when not controlling for temperature. However, the current study is the first to control for temperature while examining such relationships. Across a temperature range of 12–18°C, females demonstrate in two choice experiments a strong preference for pure tones that match the fundamental frequency of average type I males calling at that temperature (McKibben and Bass, 1998). This fundamental frequency preference by females evokes strong phonotaxis to the simulated playback of a calling male and suggests at a given temperature there is optimum fundamental frequency and associated harmonics that influence mate choice decisions. When we maintained temperature constant at ∼14°C in our recording tanks, we observed that males in relatively poorer body condition produced advertisement calls with lower fundamental frequencies and harmonics, which supports the hypothesis, at least at this temperature, that type I males in poorer body condition are unable to produce advertisement call frequencies that are preferred by females. Night temperatures recorded from the nesting grounds of plainfin midshipman at Seal Rock in Brinnon, WA, USA can range from 12 to 21°C during the breeding season (S.B., unpublished data). It remains to be seen whether the advertisement call frequencies of type I males are influenced by body condition at temperatures other than 14°C in the wild. Future studies that examine the correlation of advertisement call frequencies with body condition at other temperatures would prove useful in determining whether body condition constrains the call's harmonic frequencies across the

temperature range experienced by the plainfin midshipman in its natural environment. In addition to using their advertisement calls to attract mates, type I males may also employ nesting and chorusing strategies to enhance their probability of mating success. Based on the authors' personal field observations, nesting type I males do not appear to establish their nests randomly in the intertidal breeding zone. Instead, nests have commonly been observed to be clustered in groups, but it remains unclear what are the underlying factors responsible for the spatial distribution of the nesting clusters (e.g. the factors that may determine nest suitability such as the size, density and sound-propagating properties of the nests and how they are distributed in the intertidal zone). However, one potential explanation for the observed clustering of male nests in the intertidal nesting zone may be related to the 'hotshot' hypothesis, which was originally proposed by Bradbury and Gibson (1983) to explain why males congregate at leks. According to the hotshot hypothesis, subordinate males cluster around highly attractive males to enhance their chances of interacting and potentially mating with females that are drawn to the 'hotshots'. Likewise, type I males that are smaller and/or in poorer body condition may establish their nest sites near larger and better conditioned type I males (i.e. 'hotshots') during the breeding season as a strategy to enhance mating success. 'Hot shot' nesting type I males may only be able to spawn with a limited number of females at a time, which may allow for nearby nesting males to court and spawn with other females when multiple females are attracted to the dominant or 'hotshot' nesting male. An alternative, but not mutually exclusive, hypothesis for the clustering of nesting males in the intertidal environment maybe a hypothesis similar to the 'female preference' hypothesis proposed by Bradbury (1981) that males cluster together because females prefer sites with large groups of males, where they can more quickly and/or more safely, compare the quality of many potential mates. In terms of the plainfin midshipman, type I males may cluster in order to 'sing' or produce their advertisement calls together, which can be commonly heard in midshipman field recordings that contain overlapping 'hums that interfere acoustically to produce acoustic beats (McIver et al., 2014). The chorus of hums produced by nesting males may function to attract females to a cluster of males and allow them to access a large group of males relatively quickly. If the attractiveness of chorus calls is greater than individual calls such as in the eastern gray treefrog (Stratman et al., 2021), then such evidence would help support a female preference hypothesis for the clustering of nesting males. Future studies that examine the spatial distribution of the nests and the calling strategies of male midshipman in the natural environment would be informative in determining the adaptive strategies that type I males may use to potential enhance their reproductive success.

Conclusions

We show that nesting type I males primarily produce their multiharmonic advertisement calls during the dark photoperiod. Call duration steadily increased after the first call, rose to a peak value and then remained consistent until the early morning before light. Advertisement call loudness was strongly correlated with body size while the harmonics of the advertisement call initially increased with body condition up to a certain threshold body condition where it remained relatively constant and did not increase at higher body condition. Taken together, our results suggest that the advertisement calls of the type I male plainfin midshipman can potentially provide prospective mates with valuable condition dependent or 'honest' information about both the size and body condition of the advertising male.

References

Amorim, M. C. P., Simões, J. M., Mendonça, N., Bandarra, N. M., Almada, V. C. and Fonseca, P. J. (2010). Lusitanian toadfish song reflects male quality. J. Exp. Biol. 213, 2997-3004. doi:10.1242/jeb.044586

Amorim, M. C. P., Pedroso, S. S., Bolgan, M., Jordaõ, J. M., Caiano, M. and Fonseca, P. J. (2013). Painted gobies sing their quality out loud: acoustic rather than visual signals advertise male quality and contribute to mating success. Funct. Ecol. 27, 289-298. doi:10.1111/1365-2435.12032

Amorim, M. C. P., Vasconcelos, R. O. and Fonseca, P. J. (2015). Fish sounds and mate choice. In Sound Communication in Fishes (ed. F. Ladich), pp. 1-33. Vienna: Springer Vienna.

Amorim, M. C. P., Conti, C., Sousa-Santos, C., Novais, B., Gouveia, M. D., Vicente, J. R., Modesto, T., Gonçalves, A. and Fonseca, P. J. (2016). Reproductive success in the Lusitanian toadfish: Influence of calling activity, male quality and experimental design. Physiol. Behav. 155, 17-24. doi:10.1016/j. physbeh.2015.11.033

Balebail, S. (2022), Data for: Long duration advertisement calls of nesting male plainfin midshipman fish are honest indicators of size and condition. Dryad Dataset, doi:10.5061/dryad.pk0p2ngqf

Bass, A. H. and McKibben, J. R. (2003). Neural mechanisms and behaviors for acoustic communication in teleost fish. Prog. Neurobiol. 69, 1-26. doi:10.1016/ S0301-0082(03)00004-2

Bass, A. H., Bodnar, D. A. and Marchaterre, M. A. (1999). Complementary explanations for existing phenotypes in an acoustic communication system. In Neural Mechanisms of Communication. (ed. M. Hauser M and M. Konishi), pp. 493-514. Cambridge: MIT Press.

Bertucci, F., Ruppé, L., Van Wassenbergh, S., Compeŕe, P. and Parmentier, E. (2014). New insights into the role of the pharyngeal jaw apparatus in the sound- producing mechanism of Haemulon flavolineatum (Haemulidae). J. Exp. Biol. 217, 3862-3869. doi:10.1242/jeb.109025

Bose, A. P. H., Cogliati, K. M., Luymes, N., Bass, A. H., Marchaterre, M. A., Sisneros, J. A., Bolker, B. M. and Balshine, S. (2018). Phenotypic traits and resource quality as factors affecting male reproductive success in a toadfish. Behav. Ecol. 29, 496-507. doi:10.1093/beheco/ary002

Brackenbury, J. (1980). Respiration and production of sounds by birds. Biol. Rev. 55, 363-378. doi:10.1111/j.1469-185X.1980.tb00698.x

Bradbury, J. W. (1981). The evolution of leks. In Natural Selection and Social Behavior (ed. R. D. Alexander and T. W. Tinkle), 138-169. New York, NY: Carron Press.

Bradbury, J. W. and Gibson, R. M. (1983). Leks and mate choice. In Mate Choice (ed. P. Bateson), pp. 109-138. Cambridge: Cambridge University Press.

Bradbury, J. W. and Vehrencamp, S. L. (2011). Principles of Animal Communication. Sunderland: Sinauer Associate. Inc.

Brantley, R. K. and Bass, A. H. (1994). Alternative male spawning tactics and acoustic signals in the plainfin midshipman fish Porichthys notatus Girard (Teleostei, Batrachoididae). Ethology 96, 213-232. doi:10.1111/j.1439-0310. 1994.tb01011.x

Brenowitz, E. A., Rose, G. and Capranica, R. R. (1985). Neural correlates of temperature coupling in the vocal communication system of the gray treefrog (Hyla versicolor). Brain Res. 359, 364-367. doi:10.1016/0006-8993(85)91452-0

Brillet, C. and Paillette, M. (1991). Acoustic signals of the nocturnal lizard Gekko gecko: analysis of the ‘long complex sequence’. Bioacoustics 3, 33-44.

Brown, N. A. W., Halliday, W. D., Balshine, S. and Juanes, F. (2021). Low- amplitude noise elicits the Lombard effect in plainfin midshipman mating vocalizations in the wild. Anim. Behav. 181, 29-39. doi:10.1016/j.anbehav.2021. 08.025

Bucher, T. L., Ryan, M. J. and Bartholomew, G. A. (1982). Oxygen consumption during resting, calling, and nest building in the frog Physalaemus pustulosus. Physiol. Zool. 55, 10-22. doi:10.1086/physzool.55.1.30158439

Cardoso, G. C. (2010). Loudness of birdsong is related to the body size, syntax and phonology of passerine species. J. Evol. Biol. 23, 212-219. doi:10.1111/j.1420- 9101.2009.01883.x

Catchpole, C. K. and Slater, P. J. (2003). Bird Song: Biological Themes and Variations. Cambridge University Press.

Charif, R. A., Waack, A. M. and Strickman, L. M. (2010). Raven Pro 1.4 User's Manual, p. 25506974. Ithaca, NY: Cornell Lab Ornithol.

Charlton, B. D., Reby, D. and McComb, K. (2007). Female red deer prefer the roars of larger males. Biol. Lett. 3, 382-385. doi:10.1098/rsbl.2007.0244

Chellappa, S., Huntingford, F. A., Strang, R. H. C. and Thomson, R. Y. (1995). Condition factor and hepatosomatic index as estimates of energy status in male three-spined stickleback. J. Fish Biol. 47, 775-787. doi:10.1111/j.1095-8649. 1995.tb06002.x

Cogliati, K. M., Neff, B. D. and Balshine, S. (2013). High degree of paternity loss in a species with alternative reproductive tactics. Behav. Ecol. Sociobiol. 67, 399-408. doi:10.1007/s00265-012-1460-y

Colleye, O., Nakamura, M., Frédérich, B. and Parmentier, E. (2012). Further insight into the sound-producing mechanism of clownfishes: what structure is involved in sound radiation? J. Exp. Biol. 215, 2192-2202. doi:10.1242/jeb.067124 Davies, N. B. and Halliday, T. R. (1978). Deep croaks and fighting assessment in toads Bufo bufo. Nature 274, 683-685. doi:10.1038/274683a0

DeMartini, E. E. (1988). Spawning success of the male plainfin midshipman. I. Influences of male body size and area of spawning site. J. Exp. Mar. Biol. Ecol. 121, 177-192.

Eberhardt, L. S. (1994). Oxygen consumption during singing by male Carolina Wrens (Thryothorus ludovicianus). The Auk 111, 124-130. doi:10.2307/4088511 Fay, R. R. and Simmons, A. M. (1999). The sense of hearing in fishes and amphibians. In Comparative Hearing: Fish and Amphibians (ed. R. R. Fay and A. N. Popper), pp. 269-318. New York, NY: Springer.

Feng, N. Y. and Bass, A. H. (2016). "Singing" fish rely on circadian rhythm and melatonin for the timing of nocturnal courtship vocalization. Curr. Biol. 26, 2681-2689. doi:10.1016/j.cub.2016.07.079

Fine, M. L. and Parmentier, E. (2015). Mechanisms of fish sound production. In Sound Communication in Fishes (ed. F. Ladich), pp. 77-126. Springer.

Fine, M. L., Malloy, K. L., King, C., Mitchell, S. L. and Cameron, T. M. (2001). Movement and sound generation by the toadfish swimbladder. J. Comp. Physiol. A 187, 371-379. doi:10.1007/s003590100209

Forlano, P. M., Sisneros, J. A., Rohmann, K. N. and Bass, A. H. (2015). Neuroendocrine control of seasonal plasticity in the auditory and vocal systems of fish. Front. Neuroendocrinol. 37, 129-145. doi:10.1016/j.yfrne.2014.08.002

Gerhardt, H. C. and Huber, F. (2002). Acoustic Communication in Insects and Anurans: Common Problems and Diverse Solutions. University of Chicago Press. Given, M. F. (1988). Growth rate and the cost of calling activity in male carpenter frogs, Rana virgatipes. Behav. Ecol. Sociobiol. 22, 153-160. doi:10.1007/BF00300564

Gray, D. A. (1997). Female house crickets, Acheta domesticus, prefer the chirps of large males. Anim. Behav. 54, 1553-1562. doi:10.1006/anbe.1997.0584

Halliday, W. D., Pine, M. K., Bose, A. P. H., Balshine, S. and Juanes, F. (2018). The plainfin midshipman's soundscape at two sites around Vancouver Island, British Columbia. Mar. Ecol. Prog. Ser. 603, 189-200. doi:10.3354/meps12730

Ibara, R. M., Penny, L. T., Ebeling, A. W., van Dykhuizen, G. and Cailliet, G. (1983). The mating call of the plainfin midshipman fish, Porichthys notatus. In Predators and Prey in Fishes (ed. D.L.G. Noakes et al.), pp. 205-212. Springer.

Kavanagh, M. W. (1987). The efficiency of sound production in two cricket species, Gryllotalpa australis and Teleogryllus commodus (Orthoptera: Grylloidea). J. Exp. Biol.130, 107-119. doi:10.1242/jeb.130.1.1073

Kratochvil, H. (1978). Der Bau des Lautapparates vom Knurrenden Gurami (Trichopsis vittatus Cuvier & Valenciennes) (Anabantidae, Belontiidae). Zoomorphologie 91, 91-99. doi:10.1007/BF00994156

Ladich, F. (2004). Sound production and acoustic communication. In The Senses of Fish: Adaptations for the Reception of Natural Stimuli (ed. G. von der Emde, J. Mogdans and B. G. Kapoor), pp. 210-230. Dordrecht: Springer Netherlands.

Ladich, F. (2015). Sound Communication in Fishes. Springer.

Ladich, F. (2018). Acoustic communication in fishes: temperature plays a role. Fish Fish. 19, 598-612. doi:10.1111/faf.12277

Lindström, K. and Lugli, M. (2000). A quantitative analysis of the courtship acoustic behaviour and sound patterning in male sand goby, Pomatoschistus minutus. Environ. Biol. Fishes 58, 411-424. doi:10.1023/A:1007695526177

Mager, J. N., Walcott, C. and Piper, W. H. (2007). Male common loons, Gavia immer, communicate body mass and condition through dominant frequencies of territorial yodels. Anim. Behav. 73, 683-690. doi:10.1016/ j.anbehav.2006.10.009

Marcolin, F., Cardoso, G. C., Bento, D., Reino, L. and Santana, J. (2022). Body size and sexual selection shaped the evolution of parrot calls. J. Evol. Biol. 35, 439-450. doi:10.1111/jeb.13986

McIver, E. L., Marchaterre, M. A., Rice, A. N. and Bass, A. H. (2014). Novel underwater soundscape: acoustic repertoire of plainfin midshipman fish. J. Exp. Biol. 217, 2377-2389.

McKibben, J. R. and Bass, A. H. (1998). Behavioral assessment of acoustic parameters relevant to signal recognition and preference in a vocal fish. J. Acoust. Soc. Am. 104, 3520-3533. doi:10.1121/1.423938

Myrberg, A. A., , Jr, Ha, S. J. and Shamblott, M. J. (1993). The sounds of bicolor damselfish (Pomacentrus partitus): predictors of body size and a spectral basis for individual recognition and assessment. J. Acoust. Soc. Am. 94, 3067-3070. doi:10.1121/1.407267

Nally, R. M. and Young, D. (1981). Song energetics of the bladder cicada, Cystosoma Saundersii. J. Exp. Biol. 90, 185-196. doi:10.1242/jeb.90.1.185

Parmentier, E., Colleye, O., Fine, M. L., Frédérich, B., Vandewalle, P. and Herrel, A. (2007). Sound production in the clownfish Amphiprion clarkii. Science 316, 1006. doi:10.1126/science.1139753

Pedroso, S. S., Barber, I., Svensson, O., Fonseca, P. J. and Amorim, M. C. P. (2013). Courtship sounds advertise species identity and male quality in sympatric Pomatoschistus spp. gobies. PLoS ONE 8, e64620. doi:10.1371/journal.pone. 0064620

Pires, A. and Hoy, R. R. (1992). Temperature coupling in cricket acoustic communication. J. Comp. Physiol. A 171, 79-92. doi:10.1007/BF00195963

Prestwich, K. N. and Walker, T. J. (1981). Energetics of singing in crickets: Effect of temperature in three trilling species (Orthoptera: Gryllidae). J. Comp. Physiol. 143, 199-212. doi:10.1007/BF00797699

Radford, A. N., Kerridge, E. and Simpson, S. D. (2014). Acoustic communication in a noisy world: can fish compete with anthropogenic noise? Behav. Ecol. 25, 1022-1030. doi:10.1093/beheco/aru029

Reby, D. and McComb, K. (2003). Anatomical constraints generate honesty: acoustic cues to age and weight in the roars of red deer stags. Anim. Behav. 65, 519-530. doi:10.1006/anbe.2003.2078

Reid, M. L. (1987). Costliness and reliability in the singing vigour of Ipswich sparrows.

Anim. Behav. 35, 1735-1743. doi:10.1016/S0003-3472(87)80066-0

Robertson, J. G. M. (1986). Female choice, male strategies and the role of vocalizations in the Australian frog Uperoleia rugosa. Anim. Behav. 34, 773-784. doi:10.1016/S0003-3472(86)80061-6

Ryan, M. J. (1985). The Túngara Frog, A Study in Sexual Selection and Communication. 1985. Chicago: University of Chicago Press.

Sisneros, J. A. (2009). Seasonal plasticity of auditory saccular sensitivity in the vocal plainfin midshipman fish, Porichthys notatus. J. Neurophysiol. 102, 1121-1131. doi:10.1152/jn.00236.2009

Sisneros, J. A. and Bass, A. H. (2003). Seasonal plasticity of peripheral auditory frequency sensitivity. J. Neurosci. 23, 1049-1058. doi:10.1523/JNEUROSCI.23- 03-01049.2003

Sisneros, J. A., Forlano, P. M., Deitcher, D. L. and Bass, A. H. (2004a). Steroid-dependent auditory plasticity leads to adaptive coupling of sender and receiver. Science 305, 404-407. doi:10.1126/science.1097218

Sisneros, J. A., Forlano, P. M., Knapp, R. and Bass, A. H. (2004b). Seasonal variation of steroid hormone levels in an intertidal-nesting fish, the vocal plainfin midshipman. Gen. Comp. Endocrinol. 136, 101-116. doi:10.1016/j.ygcen.2003. 12.007

Sisneros, J. A., Alderks, P. W., Leon, K. and Sniffen, B. (2009). Morphometric

changes associated with the reproductive cycle and behaviour of the intertidal- nesting, male plainfin midshipman Porichthys notatus. J. Fish Biol. 74, 18-36. doi:10.1111/j.1095-8649.2008.02104.x

Smith, J. M. and Harper, D. (2003). Animal Signals. Oxford University Press.

Stratman, K. D., Oldehoeft, E. A. and Höbel, G. (2021). Woe is the loner: female treefrogs prefer clusters of displaying males over single “hotshot” males. Evolution 75, 3026-3036.

Sutton, S. G., Bult, T. P. and Haedrich, R. L. (2000). Relationships among fat weight, body weight, water weight, and condition factors in wild Atlantic Salmon Parr. Trans. Am. Fish. Soc. 129, 527-538. doi:10.1577/1548- 8659(2000)129<0527:RAFWBW>2.0.CO;2

Taigen, T. L. and Wells, K. D. (1985). Energetics of vocalization by an anuran amphibian (Hyla versicolor). J. Comp. Physiol. B 155, 163-170. doi:10.1007/ BF00685209

Vannoni, E. and McElligott, A. G. (2008). Low frequency groans indicate larger and more dominant fallow deer (Dama dama) males. PLoS ONE 3, e3113. doi:10.1371/journal.pone.0003113

Zar, J. H. (1972). Significance testing of the spearman rank correlation coefficient. J. Am. Stat. Assoc. 67, 578-580. doi:10.1080/01621459.1972.10481251

Ziegler, L., Arim, M. and Bozinovic, F. (2016). Intraspecific scaling in frog calls: the interplay of temperature, body size and metabolic condition. Oecologia 181, 673-681. doi:10.1007/s00442-015-3499-8

Supplementary material

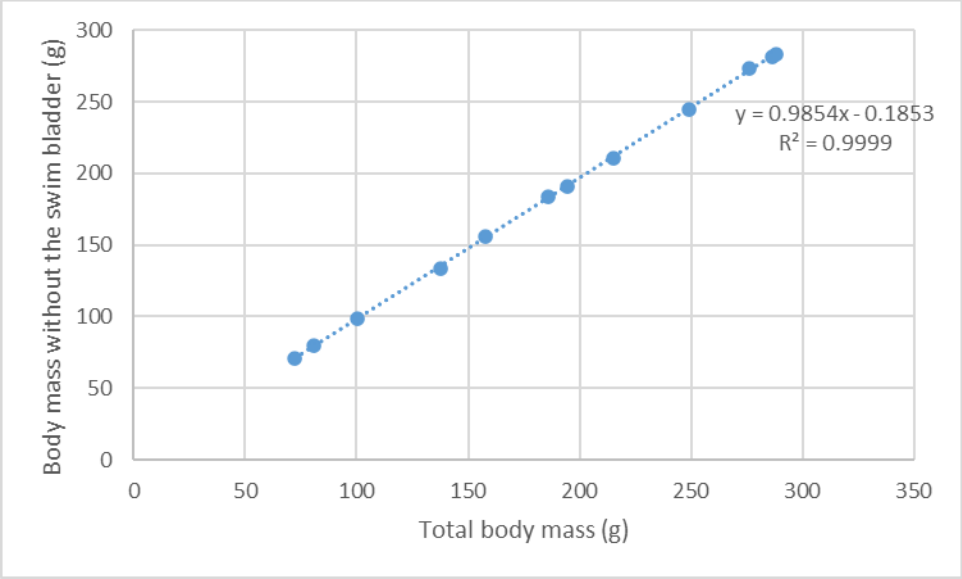

Figure S1. Body mass (without the swim bladder) versus total body mass of advertisement calling type I males.

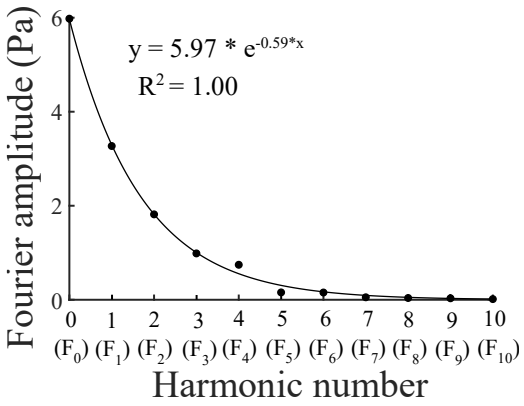

Figure S2. Fourier amplitude plotted as a function of harmonic number for a single representative 1 minute call segment. For this specific advertisement call, an exponential decay function of the form $y= a*e^{-bx}$ fit the data almost perfectly, $R^2 \approx 1$, where a= 5.97 and b=0.59. b represents the harmonic decay rate.

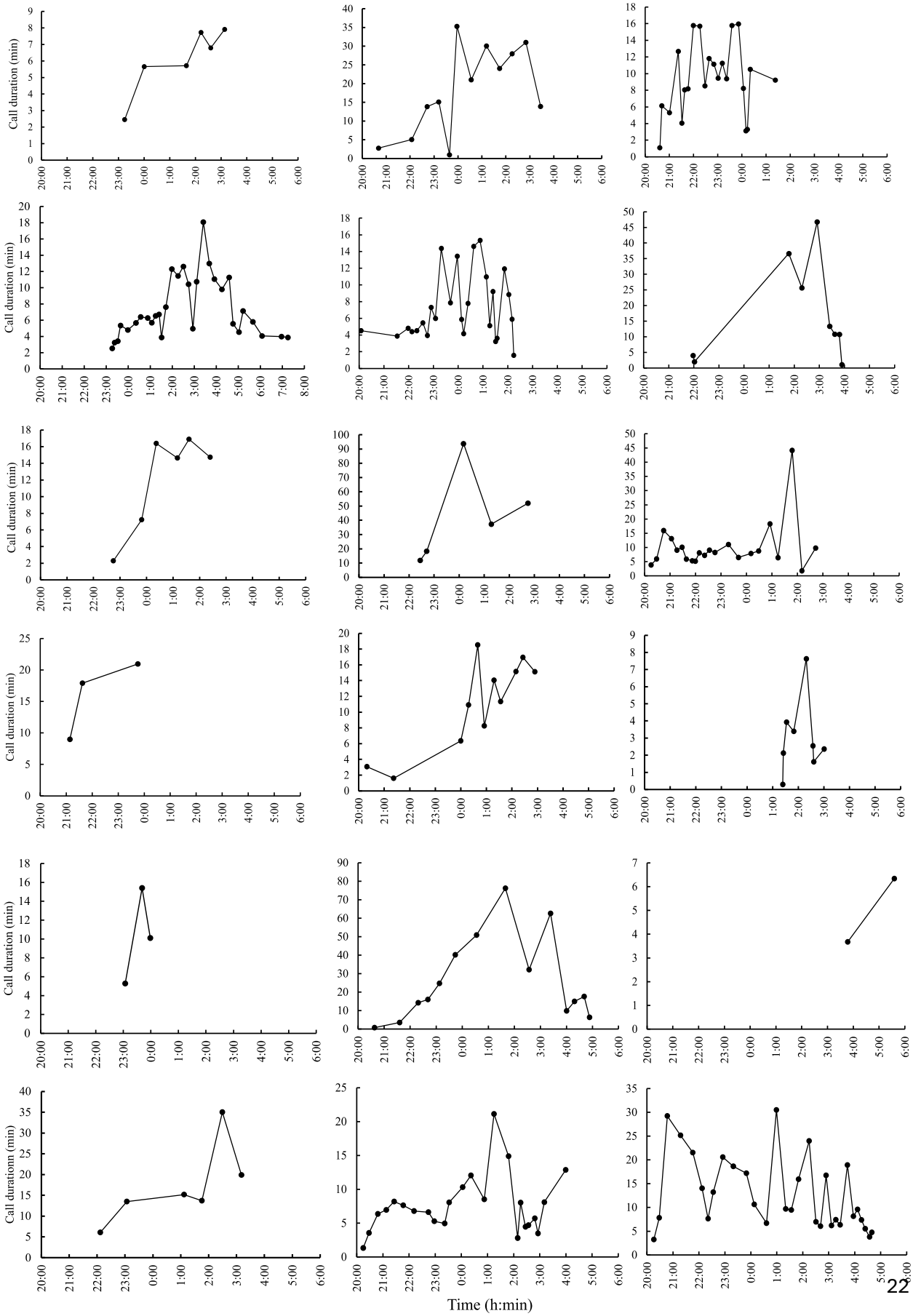
Call duration (min)
Call durationn (min)
Time (h:min)

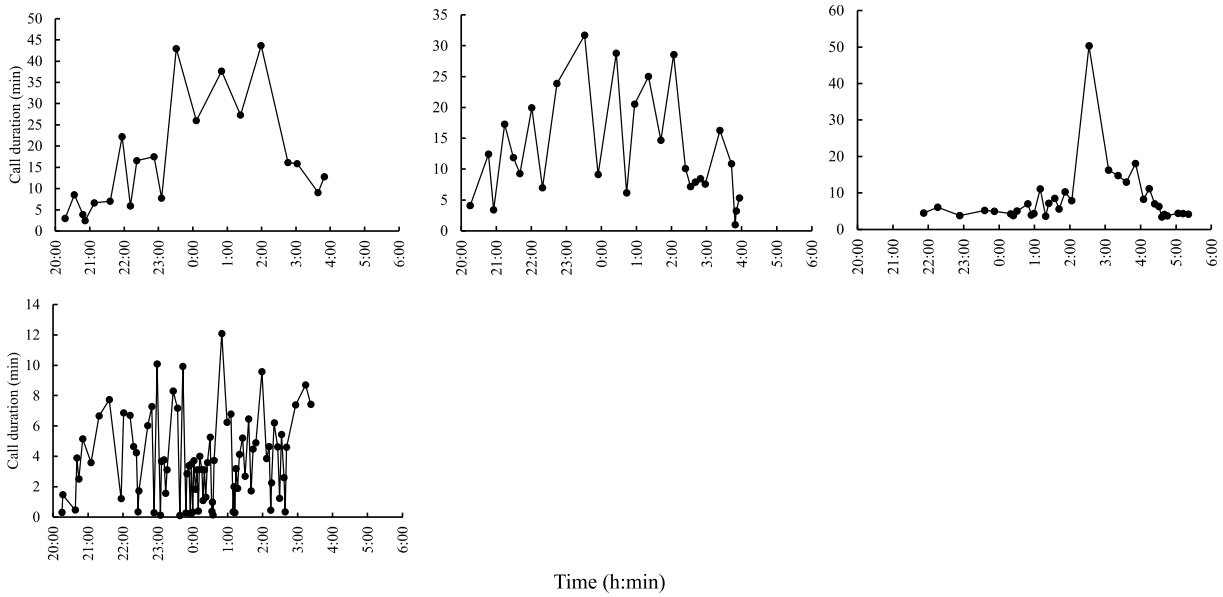

Figure S3. Call duration versus time for all 22 individuals.

Chapter 2: Finite element models suggest a mechanism by which the swim bladder helps resolve the 180-degree ambiguity in directional hearing in the plainfin midshipman fish

Abstract

Fish auditory systems primarily detect the particle motion aspect of sound, which theoretically introduces a 180-degree ambiguity in determining sound direction due to the back-and-forth nature of particle motion along a line. Despite this, directional hearing has been demonstrated in several fish species. It is hypothesized that acoustic pressure detection, facilitated by a gas-filled swim bladder scattering sound towards the inner ears, helps resolve this ambiguity. However, the impact of the swim bladder on the motion of otoliths, which activate auditory receptors (hair cells), remains poorly understood. In this study, we used the finite element method to model the effects of the swim bladder on otolith motion in response to plane wave sounds from different directions in the horizontal and vertical planes in female and type I male plainfin midshipman (*Porichthys notatus*). Our results showed that the swim bladder amplified otolith displacement and acceleration, consistent with previous studies showing the swim bladder improves auditory sensitivity. At frequencies at or below the fundamental frequency of midshipman mating vocalizations (≤ 100 Hz), the swim bladder caused the otoliths to move along elliptical orbits with opposite handedness for opposite sound directions, potentially resolving the 180-degree ambiguity. Moreover, the otoliths exhibited distinct elliptical orbits for non-opposite incident sound directions at these frequencies. At higher frequencies (200–1000 Hz), otolith motion was similar across all directions in the presence of the swim bladder. In contrast, without the swim bladder, otoliths moved back and forth in the direction of the incident sound, nearly identically for opposite sound directions at all tested frequencies (10–1000 Hz), while exhibiting different linear motions for non-opposite sound directions. These findings suggest that the swim bladder enhances directional hearing at the vocalization frequencies of the midshipman, though it may hinder directional hearing at higher frequencies. Our finite element models indicate that the swim bladder is a crucial contributor to directional hearing at behaviorally relevant frequencies in the plainfin midshipman and possibly in other fish species with swim bladders. The predictions of our model could be experimentally tested using recently developed techniques such as X-ray tomography and optical vibrometry.

Introduction

The ability to determine the direction of sounds is crucial for the survival and reproduction of many organisms. For example, animals use directional hearing to locate prey (Carr and Christensen-Dalsgaard, 2015) and find potential mates (Gerhardt et al., 2023). Sound is a mechanical disturbance that propagates as a longitudinal wave through a medium, causing local pressure fluctuations (acoustic pressure) and oscillations of particles (particle motion) (Kinsler et al., 1951). Terrestrial vertebrates utilize binaural acoustic pressure cues, such as interaural time difference (ITD) and interaural level difference (ILD), to determine sound direction (Carr and Christensen-Dalsgaard, 2016). However, in ray-finned fishes, these acoustic pressure cues are not thought to play a significant role in directional hearing. Instead, it is proposed that these fishes primarily rely on particle motion cues for directional hearing and sound source localization (Sisneros and Rogers, 2016).

Particle motion provides information about the direction of the sound source. Many natural sound sources function as monopoles, where acoustic particle motion occurs back and forth along an axis pointing towards the source (Sisneros and Rogers, 2016). Thus, by determining the direction of particle motion, the line along which the source is located can be determined, but within the line, there is a 180-degree ambiguity in determining sound direction. Despite this ambiguity, directional hearing has been demonstrated in several fish species. Fishes exhibit phonotaxis towards attractive sounds (Popper et al., 1973; Rollo et al., 2007; Winn, 1972; Zeddies et al., 2010), and conditioning experiments have shown that some fish species can discriminate between sound sources placed in different positions in the vertical and horizontal planes (Hawkins and Sand, 1977). This raises the question of how fish auditory systems resolve the 180-degree ambiguity to accurately determine sound direction.

The peripheral auditory system of ray-finned fishes appears to be adapted to detect the direction of particle motion. It includes six otolith end organs, with pairs of utricles, saccules, and lagenae on either side of the brain (Retzius, 1881). Each end organ contains an endolymph-filled sac with a calcareous otolith and the macula, which houses hair cells (Popper, 2017). Relative motion between the otoliths and hair cells causes shearing of the hair cells, (De Vries, 1950) altering their potential based on the direction of the force relative to the cell orientation (Flock and Wersäll, 1962). This changes the firing rates in the afferent fibers synapsing with the hair cells, sending auditory information to the brain via the VIIIth cranial nerve (Popper and Saidel, 1990; Walton et al., 2017). Since the acoustic properties of fish tissues are similar to those of water, the direction of particle motion is thought not to change as sound enters the fish bodies and propagates toward the inner ears. Particle motion at the otoliths will cause relative motion between the otoliths and hair cells, as otoliths are approximately three times denser than fish tissue, thereby activating hair cell fields (Sisneros and Rogers, 2016). Hair cell orientations vary within and across otolith end organs (For example, see 17,18). Different directions of particle motion will cause different hair cell activation patterns, likely allowing the auditory system to determine the direction of particle motion. However, it remains unclear if otolith movement and hair-cell activation patterns differ for opposite sound directions, potentially resolving the 180-degree ambiguity.

Gas-filled swim bladders, present in many ray-finned fishes, have been proposed to play an important role in resolving the 180-degree ambiguity problem in fish directional hearing (Schuijf, 1976). When sound waves strike the swim bladder, it expands and contracts due to changes in acoustic pressure, generating particle motion. Consequently, the otolith end organs are stimulated by both direct particle motion from the sound source and particle motion generated by the swim bladder (Van Bergeijk, 1964). The swim bladder is known to improve auditory sensitivity in several fish species (Colleye et al., 2019; Sand and Enger, 1973; Schulz-Mirbach et al., 2012), likely due to the swim bladder-generated particle motion amplifying otolith motion (Li et al., 2024; Salas et al., 2019). The phase model of directional hearing proposes that the auditory system computes the phase relationship between acoustic pressure and particle motion to resolve the 180-degree ambiguity. Proponents of this model suggest that the particle motion generated by the swim bladder due to acoustic pressure can inform the auditory system about acoustic pressure, theoretically helping the auditory system resolve the 180-degree ambiguity (Schuijf, 1976).

An important requirement for the phase model is that the swim bladder-generated component causes the otoliths to move differently for opposite sound directions, but whether this occurs is unknown. To test this, the motion of the otoliths needs to be computed for opposite sound directions. However, otolith motion is challenging to visualize. Recent developments have allowed otolith motion due to sounds to be visualized using synchrotron radiation-based tomography (Maiditsch et al., 2022; Schulz-Mirbach et al., 2020). However, in this setup, the sound loudness needs to be high (~150 dB re: 1µPa or more) to visualize otolith motion, which is generally higher than the sounds experienced by fishes in natural settings. Additionally, the small tank used in the setup likely causes reflections that change particle motion compared to natural settings (Rogers et al., 2016).

In this study, we use finite element modeling (FEM) with COMSOL Multiphysics (Burlington, MA, USA) to model how gas-filled swim bladders affect otolith motion for plane wave sounds varying in frequency and direction. We perform these simulations in the plainfin midshipman (*Porichthys notatus*), an acoustically communicating toadfish in which females locate the nests of calling males by listening to their mating calls (McKibben and Bass, 2001; Zeddies et al., 2010), making directional hearing and sound source localization ecologically important. Simulations were conducted for a female midshipman, whose swim bladder has two horns projecting close to the otoliths, and a reproductive type I male, whose swim bladder is heart-shaped with shorter horns located further from the otoliths (Mohr et al., 2017). Like previous modeling studies on the mechanics of the fish auditory system (Li et al., 2024; Salas et al., 2019; Schellart and De Munck, 1987), we assume the acoustic properties of fish tissue to be similar to water, with the swim bladder and otoliths being the only structures in the fish body with acoustic properties different from water. We predict that swim bladder-generated sound will increase otolith displacement and acceleration amplitudes, aligning with auditory evoked potential (AEP) measurements showing increased peripheral auditory sensitivity in the

plainfin midshipman (Colleye et al., 2019; Rogers et al., 2023; Vetter and Sisneros, 2020). Additionally, we predict that the swim bladder's presence will cause differential otolith motion for opposite directions, potentially resolving the 180-degree ambiguity.

Methods

CT scanning and geometry creation

In a previous study microCT scans of nine type I male plainfin midshipman and nine females were obtained (Mohr et al., 2017). For this study, we selected the CT scans of one reproductive type I male and one female. The specimens were scanned using a Skyscan 1076 microCT scanner (Bruker, Inc., USA) at 50 kV, 170 μA, with a resolution of 35.26 μm. The projection images obtained by the scanner were reconstructed into cross-sectional images using NRecon software v1.6.9.4 (Micro Photonics Inc., Allentown, PA, USA) with consistent thresholding parameters. These cross-sectional images were converted into nrrd volume data using Fiji (Schindelin et al., 2012). The otoliths and the swim bladder were segmented from the nrrd volume files using 3D Slicer (Fedorov et al., 2012). The six otoliths, being the densest structures in the fish body, are easily visible in the CT images due to their high pixel intensity. The otoliths were segmented using the “paint” and “grow from seeds” tools in 3D Slicer. The air-filled portion of the swim bladder appears as black regions in the CT images, and this space was segmented using the same tools. The swim bladder was smoothed after segmentation using the median smoothing option with a kernel size between 0.5-1 mm. Joint smoothing with the default smoothing factor of 0.5 was also applied if the swim bladder surface still possessed irregularities after median smoothing. The segmented CT scans and otoliths were saved as STL meshes.

Since the STL mesh had a coordinate system based on reference points in the microCT scanner, a local coordinate system needed to be created based on local landmarks on the otoliths to ensure that sounds could be incident on the otoliths from specific directions in later finite element simulations (see section b). To achieve this, the STL mesh was opened in Meshlab (Cignoni et al., 2008). The coordinates of the following landmarks were extracted: the centers of mass (COMs) of the six otoliths, and the dorsal and ventral tips of each otolith. The best-fit plane passing through the COMs of the utricular and lagenar otoliths was computed using custom MATLAB (MathWorks, Natick, MA, USA) code and chosen as the horizontal plane. The coordinates of the midpoint of the line segment connecting the COMs of the utricular otoliths (MUO) and the midpoint of the line segment connecting the COMs of the lagenar otoliths (MLO) were also computed using custom MATLAB scripts. The plane perpendicular to the horizontal plane and passing through the line segment connecting MUO and MLO formed the vertical (midsagittal) plane. The center of the line segment connecting MUO and MLO was the origin of the new coordinate system. The y-axis passed through the line segment containing MUO and MLO and pointed in the rostral direction, the x-axis pointed to the right, and the z-axis pointed in the dorsal direction. A matrix containing the desired coordinates of the landmarks on the otoliths in the new otolith-centered coordinate system was created. A MATLAB script was used to generate the seven Helmert parameters required to compute the transformation matrix to change the coordinate system of the STL mesh to the otolith-centered system (Wasmeier, 2010). A modified version of a MATLAB script written by Wasmeier (2010) was used to transform the STL mesh using the seven Helmert parameters (Fig. S1).

The swim bladder wall is not distinctly visible in the CT images. Since the thickness of the swim bladder wall in the plainfin midshipman is unknown, it was approximated based on the thickness of the swim bladder wall in the oyster toadfish (*Opsanus tau*), which is 824.5 μm (Fine et al., 2016; Rogers et al., 2023). The Offset tool in Meshmixer (Schmidt and Singh, 2010) was used to add this thickness to the swim bladder. STL files were generated for the swim bladders of both the female and type I male. For both the female and type I male, two 3D models of the swim bladder were generated: one with a bladder wall and another where the swim bladder was modeled as an air-filled bubble without a wall.

To reduce the number of mesh elements for subsequent finite element (FE) simulations on COMSOL while still maintaining high-quality elements with high isotropy (Bern and Eppstein, 1995), we remeshed the STL

files of the otoliths and swim bladder using Instant Meshes (Jakob et al., 2015) (Fig. 1a,b). The coordinates of the COM of each otolith were extracted from the isotropic meshes using Meshlab (Fig. 1c). The coordinates of the points on the surface of the otoliths lying on the tips of the rostrocaudal (RC), mediolateral (ML), and dorsoventral (DV) axes (henceforth termed as axis tip points) were manually estimated by carefully viewing the otoliths in Meshlab (Fig. 1d). The coordinates of the tips of the swim bladders were also estimated in Meshlab (Fig. S2).

Finite Element simulations on COMSOL

The isotropic STL meshes were exported into COMSOL Multiphysics (v5.1.0.234) and converted into a geometry. This geometry was enclosed by a water sphere with a radius of 500 mm. The volume of the sphere was approximately 8.8×10^5 times the volume of the female's swim bladder and approximately 9.7×10^5 times the volume of the type I male's swim bladder. The origin of the geometry was located at the center of the sphere. The water sphere was given the default acoustic properties of water (compressional wave speed of sound (c_p) = 1481 ms^{-1}, density = 1000 kgm^{-3}). The otoliths were assigned the compressional and shear wave speeds (c_s) of bone, c_p = 3000 ms^{-1} and c_s = 1400 ms^{-1}, as used in a previous study on how the swim bladder affects otolith motion (Salas et al., 2019). The utricular and saccular otoliths in ray-finned fishes are primarily composed of aragonite, and the lagenar otoliths are primarily composed of vaterite (Oliveira et al., 1996). The density of the utricular and saccular otoliths was set to the density of aragonite, 2930 kgm^{-3}, and the density of the lagenar otoliths was set to the density of vaterite, 2540 kgm^{-3} (Li et al., 2024; Tomás and Geffen, 2003). The swim bladder wall was assumed to possess the density of water (1000 kgm^{-3}). The Young's modulus (E) of the plainfin midshipman's swim bladder has not been measured; however, it was assumed to be similar to that of the closely related oyster toadfish (1 MPa) (Fine et al., 2016). The Poisson's ratio (v) of soft biological tissues is generally assumed to be very close to 0.5 (Fung, 2013). A value of 0.4999 was used for the Poisson's ratio of the swim bladder. c_p and c_s of the swim bladder were computed from the Young's modulus (E) and Poisson's ratio (v) using the following formulae (Craig Jr and Taleff, 2020):

$$c_p = \sqrt{\frac{E\,(1-v)}{\rho\,(1+v)\,(1-2v)}} \quad (1)$$

$$c_s = \sqrt{\frac{E}{2\rho\,(1+v)}} \quad (2)$$

Where ρ is the density of the swim bladder wall. c_p and c_s computed using equations 1 and 2 respectively, were 1291.2 ms^{-1} and 18.258 ms^{-1}. In equation 1, the value of c_p is sensitive to the value of the Poisson's ratio (v). Since the speed of sound (c_s) in fish tissue is thought to be very similar to water (1481 ms^{-1}) (Rogers and Cox, 1988), a value of 0.4999 was chosen for v, as this value led to a c_s closer to water (1291.2 ms^{-1}) compared to v values of 0.49, 0.499, and 0.49999. The air bubble part of the swim bladder was given the default acoustic properties of air (c_p = 343.2 ms^{-1}, density = 1.2 kgm^{-3}). Shear viscosity of fish tissue is an important factor determining the target strength (TS) of fishes with a swim bladder in fisheries acoustics (Khodabandeloo et al., 2021a). TS is a measure for the amount of acoustic backscatter from an acoustic target. Therefore, the swim bladder was assigned the value for shear viscosity of fish tissue (2 Pa·s) (Khodabandeloo et al., 2021b). Thus, the acoustic properties of fish tissues other than the otoliths and swim bladder were assumed to be the same as water (Tavolga, 1971).

For both the type I male and female, three geometries were created in COMSOL. In one geometry, the swim bladder had a wall; in another, the swim bladder was modeled as a bladder-shaped air bubble (henceforth called "air-bubble swim-bladder"; and in the third, the swim bladder was absent (Fig. 1e). The geometries were meshed using tetrahedral elements (Fig. 1f). The minimum element size was chosen to be 0.1 mm to ensure that the lagenar otoliths, the smallest structures in the geometry, had sufficient detail. Care was taken to ensure that the maximum mesh size was smaller than 1/5th of the wavelengths of the incident sounds in the simulations to accurately model the sound waves in the finite element simulations.

The number of mesh elements ranged from approximately 70,000 to 250,000. Generally, geometries containing the swim bladder wall had the maximum number of elements, while those lacking a swim bladder had the minimum number of elements.

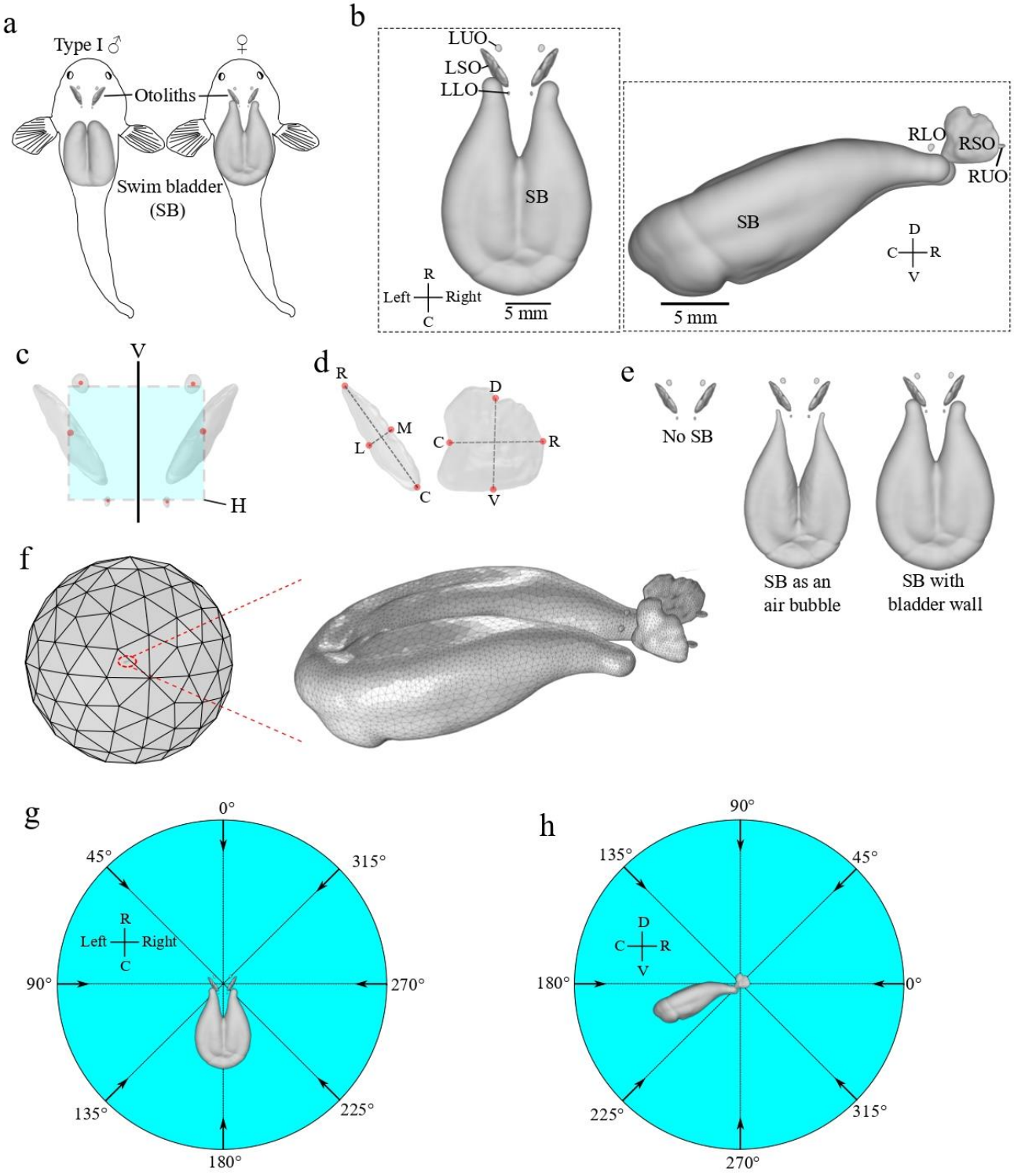

Figure 1. Finite element simulations on COMSOL Multiphysics. (a) Cartoons of the approximate locations of the swim bladder and otoliths in a type I male (left) and female (right) plainfin midshipman (Porichthys

notatus). (b) Left: Dorsal view of the 3D model of the swim bladder and otoliths of a female plainfin midshipman created by segmenting a CT scan. Right: Lateral view of the same 3D model. LUO, LSO, and LLO stand for left utricular otolith, left saccular otolith, and left lagenar otolith, respectively. RUO, RSO, and RLO stand for right utricular otolith, right saccular otolith, and right lagenar otolith, respectively. (c) Red dots represent the center of mass (COM) of each otolith. The best fit plane through the COMs of the utricular and lagenar otoliths was chosen to be the horizontal plane (H). The midsagittal (vertical, V) plane was the plane perpendicular to the horizontal plane and passed through the midpoints of the line segments connecting the COMs of the lagenar otoliths and the utricular otoliths. (d) Points at the ends of the rostrocaudal (RC), dorsoventral (DV), and mediolateral (ML) axes were manually selected. The change in coordinates of these points was used to later compute the angular motion of the otoliths. (e) Three geometries were generated: one containing the otoliths, another in which the swim bladder was composed of air and did not possess a bladder wall (air bubble swim bladder), and a third geometry containing the otoliths and a swim bladder with a bladder wall. (f) The otolith-swim bladder system was enclosed in a water sphere (r = 500 mm). The swim bladder-otolith-water sphere geometry was meshed in COMSOL using tetrahedral elements. In the finite element (FE) simulations, sounds were incident on the otoliths and/or swim bladder from different directions in (g) the horizontal plane and (h) the vertical (midsagittal) plane.

Frequency domain simulations of the swim bladder-otolith-water system were conducted. The regions of the geometry containing fluids (water sphere and the air bubble inside the swim bladder) were modeled using the Pressure Acoustics, Frequency Domain physics interface, which solves the Helmholtz equation for acoustic pressure. The regions of the geometry containing solids (otoliths and the swim bladder wall) were modeled using the Solid Mechanics physics interface. This interface solves the Navier-Cauchy equation in the frequency domain to compute movements inside elastic solids in response to external forces, internal stresses, or both. A spherical wave radiation condition was applied to the boundary of the water sphere, allowing outgoing spherical waves to leave the geometry without reflections, simulating a situation where the fish is in a large body of water with no reflecting surfaces around it.

In one set of simulations, the displacement and acceleration amplitudes of the COM of each otolith were computed for frequencies ranging from 8 Hz, then 10 Hz to 2000 Hz in steps of 10 Hz. The incident sound direction was directly in front of the animal. These simulations were conducted to determine if the presence of the swim bladder amplifies the motion of the otoliths. In another set of simulations, sounds were incident on the swim bladder and otoliths from multiple directions in the horizontal plane (Fig. 1g). Simulations were also conducted with sounds incident from different directions in the vertical plane (Fig. 1h). For both sets of simulations, the amplitude of displacement of the COMs of each otolith and the phase of displacement relative to the phase of the input pressure stimulus in the left to right direction (along the x-axis), caudal to rostral direction (along the y-axis), and ventral to dorsal direction (along the z-axis) were extracted. This information was used to compute the trajectory of the COMs of the otoliths along the x, y, and z for one time period (T) using the following Lissajous equations:

$$u = A_x \cdot \sin(2\pi f \cdot t + \Phi_x) \quad (3)$$

$$v = A_y \cdot \sin(2\pi f \cdot t + \Phi_y) \quad (4)$$

$$w = A_z \cdot \sin(2\pi f \cdot t + \Phi_z) \quad (5)$$

Where u, v, and w represent displacement in the x, y, and z directions respectively. A_x, A_y, and A_z are the amplitudes of displacement in the x, y, and z directions respectively, and Φ_x ,Φ_y , and Φ_z are the phases of displacement in the x, y, and z directions. The time t ranges from 0 to 1/f s (or one time period, T s), where f is the frequency of incident sound. Custom MATLAB scripts were written to plot the trajectory of the COM of the otoliths in the horizontal plane (by plotting u, and v), and the midsagittal (vertical) plane by plotting v and w. Vector plots were utilized to represent the direction of motion in each time step. The trajectories of motion of the tips of the swim bladders, and the axis tip points of the otoliths were also extracted similarly. The trajectories of the axis tip points were used to compute the angles made by the three axes of the otoliths (rostrocaudal, mediolateral, and dorsoventral) with the horizontal and vertical planes. These simulations

were conducted for multiple sound frequencies ranging from 10 to 1000 Hz. In all the above simulations, incident sound was applied as a plane wave pressure field with a peak pressure amplitude of 130 dB re: 1 µPa, which is similar to the loudness of the sound experienced by female plainfin midshipman in the sound source localization experiments performed by Zeddies et al., (2010).

A set of simulations was also conducted to examine how changing the phase relationship between pressure and the particle motion aspect of sound affects otolith motion. In one case, an incident sound arrived from the right of the swim bladder-otolith system (270° incident direction, fig. 1g), with a peak pressure amplitude of 3.16 Pa (130 dB re: 1 µPa). In a second simulation, three incident sounds arrived at the swim bladder and otoliths: one from the left with a peak pressure amplitude of 3.16 Pa, and two from the dorsal and ventral directions with inverted peak pressure amplitudes of -3.16 Pa. These sounds shifted the pressure at the geometry by 180 degrees to -3.16 Pa but did not affect the particle motion of the sound coming from the left. The frequency of the incident sound for both these simulations was 100 Hz. The amplitudes and phases of the displacement of the COMs along the left to right (x), caudal to rostral (y), and ventral to dorsal (z) directions were extracted.

Results

Effect of the swim bladder on the amplitude of motion of the otoliths

When sound was incident from the front of the animal, the presence of the swim bladder increased the displacement and acceleration amplitudes of the otoliths. In finite element (FE) simulations, the displacement amplitude of the center of mass (COM) of the right saccular otolith (RSO) was greater when a swim bladder with a bladder wall or an air bubble swim bladder was present, compared to simulations lacking a swim bladder, for the female across frequencies ranging from 8 to 2000 Hz (Fig. 2a). Similarly, the presence of a swim bladder also increased the acceleration of the COM of the RSO at these frequencies (Fig. 2b). There were peaks in displacement and acceleration at 600 Hz for the air bubble swim bladder. The presence of the swim bladder also increased the displacement (Fig. S3) and acceleration (Fig. S4) of other otoliths in the female, with similar results for the reproductive type I male (Fig. S5, S6). Thus, the swim bladder increased the displacement and acceleration of the otoliths.

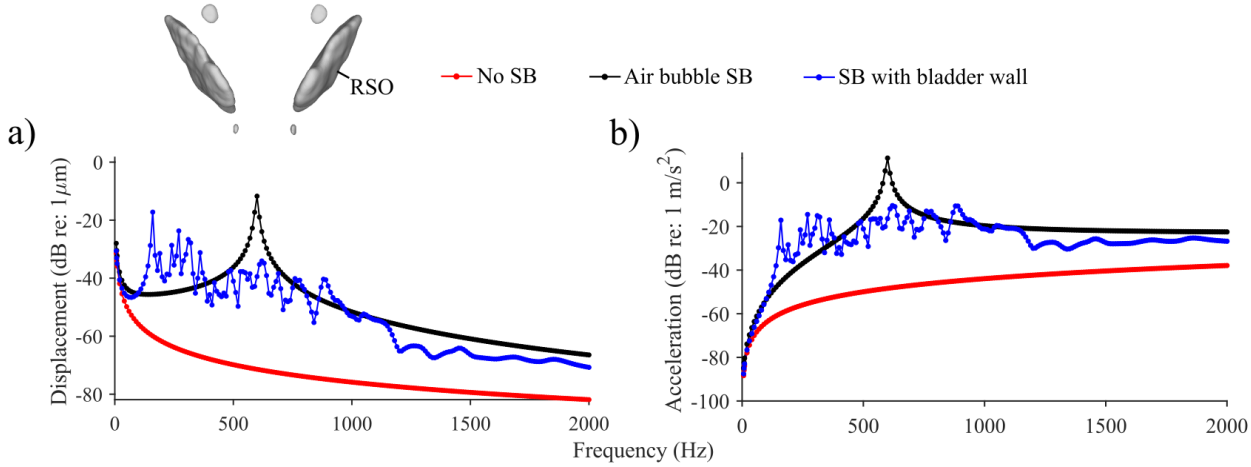

Figure 1. (a) Displacement and (b) acceleration amplitudes of the center of mass (COM) of the right saccular otolith (RSO) when sounds were incident from the front of the animal for the female midshipman (0°).

Motion of the otoliths in the absence of the swim bladder

Fish hearing is generally most sensitive to frequencies below 1000 Hz (Ladich and Fay 2013). To better understand how the swim bladder affects otolith motion at behaviorally relevant frequencies, finite element

simulations were first conducted at 100 Hz - near the fundamental frequency of the midshipman's hum (Balebail and Sisneros, 2022; Brantley and Bass, 1994) and at 1000 Hz, which is close to the upper hearing limit of the midshipman. These simulations were performed both in the presence and absence of the swim bladder. If otolith motion differed at these two frequencies, additional simulations were conducted at intermediate frequencies (e.g., 50 Hz and 200 Hz) to explore any frequency-dependent trends in otolith movement in response to sounds from different directions. Preliminary simulations indicated no consistent differences between the motion of the left and right otoliths in response to sound. To illustrate this, the motion of the right otoliths is plotted for female midshipman and the left otoliths for type I male midshipman, with overall trends being consistent across the right otoliths of females and the left otoliths of type I males (Fig. 3-6, S7-23).

In the absence of the swim bladder, when the motion of the COMs of the right otoliths (RUO, RSO, and RLO) were projected onto the horizontal plane, the COMs moved back and forth along a straight line at 100 and 1000 Hz, when sounds were incident from various directions in the horizontal plane for the female midshipman (Fig. 3). The trajectories of the COMs of the otoliths differed for non-opposite sound directions (e.g., 0° and 45°) but were almost identical for opposite directions (e.g., 0° and 180°). Similar trends were observed at 100 and 1000 Hz for the left otoliths of the type I male (Fig. S7). When sounds were incident from different directions on the horizontal plane, the projections of the motion of the COMs of the right otoliths onto the vertical (midsagittal) plane moved along the same line for all incident sound directions at 100 and 1000 Hz for the female (Fig. S8).

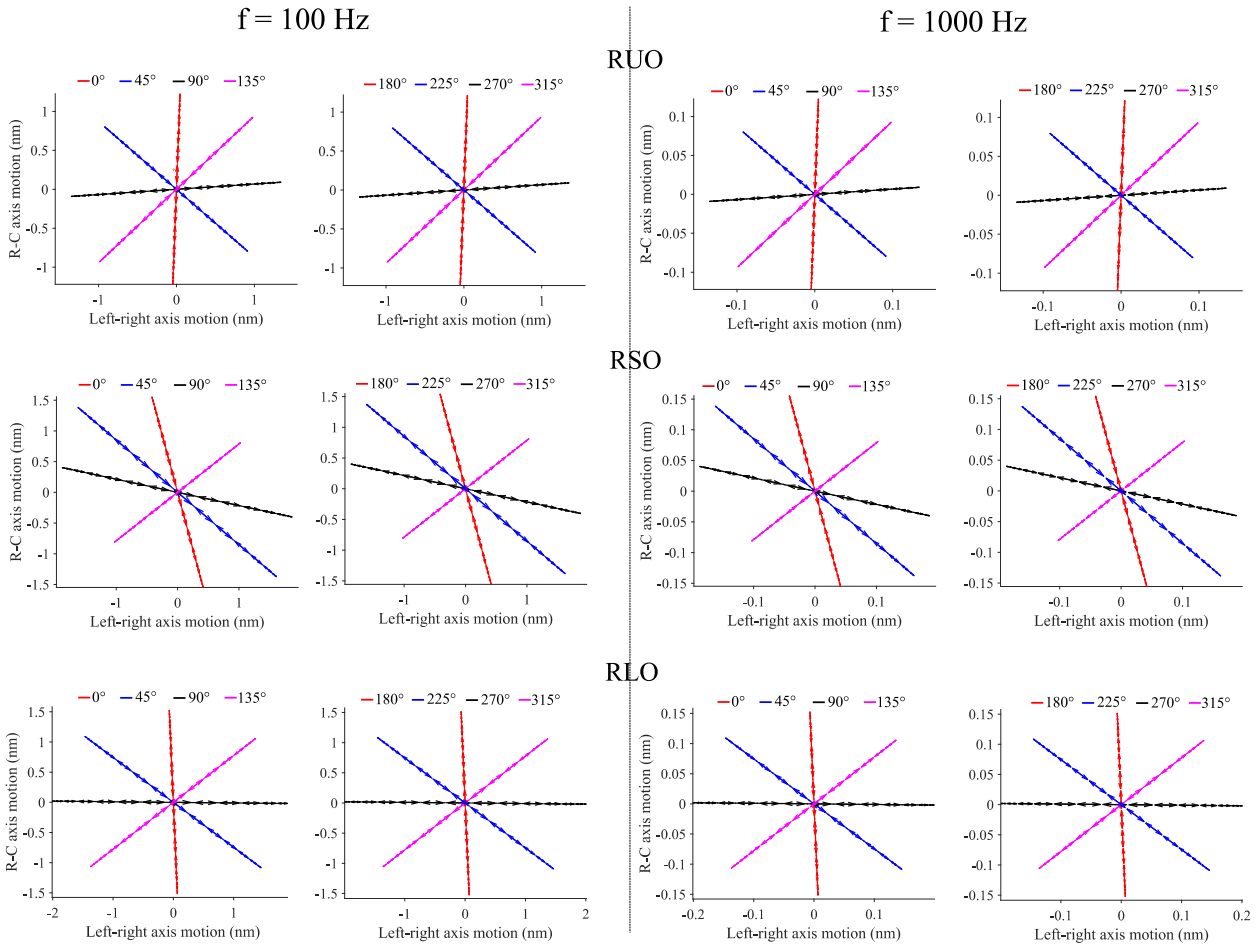

Figure 2. Projection of the motion of the COM of the right otoliths onto the horizontal plane when sounds were incident from various directions in the horizontal plane (0-315°) in the simulations without a swim bladder for the female midshipman for frequencies 100 and 1000 Hz.

In the absence of the swim bladder, the motion of the COMs of the right otoliths, when projected onto the vertical plane, moved back and forth along a line at frequencies of 100 and 1000 Hz. This occurred when sounds were incident from various directions in the vertical plane for the female (Fig. S9). Similarly, for the type I male, the vertical projection of the COMs of the left otoliths also moved back and forth along a line when sounds were incident from multiple directions in the vertical plane (Fig. S10). Consistent with the results for sounds incident in the horizontal plane, the COMs of the otoliths followed different paths for non-opposite sound directions but identical paths for opposite sound directions. For the female, when the motion of the COMs of the right otoliths was projected onto the horizontal plane, they moved back and forth along the same line when sounds were incident from different directions in the vertical plane (Fig. S11).

Motion of the otoliths in the presence of the swim bladder with a wall

For the female, in the simulations containing a swim bladder with a wall, when the motion of the COMs of the right otoliths was projected onto the horizontal plane, the COMs moved along elliptical orbits when sounds were incident from multiple directions in the horizontal plane for frequencies 50 Hz, 100 Hz, 200 Hz, and 1000 Hz (Fig. 4). At 50 and 100 Hz, when sounds were incident from opposite directions, the COMs of the right otoliths moved along the same elliptical orbits but with opposite handedness of rotation (clockwise vs anticlockwise). At frequencies 200 Hz and 1000 Hz, the trajectories of the COM of the otoliths were similar for different incident sound directions, with the trajectories of the COMs generally being more similar for different directions at 1000 Hz compared to 200 Hz (Fig. 4). In general, the trajectories of the

COMs of the right otoliths were more different for different directions at 50 Hz, compared to 100 Hz, and very similar for different directions at 200 and 1000 Hz. Compared to the RUO and RSO, the COM of the RLO had more similar trajectories of motion for different incident sound directions at 100 Hz. Similar results were observed for the left otoliths for the type I male, when sounds were incident from different directions in the horizontal plane, for frequencies 100 and 1000 Hz (Fig. S12). The component of motion of the COMs of the left otoliths (LUO, LSO, and LLO) in the horizontal plane also followed the same elliptical orbits for opposite directions at 100 Hz, but with opposite handedness of rotation. The horizontal component of the motion trajectories of the COMs of the left otoliths was similar for all incident sound directions at 1000 Hz. At 100 Hz, the trajectories differed for non-opposite sound directions (like 0° and 90°).

RUO

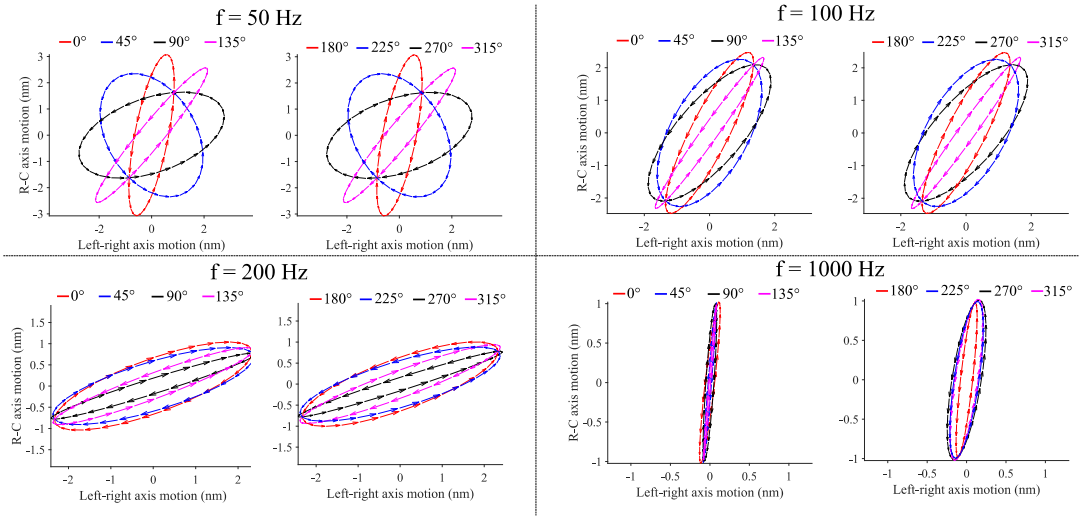
f = 50 Hz
f = 100 Hz
f = 200 Hz
f = 1000 Hz
0° 45° 90° 135°
180° 225° 270° 315°
R-C axis motion (nm)
Left-right axis motion (nm)

RSO

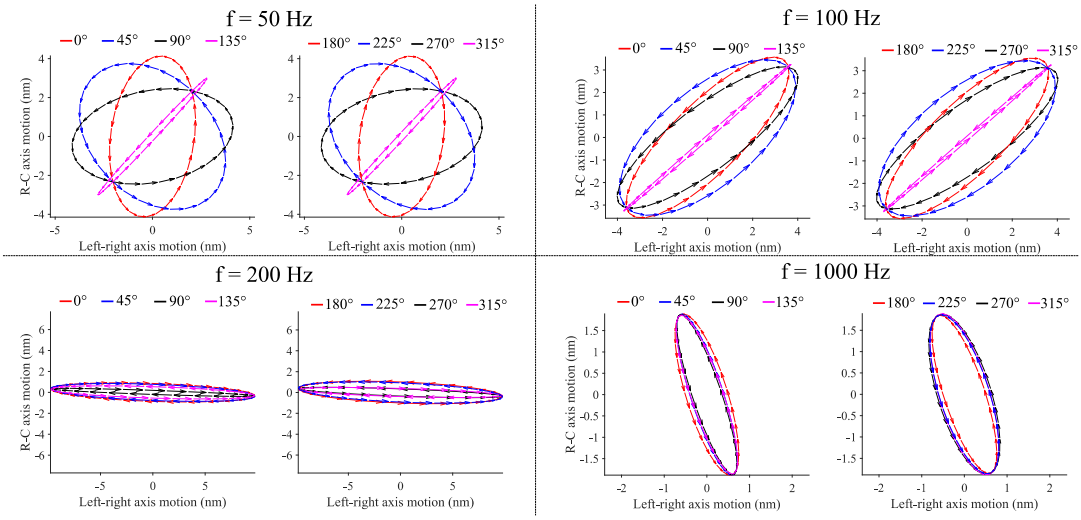
f = 50 Hz
f = 100 Hz
f = 200 Hz
f = 1000 Hz
0° 45° 90° 135°
180° 225° 270° 315°
R-C axis motion (nm)
Left-right axis motion (nm)

RLO

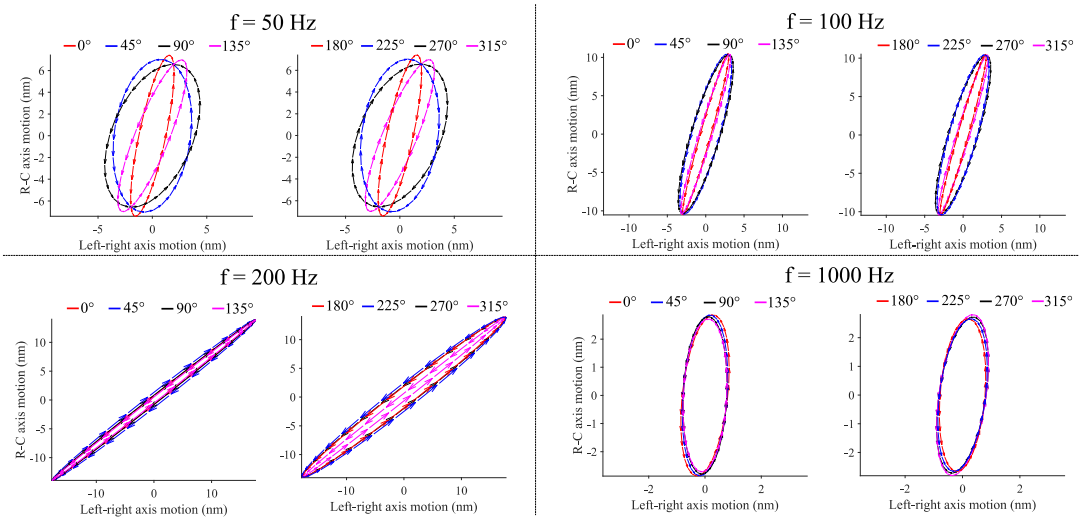
f = 50 Hz
f = 100 Hz
f = 200 Hz
f = 1000 Hz
0° 45° 90° 135°
180° 225° 270° 315°
R-C axis motion (nm)
Left-right axis motion (nm)

Figure 3. Projection of the motion of the COM of the right otoliths onto the horizontal plane when sounds were incident from various directions in the horizontal plane in the simulations containing a swim bladder with a bladder wall, for the female midshipman.

When sounds were incident in the horizontal plane, the vertical component of the motion of the COMs of the right otoliths was similar at 1000 Hz for all incident sound directions, for the female (Fig. S13). At 100 Hz however, the patterns resembled the horizontal component of otolith motion, with the vertical component of the motion trajectory of the COM following the same elliptical orbits but with opposing handedness for opposite sound directions, and the trajectories of the COMs of the RUO and RSO also following different paths for non-opposite directions.

For the female, in the simulations containing a swim bladder with a wall, the projection of motion of the COMs of the right otoliths in the vertical plane followed elliptical orbits when sounds were incident from multiple directions in the vertical plane for frequencies 50 Hz, 100 Hz, 200 Hz, and 1000 Hz (Fig. 5). At 50 and 100 Hz, when sounds were incident from opposite directions, the vertical component of the motion of the COMs of the right otoliths followed the same elliptical orbit but with opposite handedness of rotation. At frequencies 200 and 1000 Hz, the trajectories of the vertical component of motion of the COMs of the right otoliths were generally similar for different incident sound directions (Fig. 5). In general, the vertical component of the trajectories of the COMs of the right otoliths was more different for different directions at 50 Hz, compared to 100 Hz, and very similar for different directions at 200 and 1000 Hz. Compared to the RUO and the RSO, the vertical component of the trajectory of the COM of the RLO had more similarities for different incident sound directions at both 50 and 100 Hz. Similar patterns were observed for the left otoliths for the type I male for 100 and 1000 Hz, when sounds were incident from different directions along the vertical plane (Fig. S14). The vertical component of the motion of the COMs of the left otoliths followed the same elliptical orbits with opposite handedness of rotation for opposite directions at 100 Hz, and very similar trajectories for all incident sound directions at 1000 Hz. Additionally, at 100 Hz, the vertical component of the motion of the COMs of the left otoliths followed different elliptical orbits for non-opposite sound directions (like 0° and 90°).

RUO

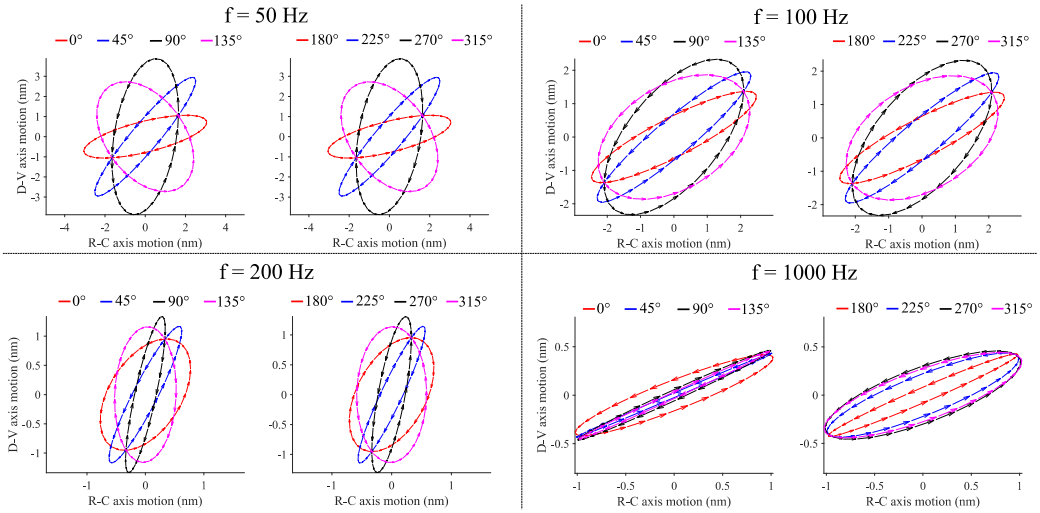
f = 50 Hz
f = 100 Hz
f = 200 Hz
f = 1000 Hz
0° 45° 90° 135° 180° 225° 270° 315°
D-V axis motion (nm)
R-C axis motion (nm)

RSO

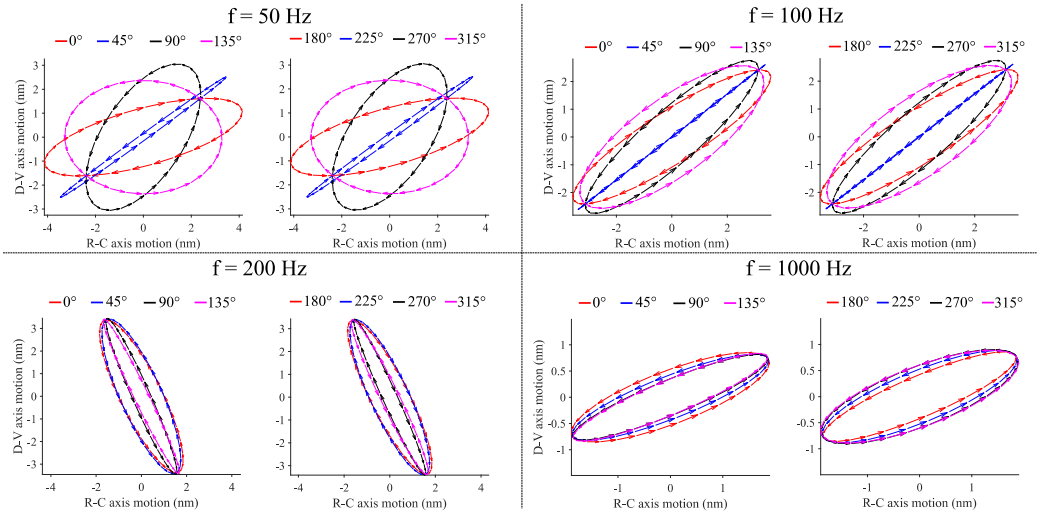
f = 50 Hz
f = 100 Hz
f = 200 Hz
f = 1000 Hz
0° 45° 90° 135° 180° 225° 270° 315°
D-V axis motion (nm)
R-C axis motion (nm)

RLO

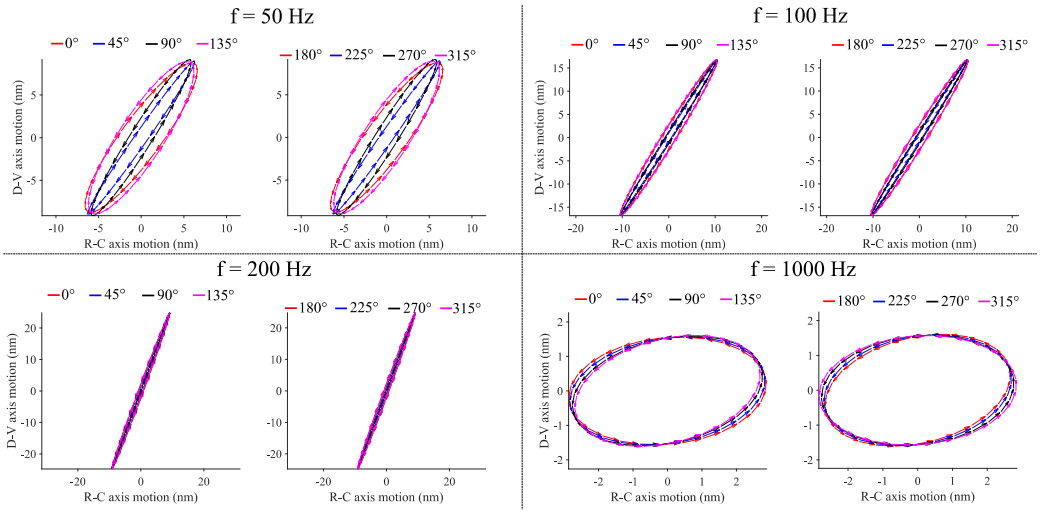
f = 50 Hz
f = 100 Hz
f = 200 Hz
f = 1000 Hz
0° 45° 90° 135° 180° 225° 270° 315°
D-V axis motion (nm)
R-C axis motion (nm)

Figure 4. Projection of the motion of the COM of the right otoliths onto the vertical plane when sounds were incident from various directions in the vertical plane in the simulations containing a swim bladder with a bladder wall, for the female midshipman.

When sounds were incident from the vertical plane, the horizontal component of the motion of the COMs of the right otoliths was similar at 1000 Hz for all incident sound directions, for the female (Fig. S15). At 100 Hz, the patterns resembled the component of otolith motion along the vertical plane, with the horizontal component of motion of the COMs of the otoliths following the same elliptical orbits with opposite handedness for opposite sound directions, and the COMs of the RUO and RSO moving along different paths for different directions.

Motion of the swim bladder

For the female, the motion of the tip of the right horn of the swim bladder is projected onto the horizontal (Fig. S16) and vertical (Fig. S17) planes for sounds incident from multiple directions in the horizontal plane, at 100 and 1000 Hz. At 100 Hz, the horizontal component of the motion of the tip of the right horn followed a similar elliptical orbit for all incident sound directions, whereas the vertical component had more differences in the motion trajectory for different incident sound directions. Additionally, for both components, the handedness of elliptical motion of the right bladder tip was opposite for opposite directions. At 1000 Hz, the tip of the right horn of the swim bladder moved similarly in the horizontal and vertical planes for different incident sound directions. For the type I male, the trajectory of motion of the tip of the left horn of the swim bladder is projected onto the horizontal (Fig. S18) and vertical (Fig. S19) planes for sounds incident from different directions in the horizontal plane at 100 Hz. The horizontal and vertical components of the motion of the tip of the left horn underwent elliptical motion with opposite handedness of rotation for opposite sound directions, with different elliptical orbits for non-opposite sound directions.

When sounds were incident from different directions in the vertical plane, the horizontal component of the motion of the tip of the right horn of the swim bladder of the female followed similar elliptical orbits for all incident sound directions at 100 and 1000 Hz (Fig. S20). The vertical component of the motion of the right horn tip of the swim bladder tip showed more differences for different incident sound directions at 100 Hz (Fig. S21). Additionally, the handedness of the elliptical orbits were opposite for opposite directions. In contrast, at 1000 Hz, the tip of the right horn moved similarly in the vertical plane for all directions.

Motion of the otoliths in the presence of the air bubble swim bladder

The results of the simulations with the swim bladder modeled as an air bubble without a wall resembled those where the swim bladder had a wall. For the female, when the motion of the COMs of the right otoliths was projected onto the horizontal plane, the COMs traced elliptical orbits at frequencies of 100 and 1000 Hz when sounds were incident from multiple directions in the horizontal plane (Fig. S22). At 100 Hz, the COMs followed the same elliptical orbits with opposite handedness for opposite sound directions and different orbits for non-opposite directions. Among the otoliths, the COM of the RLO showed greater similarity in trajectories for non-opposite directions compared to the COMs of the RUO and RSO. At 1000 Hz, the trajectories of the COMs of all three right otoliths became similar for all directions. Similar results were observed for the left otoliths of the type I male when sounds were incident from different directions in the vertical plane at 100 and 1000 Hz (Fig. S23). The vertical component of the COMs' motion followed the same elliptical paths with opposite handedness for opposite directions. At 100 Hz, the vertical component of the right otoliths' COMs followed different elliptical paths for non-opposite directions but similar elliptical paths for opposite directions at 1000 Hz. In contrast to the simulations where the swim bladder had a wall (Fig. 4, 5, S12, S14), the handedness of the otoliths' elliptical orbits at 1000 Hz was opposite for opposite incident sound directions, even though the orbits were very similar for all directions (Fig. S22, S23).

Frequency-dependence of the trajectory of otolith motion

In the absence of the swim bladder, the COMs of the otoliths move along the same path for the same incident sound directions in a frequency-independent manner (Fig. 3, S7-S11). In the presence of the swim

bladder, however, the trajectories of the otoliths for different frequencies for the same incident sound direction are different (Fig. 4, 5, S12-22). In figure 6, horizontal projections of the trajectory of the motion of the COM of the right saccular otolith (LSO) are plotted for frequencies 10, 50, 100, 200, 500, and 1000 Hz for different incident sound directions in the horizontal plane (0°, 45°, and 90°) in the simulations lacking a swim bladder and in the simulations containing a swim bladder with a wall, for the female. The COM of the RSO moves along the same path in the horizontal plane for all frequencies, in the absence of the swim bladder, but the trajectories in the horizontal plane are different for the same incident sound directions for different frequencies in the presence of the swim bladder with a wall.

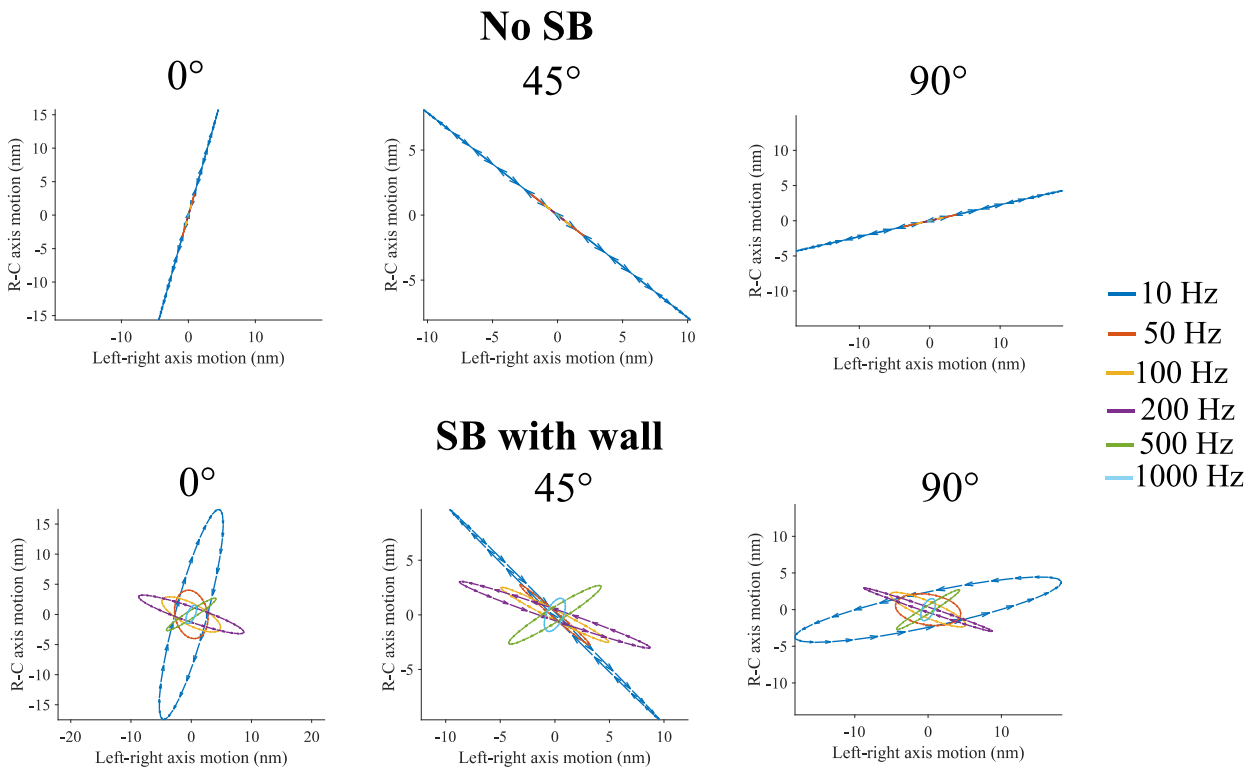

Figure 5. Horizontal projections of the trajectory of the motion of the COM of the right saccular otolith for various frequencies (10, 50, 100, 200, 500, and 1000 Hz), and incident sound directions in the horizontal plane (0°, 45°, and 90°) in the simulations lacking a swim bladder (top row) and in the simulations containing a swim bladder with a bladder wall (bottom row) for the female midshipman.

Effect of the swim bladder on the rotational motion of the otoliths

Apart from undergoing elliptical motion, the otoliths also undergo rotational motion when exposed to sound. For the female, the angle made by the rostrocaudal (RC) axis of the right saccular otolith (RSO) with the horizontal and vertical planes for two oscillation cycles at 100 Hz is plotted in fig. 7 for 0° incident sound direction. The presence of the swim bladder increased the amplitude of rotational motion of the otoliths. For 0° incident sound direction, the presence of the swim bladder (with wall) increased the peak amplitude of the angular oscillations of all the otoliths at 100 Hz (Table 1) and 1000 Hz (Table 2). The angles made by the RC, dorsoventral (DV), and mediolateral (ML) axes of the otoliths with the horizontal and vertical planes increased in the presence of the swim bladder by a factor of ~5 to 3000 at both 100 Hz and 1000 Hz. Similar results were observed when sounds were incident from 90° direction in the horizontal plane at 100 Hz (Table S1).

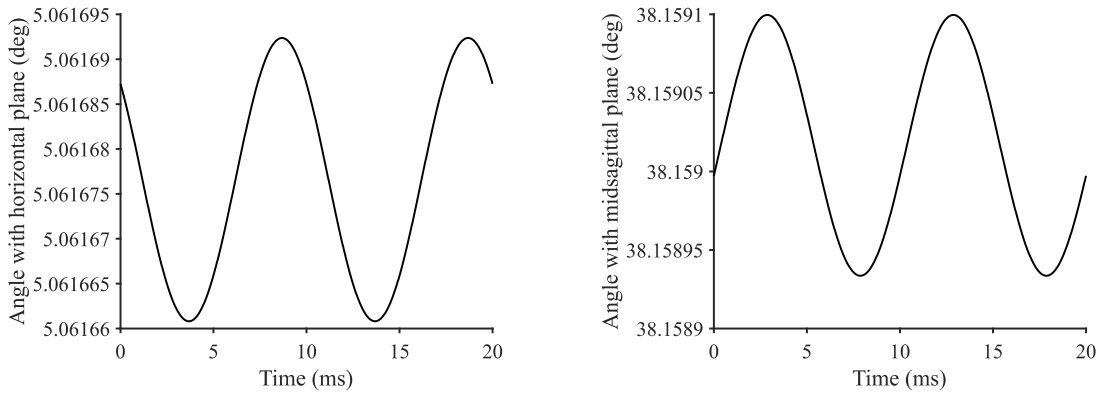

Figure 6. Angle made by the rostrocaudal (RC) axis of the right saccular otolith (RSO) with the horizontal and midsagittal (vertical) planes for two oscillation cycles at 100 Hz and 0° incident sound direction.

Otolith	Simulation type	RC (H)°	RC (V)°	DV (H)°	DV (H)°	ML (H)°	ML (V)°
LUO	SB with wall	1.1×10^{-4}	1.1×10^{-5}	3.2×10^{-4}	2.0×10^{-4}	1.9×10^{-4}	6.8×10^{-5}
LUO	No SB	8.3×10^{-6}	5.7×10^{-7}	5.9×10^{-6}	3.5×10^{-6}	3.8×10^{-6}	1.6×10^{-6}
RUO	SB with wall	1.9×10^{-4}	4.8×10^{-5}	3.6×10^{-4}	3.4×10^{-4}	2.3×10^{-4}	1.4×10^{-4}
RUO	No SB	6.3×10^{-6}	1.3×10^{-6}	8.4×10^{-6}	5.9×10^{-6}	5.4×10^{-6}	3.0×10^{-6}
LSO	SB with wall	3.6×10^{-5}	9.3×10^{-5}	1.3×10^{-4}	1.3×10^{-4}	1.1×10^{-4}	3.2×10^{-4}
LSO	No SB	2.6×10^{-7}	1.9×10^{-6}	3.8×10^{-7}	2.1×10^{-6}	2.0×10^{-6}	2.0×10^{-6}
RSO	SB with wall	1.6×10^{-5}	8.3×10^{-5}	1.3×10^{-4}	1.3×10^{-4}	3.2×10^{-5}	2.6×10^{-4}
RSO	No SB	9.7×10^{-8}	1.4×10^{-6}	1.0×10^{-6}	1.4×10^{-6}	1.4×10^{-6}	1.6×10^{-6}
LLO	SB with wall	1.9×10^{-4}	1.1×10^{-3}	5.5×10^{-4}	7.0×10^{-4}	2.3×10^{-4}	1.5×10^{-3}
LLO	No SB	3.0×10^{-6}	1.1×10^{-5}	7.9×10^{-7}	2.7×10^{-6}	3.1×10^{-6}	1.0×10^{-5}
RLO	SB with wall	2.8×10^{-4}	7.0×10^{-4}	3.4×10^{-4}	4.9×10^{-4}	6.1×10^{-4}	5.3×10^{-4}
RLO	No SB	3.3×10^{-6}	1.3×10^{-5}	4.7×10^{-6}	8.6×10^{-6}	9.2×10^{-6}	7.6×10^{-6}

Table 1. The angles made by the rostrocaudal (RC), dorsoventral (DV), and mediolateral (ML) axes of the otoliths with the horizontal (H) and vertical (V) planes in degrees at 100 Hz when the sound was incident from in front of the animal (0°).

Otolith	Simulation type	RC (H)°	RC (V)°	DV (H)°	DV (V)°	ML (H)°	ML (V)°
LUO	SB with wall	4.0×10^{-5}	4.7×10^{-6}	1.7×10^{-4}	2.1×10^{-5}	4.9×10^{-6}	6.2×10^{-5}
LUO	No SB	8.6×10^{-7}	1.4×10^{-7}	5.9×10^{-7}	3.6×10^{-7}	3.9×10^{-7}	2.0×10^{-7}
RUO	SB with wall	5.9×10^{-5}	1.0×10^{-5}	2.0×10^{-4}	2.3×10^{-5}	6.4×10^{-5}	8.5×10^{-5}
RUO	No SB	6.4×10^{-7}	1.7×10^{-7}	8.5×10^{-7}	6.0×10^{-7}	5.5×10^{-7}	3.2×10^{-7}
LSO	SB with wall	4.1×10^{-6}	2.1×10^{-5}	1.6×10^{-5}	2.8×10^{-5}	6.2×10^{-5}	1.4×10^{-4}
LSO	No SB	1.6×10^{-8}	1.2×10^{-6}	5.2×10^{-8}	2.9×10^{-7}	1.9×10^{-7}	1.3×10^{-6}
RSO	SB with wall	2.1×10^{-5}	5.9×10^{-6}	3.8×10^{-5}	3.9×10^{-5}	4.9×10^{-5}	1.8×10^{-4}
RSO	No SB	3.6×10^{-8}	1.1×10^{-6}	1.1×10^{-7}	1.5×10^{-7}	5.1×10^{-8}	1.2×10^{-6}
LLO	SB with wall	1.6×10^{-4}	1.8×10^{-4}	6.1×10^{-4}	1.8×10^{-4}	2.7×10^{-4}	2.0×10^{-4}
LLO	No SB	3.7×10^{-7}	1.3×10^{-6}	2.0×10^{-7}	2.9×10^{-7}	3.1×10^{-7}	1.0×10^{-6}

RLO	SB with wall	3.9×10^{-4}	2.2×10^{-4}	1.5×10^{-4}	1.6×10^{-4}	3.0×10^{-4}	2.9×10^{-4}
RLO	No SB	4.7×10^{-7}	1.5×10^{-6}	3.4×10^{-7}	9.7×10^{-7}	9.4×10^{-7}	7.7×10^{-7}

Table 2. The angles made by the rostrocaudal (RC), dorsoventral (DV), and mediolateral (ML) axes of the otoliths with the horizontal (H) and vertical (V) planes in degrees at 1000 Hz when the sound was incident from in front of the animal (0°).

Otolith motion in the presence of the swim bladder when the phase relationship between pressure and particle motion is inverted

Reversing the phase relationship between sound pressure and particle motion changes otolith motion such that the otoliths move as if the sound is coming from the opposite direction. In Figure 8, the horizontal component of the center of mass (COM) of the otoliths is plotted for a sound at 100 Hz incident from the right of the animal for the female. The same horizontal component is also plotted for a sound incident at 100 Hz coming from the left, but with the phase relationship between sound pressure and particle motion inverted by playing sounds at the same frequency and pressure amplitude (3.16 Pa) in the dorsal and ventral directions, with the phase of pressure reversed by 180° for both sounds incident on the vertical (z) axis. For both simulations, with sound from the right and sound from the left (pressure phase inverted), the swim bladder had a wall. The motion of the horizontal component of the COMs of all the otoliths followed the same elliptical orbits with the same handedness for both incident sound stimuli.

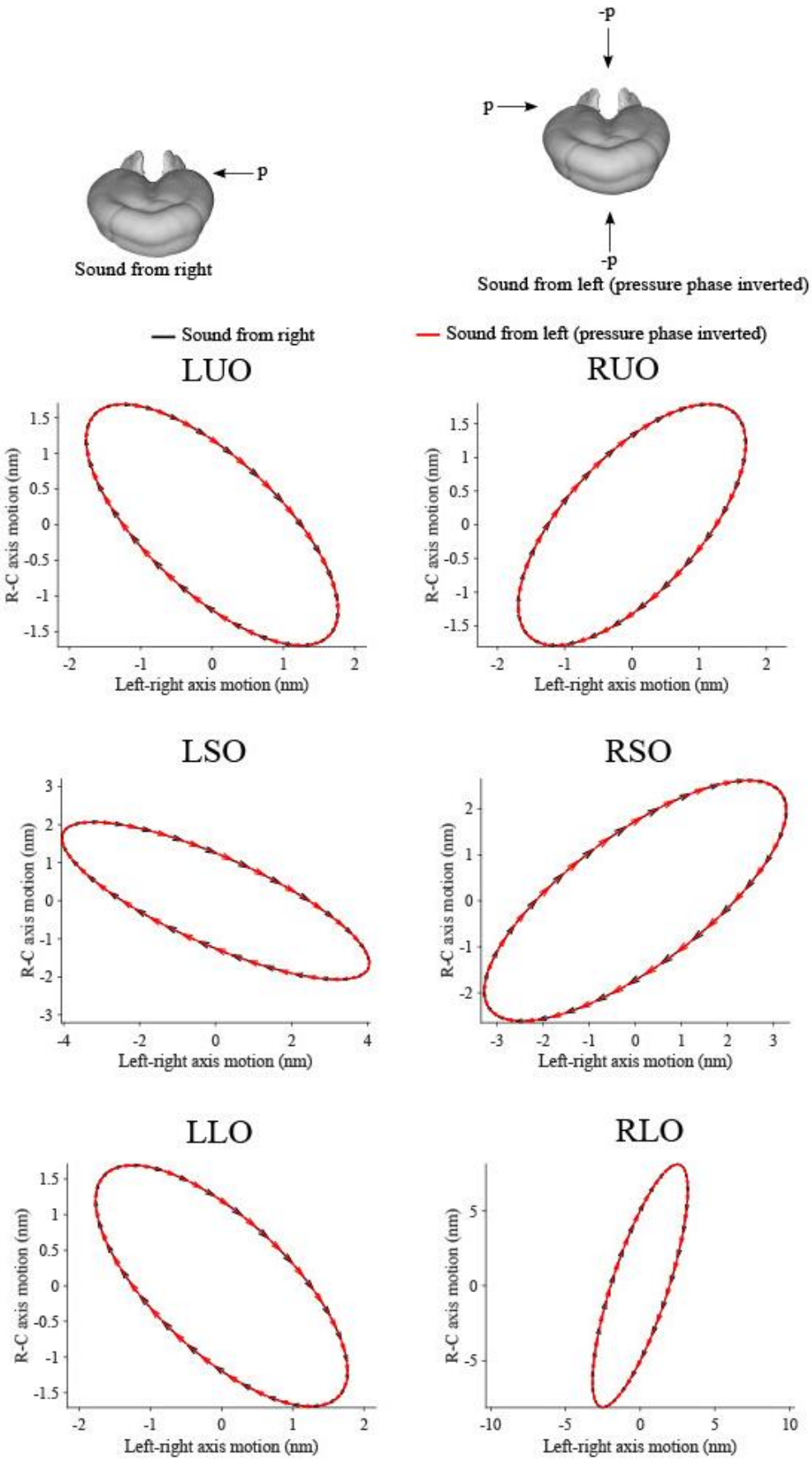
p
Sound from right
-p
p
-p
Sound from left (pressure phase inverted)
Sound from right
Sound from left (pressure phase inverted)
LUO
RUO
LSO
RSO
LLO
RLO
R-C axis motion (nm)
Left-right axis motion (nm)

Figure 7. Horizontal projection of the motion of the COM of the otoliths of the female midshipman when a sound was incident from the right, and when a sound was incident from the left at the same amplitude and frequency (100 Hz), but with the phase relationship between pressure and particle motion being inverted by applying two sounds in the vertical (dorsoventral) axis with the same pressure amplitude but opposite phase compared to the sound incident from the left. These simulations contained a swim bladder with a bladder wall.

Discussion

In this study, we constructed finite element models to investigate how the presence of a gas-filled swim bladder affects the motion of the otoliths to sounds incident from different directions in the horizontal and vertical planes to help elucidate the role of the swim bladder in directional hearing in the plainfin midshipman fish. We found that in both the female and type I male, the presence of the swim bladder increases the displacement and acceleration of the otoliths. Additionally, in the absence of the swim bladder, the otoliths move back and forth in the direction of sound, with the same motion for different directions. However, they move differently for non-opposite incident sound directions. When the swim bladder was present in the finite element (FE) simulations, the otoliths moved along elliptical orbits with opposite handedness for opposite directions and along different elliptical orbits for non-opposite incident sound directions at low frequencies (≤ 100 Hz). At higher frequencies (200 - 1000 Hz), the otoliths moved similarly for all incident sound directions. The swim bladder moved differently for different incident sound directions at 100 Hz but almost identically for different sound directions at 1000 Hz. In the absence of the swim bladder, the otoliths moved back and forth in the same direction for a given incident sound direction in a frequency-independent manner. However, in the presence of the swim bladder, the otoliths move along different paths for the same incident sound direction at different frequencies. The presence of the swim bladder also increased the amplitude of rotational motion of the otoliths. Furthermore, reversing the phase relationship between sound pressure and particle motion changed otolith motion in a way such that otoliths moved as if the sound was coming from the opposite direction, in the presence of the swim bladder. Below we discuss the main results of this study and their implications.

Swim bladder amplifies otolith motion

Previous studies have shown that the presence of the swim bladder improves physiological auditory sensitivity in the plainfin midshipman (Brown et al., 2019; Colleye et al., 2019; Rogers et al., 2023; Vetter and Sisneros, 2020), as well as in other fishes like the Atlantic cod (Sand and Enger, 1973) and cichlids (Schulz-Mirbach et al., 2012). The scattering of sound by the swim bladder to the inner ears is thought to increase the amplitude of displacement of the otoliths, leading to increased activation of the hair cells, which in turn increases physiological auditory sensitivity as measured through auditory evoked potential (AEP) measurements. In our study, the increase in the amplitude of displacement and acceleration of the otoliths in the presence of the swim bladder is consistent with these observations. Other finite element model (FEM) studies have also shown that the presence of a gas-filled swim bladder near the otoliths amplifies the acceleration of the otoliths (Li et al., 2024; Salas et al., 2019).

Swim bladder helps resolve the 180-degree ambiguity in directional hearing

At frequencies around 100 Hz and lower, the presence of the swim bladder causes the otoliths to move along the same elliptical orbits with different handedness for opposite sound directions. This likely activates the directionally sensitive hair cell fields around the otoliths (Sienknecht et al., 2014) differently for opposite sound directions, potentially providing higher-order centers in the auditory system with sufficient information to resolve the 180-degree ambiguity in directional hearing. At 100 Hz and lower frequencies, the elliptical orbits of the otoliths are also different for non-opposite sound directions, suggesting different hair-cell activation patterns for non-opposite directions. At frequencies of 200 Hz and greater, the otoliths move similarly for all incident sound directions. Thus, at these frequencies, the swim bladder may impede directional hearing capabilities.

The fundamental frequency of the hums produced by type I male plainfin midshipman is around 100 Hz (Balebail and Sisneros, 2022; Brantley and Bass, 1994), which is at the limit where the otoliths show differential motion for different incident sound directions. In our FE simulations, as the frequency increased from 50 to 2000 Hz, the difference in otolith motion for different sound directions increased. Thus, according to our simulations, the female midshipman's auditory system would theoretically be better at determining sound direction at 50 Hz rather than 100 Hz, raising the question as to why the fundamental frequency of the hum evolved to be close to 100 Hz. One possible reason is that in shallow water environments, there is a cutoff frequency above which sounds do not propagate, and the cutoff frequency in the rocky intertidal habitats in which midshipman breed is around 100 Hz (Bass and Clark, 2003). Therefore, it is possible that the hum evolved at a frequency that ensures directional hearing but also the propagation of the hum underwater. Many fish species in shallow water environments communicate at around 100 Hz, and it has been suggested that these communication frequencies evolved because there is a "quiet window" in local ambient sound spectra at this frequency (Lugli, 2010). Our study raises a second possibility, namely that fishes evolved to vocalize at frequencies that allow directional hearing but also propagate in shallow water environments, which needs to be investigated further.

Thus, our study makes testable predictions about how the swim bladder affects otolith motion in fishes possessing a swim bladder like the plainfin midshipman. Namely, that the swim bladder causes elliptical motion in the otoliths with opposite handedness for opposite directions. As the frequency increases, the elliptical orbits of the otoliths begin to lose their dependency on incident sound direction and become more similar for all incident sound directions. There have been recent studies in which otolith motion inside fishes has been experimentally measured for incident sounds using techniques such as X-ray tomography and optical vibrometry (Maiditsch et al., 2022; Schulz-Mirbach et al., 2020; Veith et al., 2024). The predictions raised by our simulations can be tested using such techniques.

Our study is not the first to predict elliptical motion of auditory structures due to sounds emanating from opposite directions. This was first predicted by Schellart and De Munck, (1987), where the authors constructed an analytical model where a cod's swim bladder was modeled as an oblate spheroid, and the particle displacement of water at the approximate location of the hair cells was calculated. The results they obtained were similar to ours: the particle motion followed the same elliptical orbits for opposite sound directions but with opposite handedness. As the frequencies of sound increased, the particle displacement became more similar for all directions. Our model extends the results obtained by Schellart and De Munck, (1987) by incorporating more realistic geometry for the swim bladder, based on CT scans. Additionally, our model includes the calcareous otoliths, which have different acoustic impedances compared to water and likely also considerably influence the particle motion fields near the hair cells. In addition to sounds being incident from the horizontal plane as in Schellart and De Munck, (1987), we also had sound incident from different directions in the vertical plane and showed that the swim bladder could potentially resolve the 180-degree ambiguity for sounds incident from both planes. Additionally, we computed the component of otolith motion both in the horizontal and vertical (midsagittal) planes. Schellart and De Munck, (1987) showed that the phase difference between the sound from the source and the sound scattered by the otoliths creates elliptical particle motion displacement, which is likely the reason for the elliptical motion of the otoliths in our simulations as well.

The results from the simulations in which the swim bladder was an air bubble resembled those in which the swim bladder had a wall, with the otoliths moving along elliptical orbits with opposite handedness of rotation for opposite incident sound directions. In our simulations, we assumed the acoustic properties of fish tissues (apart from the swim bladder and the otoliths) to be the same as water, a commonly held assumption in the fish hearing community. In an FEM study by Salas et al., (2019), the addition of ribs had little effect on how the swim bladder increased the magnitude of acceleration of the otoliths. In our study, the properties of the swim bladder material had little effect on the main trends observed in how the swim bladder affects otolith motion. This suggests that the presence of other tissues in the fish, such as bones and connective tissue, may not significantly impact the main predictions of our FE model. However, some fishes do not possess a gas-filled bladder. These species may possess biological tissues with different acoustic impedances than

water, which can still create elliptical motion in the otoliths' orbits in the absence of the swim bladder, helping resolve the 180-degree ambiguity in directional hearing. This hypothesis remains to be investigated.

The presence of the swim bladder caused otoliths of the same type on the left and right sides to move along different paths in response to sounds (Fig. 8). This observed asymmetry in the motion of the left and right otoliths may have implications for directional hearing and warrants further investigation.

Sufficiency of a single inner ear end-organ to encode sound direction

In recent experiments on sound source localization in female plainfin midshipman (Rogers et al., in prep), we found that none of the end-organs were necessary for sound source localization. Female midshipman could localize a sound source even when three end organs on one side were ablated, suggesting that binaural cues are not necessary for sound source localization. However, when one or more of the end-organs were ablated, the paths taken by the females to localize a sound source were more erratic. This suggests that inputs from multiple otoliths provide redundant information to the fish brain about sound direction and minimize errors in the computation of sound direction. The results from our simulations support this hypothesis. Since all six otoliths responded differently to sounds from various directions, a single inner-ear end-organ (utricle, saccule, or lagena) may be sufficient for determining sound direction at the communication frequencies of the midshipman (~100 Hz) and for sounds incident in both the horizontal and vertical planes.

Dependence of swim bladder motion on the direction of sound

Our FE simulations showed that the tips of the swim bladder wall moved differently for different incident sound directions at 100 Hz but not at 1000 Hz. When a gas-filled swim bladder is present, the otoliths are excited both by sound directly from the source and by sound scattered by the swim bladder. The direct motion of the otoliths due to sound from the source is represented by the simulations lacking a swim bladder, which differ for non-opposite directions. Our study suggests that at the frequencies at which the midshipman communicates (~100 Hz), the swim bladder-derived component of otolith motion may also depend on sound direction.

Frequency dependence of the motion trajectory of the otoliths in the presence of the swim bladder

We found that at different incident sound frequencies, the otoliths moved differently for the same sound direction in the presence of the swim bladder. In fishes like the plainfin midshipman, the frequency of sound is thought to be encoded temporally, with afferent fibers innervating the end organs synchronizing their action potentials with the phase of the input sound (Fay, 1978; McKibben and Bass, 2001; Sisneros and Bass, 2003). However, since the trajectories of the otoliths in response to sound in our FE simulations were frequency-dependent, it is possible that sound frequency is also encoded by a “dynamic place code,” wherein the spatio-temporal pattern of stimulation of hair cells encodes not only sound direction but also provides the auditory system with information about frequency. Our prediction of different trajectories of the otoliths for the same incident sound direction (but different frequency) can be tested experimentally using techniques like optical vibrometry (Veith et al., 2024) and X-ray tomography (Maiditsch et al., 2022; Schulz-Mirbach et al., 2020).

Increased rotational motion of the otoliths in the presence of the swim bladder

A FEM study by Krysl et al., (2012) found that a hemispherical-shaped structure undergoes both rotational and translational motion in response to plane wave incident sounds. Krysl et al., (2012) also suggested that asymmetric structures like otoliths will undergo rotational motion when struck by incident sound. Visualization of otolith motion due to sound by Maiditsch et al., (2022) showed that otoliths did undergo rotational motion. Our simulations showed that in the presence of the swim bladder, otolith motion has multiple degrees of freedom: the otoliths move along elliptical orbits and rotate about axes passing through them. Otoliths also underwent rotational motion in the absence of the swim bladder, but with angular

amplitudes that were one to three orders of magnitude lower than in the presence of the swim bladder. It remains to be tested how rotational motion of the otoliths affects the motion of the hair cells.

A possible mechanism for sensing the phase relationship between acoustic pressure and particle motion

The phase model proposed that the swim bladder allows the fish auditory system to detect the phase difference between sound pressure and particle motion, theoretically allowing the resolution of the 180-degree ambiguity in directional hearing (Schuijf, 1976). Some studies have shown evidence for the phase model, wherein if the phase difference between sound pressure and particle motion of a sound emanating from a speaker is inverted to resemble the phase difference between sound pressure and particle motion of a sound incident from the opposite direction, the fishes respond as if the sound is coming from the opposite direction (Buwalda et al., 1983; Schuijf and Buwalda, 1975; Veith et al., 2024). However, the mechanism by which the fish's auditory system computes the phase between pressure and particle motion is not known. In our FE simulations, when we inverted the phase relationship between sound pressure and particle motion for a sound incident from the left side of the animal, we found that the otoliths moved along the same trajectory as a sound emanating from the right side with the same frequency and amplitude. Thus, the handedness of rotation of the elliptical orbits of the otoliths could encode the phase relationship between sound pressure and particle motion.

Our study has focused on otolith motion in response to sinusoidal plane wave sounds. However, natural sounds are more complex, featuring non-sinusoidal waveforms and background ambient noise in addition to the primary sound signal. Future research should explore how otoliths respond to more naturalistic stimuli. Time-domain finite element (FE) simulations, incorporating sound waveforms recorded in natural environments, are needed to address these questions. Furthermore, our FE simulations investigated the steady-state motion of the otoliths. Transient dynamics, such as the initial response when sound first strikes the otoliths - may offer valuable cues for directional hearing and sound source localization, including interaural time differences. These aspects require further exploration.

Recent advancements have enabled the acquisition of 3D coordinates of the macula containing hair cells (Schulz-Mirbach et al., 2013). Additionally, the polarity patterns of hair cell fields in the macula are known for many species, including the plainfin midshipman (Coffin et al., 2012), and could be mapped onto the 3D coordinates of the maculae of the three end-organs. By computing the displacement of the hair cells and modeling changes in their electrical activity in response to sound, we can gain insights into the auditory inputs being sent to the brain for different incident sound directions.

References

Balebail, S. and Sisneros, J. A. (2022). Long duration advertisement calls of nesting male plainfin midshipman fish are honest indicators of size and condition. Journal of Experimental Biology 225, jeb243889.

Bass, A. H. and Clark, C. W. (2003). The Physical Acoustics of Underwater Sound Communication. In Acoustic Communication (ed. Simmons, A. M.), Fay, R. R.), and Popper, A. N.), pp. 15–64. New York: Springer-Verlag.

Bern, M. and Eppstein, D. (1995). MESH GENERATION AND OPTIMAL TRIANGULATION. In Lecture Notes Series on Computing, pp. 47–123. WORLD SCIENTIFIC.

Brantley, R. K. and Bass, A. H. (1994). Alternative male spawning tactics and acoustic signals in the plainfin midshipman fish Porichthys notatus Girard (Teleostei, Batrachoididae). Ethology 96, 213–232.

Brown, A. D., Zeng, R. and Sisneros, J. A. (2019). Auditory evoked potentials of the plainfin midshipman fish (Porichthys notatus): implications for directional hearing. Journal of Experimental Biology 222, jeb198655.

Bui, S., Oppedal, F., Korsøen, Ø. J., Sonny, D. and Dempster, T. (2013). Group behavioural responses of Atlantic salmon (Salmo salar L.) to light, infrasound and sound stimuli. PloS one 8, e63696.

Buwalda, R. J. A., Schuijf, A. and Hawkins, A. D. (1983). Discrimination by the cod of sounds from opposing directions. J. Comp. Physiol. 150, 175–184.

Carr, C. E. and Christensen-Dalsgaard, J. (2015). Sound localization strategies in three predators. Brain Behavior and Evolution 86, 17–27.

Carr, C. E. and Christensen-Dalsgaard, J. (2016). Evolutionary trends in directional hearing. Current opinion in neurobiology 40, 111–117.

Cignoni, P., Callieri, M., Corsini, M., Dellepiane, M., Ganovelli, F. and Ranzuglia, G. (2008). Meshlab: an open-source mesh processing tool. In Eurographics Italian chapter conference, pp. 129–136. Salerno, Italy.

Coffin, A.B., Mohr, R.A. and Sisneros, J.A., 2012. Saccular-specific hair cell addition correlates with reproductive state-dependent changes in the auditory saccular sensitivity of a vocal fish. Journal of Neuroscience, 32(4), pp.1366-1376.

Colleye, O., Vetter, B. J., Mohr, R. A., Seeley, L. H. and Sisneros, J. A. (2019). Sexually dimorphic swim bladder extensions enhance the auditory sensitivity of female plainfin midshipman fish, Porichthys notatus. Journal of Experimental Biology 222, jeb204552.

Craig Jr, R. R. and Taleff, E. M. (2020). Mechanics of materials. John Wiley & Sons.

De Vries, Hl. (1950). The Mechanics of the Labyrinth Otoliths. Acta Oto-Laryngologica 38, 262–273.

Duarte, C. M., Chapuis, L., Collin, S. P., Costa, D. P., Devassy, R. P., Eguiluz, V. M., Erbe, C., Gordon, T. A. C., Halpern, B. S., Harding, H. R., et al. (2021). The soundscape of the Anthropocene ocean. Science 371, eaba4658.

Fay, R. R. (1978). Coding of information in single auditory-nerve fibers of the goldfish. The Journal of the Acoustical Society of America 63, 136–146.

Fedorov, A., Beichel, R., Kalpathy-Cramer, J., Finet, J., Fillion-Robin, J.-C., Pujol, S., Bauer, C., Jennings, D., Fennessy, F. and Sonka, M. (2012). 3D Slicer as an image computing platform for the Quantitative Imaging Network. Magnetic resonance imaging 30, 1323–1341.

Fine, M. L., King, T. L., Ali, H., Sidker, N. and Cameron, T. M. (2016). Wall structure and material properties cause viscous damping of swimbladder sounds in the oyster toadfish Opsanus tau. Proc. R. Soc. B. 283, 20161094.

Flock, Å. and Wersäll, J. (1962). A study of the orientation of the sensory hairs of the receptor cells in the lateral line organ of fish, with special reference to the function of the receptors. The Journal of cell biology 15, 19–27.

Fung, Y. (2013). Biomechanics: mechanical properties of living tissues. Springer Science & Business Media.

Gerhardt, H. C., Bee, M. A. and Christensen-Dalsgaard, J. (2023). Neuroethology of sound localization in anurans. J Comp Physiol A 209, 115–129.

Hawkins, A. D. and Sand, O. (1977). Directional hearing in the median vertical plane by the cod. J. Comp. Physiol. 122, 1–8.

Jakob, W., Tarini, M., Panozzo, D. and Sorkine-Hornung, O. (2015). Instant field-aligned meshes. ACM Trans. Graph. 34, 189–1.

Khodabandeloo, B., Agersted, M. D., Klevjer, T., Macaulay, G. J. and Melle, W. (2021a). Estimating target strength and physical characteristics of gas-bearing mesopelagic fish from wideband in situ echoes using a viscous-elastic scattering model. The Journal of the Acoustical Society of America 149, 673–691.

Khodabandeloo, B., Agersted, M. D., Klevjer, T. A., Pedersen, G. and Melle, W. (2021b). Mesopelagic flesh shear viscosity estimation from in situ broadband backscattering measurements by a viscous–elastic model inversion. ICES Journal of Marine Science 78, 3147–3161.

Kinsler, L. E., Frey, A. R., Coppens, A. B. and Sanders, J. V. (1951). Fundamentals of acoustics. American Journal of Physics 19, 254–255.

Krysl, P., Hawkins, A. D., Schilt, C. and Cranford, T. W. (2012). Angular oscillation of solid scatterers in response to progressive planar acoustic waves: Do fish otoliths rock?

Ladich F and Fay RR (2013) Auditory evoked potential audiometry in fish. Rev Fish Biol Fish 23: 317–364. https://doi.org/10.1007/s11160-012-9297-z

Leis, J. M., Carson-Ewart, B. M., Hay, A. C. and Cato, D. H. (2003). Coral-reef sounds enable nocturnal navigation by some reef-fish larvae in some places and at some times. Journal of Fish Biology 63, 724–737.

Li, H., Gao, Z., Song, Z., Su, Y., Hui, J., Ou, W., Zhang, J. and Zhang, Y. (2024). Investigation on the contribution of swim bladder to hearing in crucian carp (Carassius carassius). The Journal of the Acoustical Society of America 155, 2492–2502.

Lu, Z. and Popper, A. N. (1998). Morphological polarizations of sensory hair cells in the three otolithic organs of a teleost fish: fluorescent imaging of ciliary bundles. Hearing research 126, 47–57.

Luczkovich, J. J., Daniel, H. J., Hutchinson, M., Jenkins, T., Johnson, S. E., Pullinger, R. C. and Sprague, M. W. (2000). Sounds of sex and death in the sea: Bottlenose dolphin whistles suppress mating choruses of silver perch. Bioacoustics 10, 323–334.

Lugli, M. (2010). Sounds of shallow water fishes pitch within the quiet window of the habitat ambient noise. J Comp Physiol A 196, 439–451.

Maiditsch, I. P., Ladich, F., Heß, M., Schlepütz, C. M. and Schulz-Mirbach, T. (2022). Revealing sound-induced motion patterns in fish hearing structures in 4D: a standing wave tube-like setup designed for high-resolution time-resolved tomography. Journal of Experimental Biology 225, jeb243614.

McKibben, J. R. and Bass, A. H. (2001). Peripheral encoding of behaviorally relevant acoustic signals in a vocal fish: harmonic and beat stimuli. Journal of Comparative Physiology A 187, 271–285.

Mohr, R. A., Whitchurch, E. A., Anderson, R. D., Forlano, P. M., Fay, R. R., Ketten, D. R., Cox, T. C. and Sisneros, J. A. (2017). Intra- and Intersexual swim bladder dimorphisms in the plainfin midshipman fish (Porichthys notatus): Implications of swim bladder proximity to the inner ear for sound pressure detection. Journal of Morphology 278, 1458–1468.

Multiphysics, C. (1998). Introduction to comsol multiphysics®. COMSOL Multiphysics, Burlington, MA, accessed Feb 9, 32.

Oliveira, A. M., Farina, M., Ludka, I. P. and Kachar, B. (1996). Vaterite, calcite, and aragonite in the otoliths of three species of piranha. Naturwissenschaften 83, 133–135.

Popper, A. N. (2017). Auditory system morphology.

Popper, A. N. and Saidel, W. M. (1990). Variations in receptor cell innervation in the saccule of a teleost fish ear. Hearing research 46, 211–227.

Popper, A. N., Salmon, M. and Parvulescu, A. (1973). Sound localization by the Hawaiian squirrelfishes, Myripristis berndti and M. argyromus. Animal Behaviour 21, 86–97.

Radford, C., Jeffs, A., Tindle, C. and Montgomery, J. (2008). Resonating sea urchin skeletons create coastal choruses. Mar. Ecol. Prog. Ser. 362, 37–43.

Remage-Healey, L., Nowacek, D. P. and Bass, A. H. (2006). Dolphin foraging sounds suppress calling and elevate stress hormone levels in a prey species, the Gulf toadfish. Journal of Experimental Biology 209, 4444–4451.

Retzius, G. (1881). Das gehörorgan der fische und amphibien. Gedruckt in der Centraldruckerei in Commission bei Samson & Wallin.

Richard, J. D. (1968). Fish Attraction with Pulsed Low-Frequency Sound. J. Fish. Res. Bd. Can. 25, 1441–1452.

Rogers, P. H. and Cox, M. (1988). Underwater Sound as a Biological Stimulus. In Sensory Biology of Aquatic Animals (ed. Atema, J.), Fay, R. R.), Popper, A. N.), and Tavolga, W. N.), pp. 131–149. New York, NY: Springer New York.

Rogers, P. H., Hawkins, A. D., Popper, A. N., Fay, R. R. and Gray, M. D. (2016). Parvulescu Revisited: Small Tank Acoustics for Bioacousticians. In The Effects of Noise on Aquatic Life II (ed. Popper, A. N.) and Hawkins, A.), pp. 933–941. New York, NY: Springer New York.

Rogers, L. S., Lozier, N. R., Sapozhnikova, Y. P., Diamond, K. M., Davis, J. L. and Sisneros, J. A. (2023). Functional plasticity of the swim bladder as an acoustic organ for communication in a vocal fish. Proc. R. Soc. B. 290, 20231839.

Rollo, A., Andraso, G., Janssen, J. and Higgs, D. (2007). Attraction and localization of round goby (Neogobius melanostomus) to conspecific calls. Behav 144, 1–21.

Salas, A. K., Wilson, P. S. and Fuiman, L. A. (2019). Ontogenetic change in predicted acoustic pressure sensitivity in larval red drum (Sciaenops ocellatus). Journal of Experimental Biology 222, jeb201962.

Sand, O. and Enger, P. S. (1973). Evidence for an auditory function of the swimbladder in the cod. Journal of Experimental Biology 59, 405–414.

Sand, O., Enger, P. S., Karlsen, H. E., Knudsen, F. and Kvernstuen, T. (2000). Avoidance responses to infrasound in downstream migrating European silver eels, Anguilla anguilla. Environmental Biology of Fishes 57, 327–336.

Schellart, N. A. M. and De Munck, J. C. (1987). A model for directional and distance hearing in swimbladder-bearing fish based on the displacement orbits of the hair cells. The Journal of the Acoustical Society of America 82, 822–829.

Schindelin, J., Arganda-Carreras, I., Frise, E., Kaynig, V., Longair, M., Pietzsch, T., Preibisch, S., Rueden, C., Saalfeld, S., Schmid, B., et al. (2012). Fiji: an open-source platform for biological-image analysis. Nature Methods 9, 676–682.

Schmidt, R. and Singh, K. (2010). meshmixer: an interface for rapid mesh composition. In ACM SIGGRAPH 2010 Talks, pp. 1–1. Los Angeles California: ACM.

Schuijf, A. (1976). The phase model of directional hearing in fish. Sound reception in fish 63–86.

Schuijf, A. and Buwalda, R. J. A. (1975). On the mechanism of directional hearing in cod (Gadus morhua L.). J. Comp. Physiol. 98, 333–343.

Schulz-Mirbach, T., Metscher, B. and Ladich, F. (2012). Relationship between swim bladder morphology and hearing abilities–a case study on Asian and African cichlids.

Schulz-Mirbach, T., Heß, M. and Metscher, B. D. (2013). Sensory epithelia of the fish inner ear in 3D: studied with high-resolution contrast enhanced microCT. Front Zool 10, 63.

Schulz-Mirbach, T., Ladich, F., Plath, M., Metscher, B. D. and Heß, M. (2014). Are accessory hearing structures linked to inner ear morphology? Insights from 3D orientation patterns of ciliary bundles in three cichlid species. Front Zool 11, 25.

Schulz-Mirbach, T., Ladich, F., Mittone, A., Olbinado, M., Bravin, A., Maiditsch, I. P., Melzer, R. R., Krysl, P. and Heß, M. (2020). Auditory chain reaction: Effects of sound pressure and particle motion on auditory structures in fishes. PLoS One 15, e0230578.

Sienknecht, U. J., Köppl, C. and Fritzsch, B. (2014). Evolution and development of hair cell polarity and efferent function in the inner ear. Brain, behavior and evolution 83, 150–161.

Sisneros, J. A. and Bass, A. H. (2003). Seasonal plasticity of peripheral auditory frequency sensitivity. Journal of Neuroscience 23, 1049–1058.

Sisneros, J. A. and Rogers, P. H. (2016). Directional hearing and sound source localization in fishes. Fish hearing and bioacoustics: An anthology in honor of Arthur N. Popper and Richard R. Fay 121–155.

Tavolga, W. N. (1971). 6 Sound production and detection. In Fish physiology, pp. 135–205. Elsevier.

Tolimieri, N., Jeffs, A. and Montgomery, J. (2000). Ambient sound as a cue for navigation by the pelagic larvae of reef fishes. Mar. Ecol. Prog. Ser. 207, 219–224.

Tomás, J. and Geffen, A. J. (2003). Morphometry and composition of aragonite and vaterite otoliths of deformed laboratory reared juvenile herring from two populations. Journal of Fish Biology 63, 1383–1401.

Van Bergeijk, W. A. (1964). Directional and nondirectional hearing in fish. Marine bio-acoustics 1, 281–299.

Veith, J., Chaigne, T., Svanidze, A., Dressler, L. E., Hoffmann, M., Gerhardt, B. and Judkewitz, B. (2024). The mechanism for directional hearing in fish. Nature 1–7.

Vetter, B. J. and Sisneros, J. A. (2020). Swim bladder enhances lagenar sensitivity to sound pressure and higher frequencies in female plainfin midshipman (Porichthys notatus). Journal of Experimental Biology jeb.225177.

Walton, P. L., Christensen-Dalsgaard, J. and Carr, C. E. (2017). Evolution of sound source localization circuits in the nonmammalian vertebrate brainstem. Brain Behavior and Evolution 90, 131–153.

Wang, Y.-L., Lin, C.-Y., Huang, S.-P., Lee, C.-Y., Tuanmu, M.-N. and Wang, T.-Y. (2022). Chub movement is attracted by the collision sounds associated with spawning activities. Zootaxa 5189, 308–317.

Wasmeier, P. (2010). Geodetic transformations.

Winn, H. E. (1972). Acoustic Discrimination by the Toadfish with Comments on Signal Systems. In Behavior of Marine Animals: Current Perspectives in Research Volume 2: Vertebrates (ed. Winn, H. E.) and Olla, B. L.), pp. 361–385. Boston, MA: Springer US.

Zeddies, D. G., Fay, R. R., Alderks, P. W., Shaub, K. S. and Sisneros, J. A. (2010). Sound source localization by the plainfin midshipman fish, Porichthys notatus. J. Acoust. Soc. Am. 127, 11.

Supplementary material

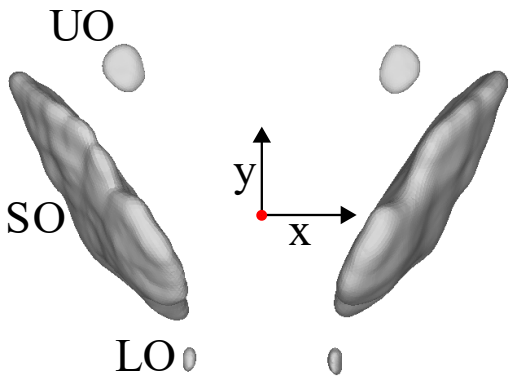

Figure S1. Coordinate system of the geometry.

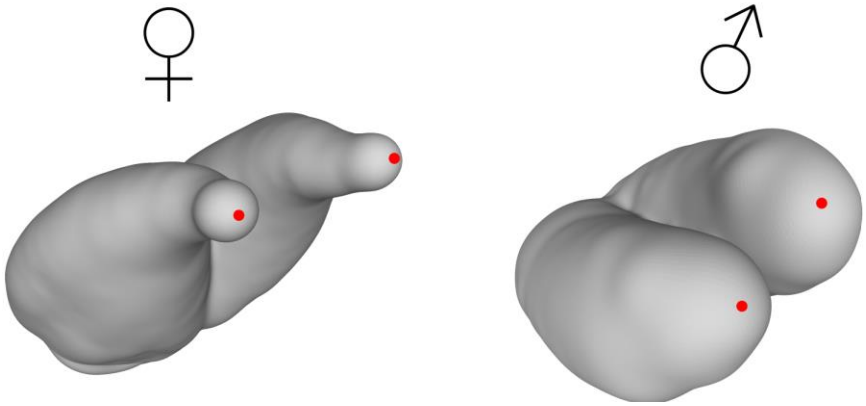

Figure S2. Tips of the swim bladder wall of the female (left) and type I male (right) plainfin midshipman.

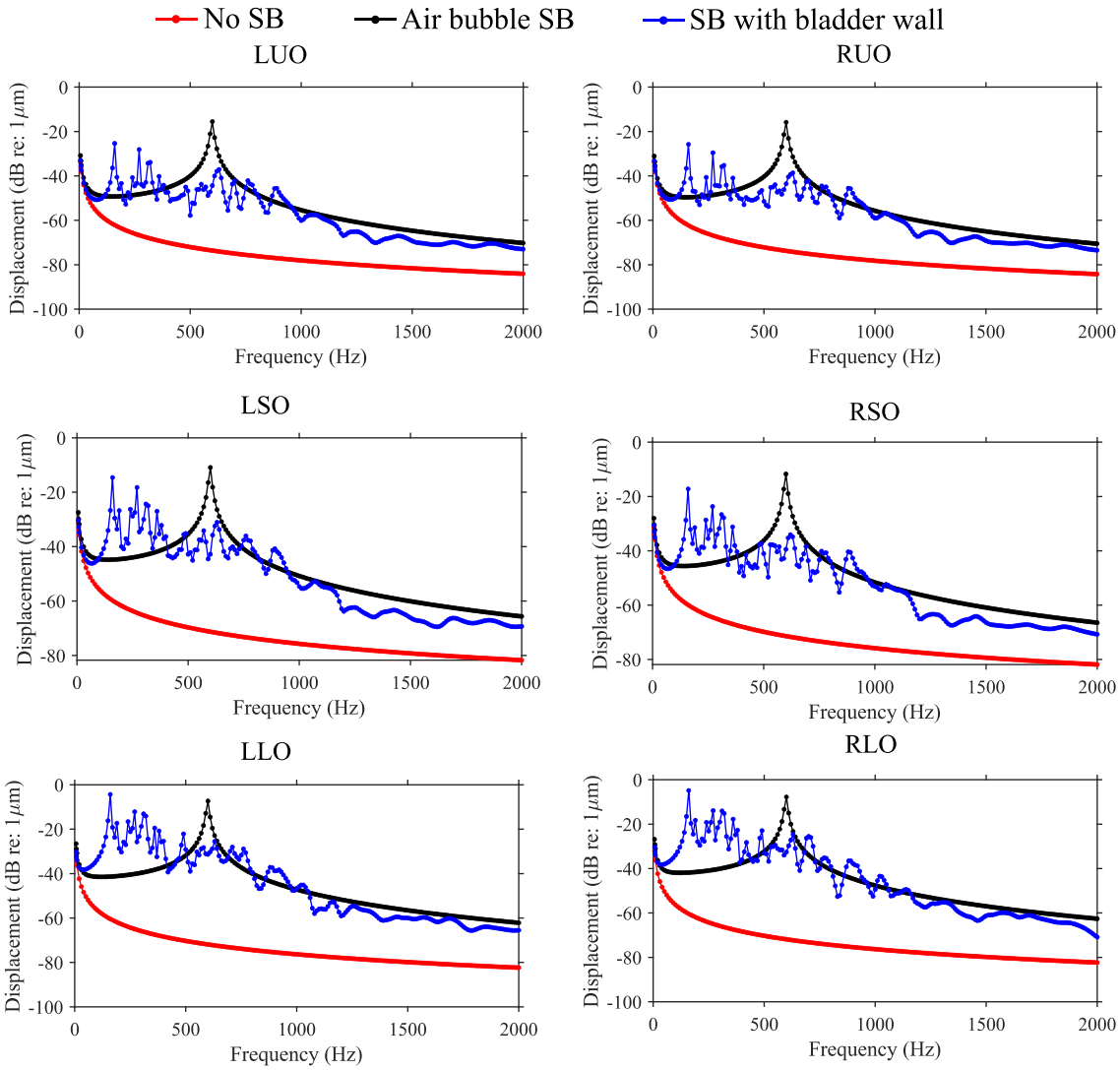

Figure S3. Displacement amplitudes of the center of masses (COMs) of the otoliths when sounds were incident from the front of the animal (0°) for the female midshipman.

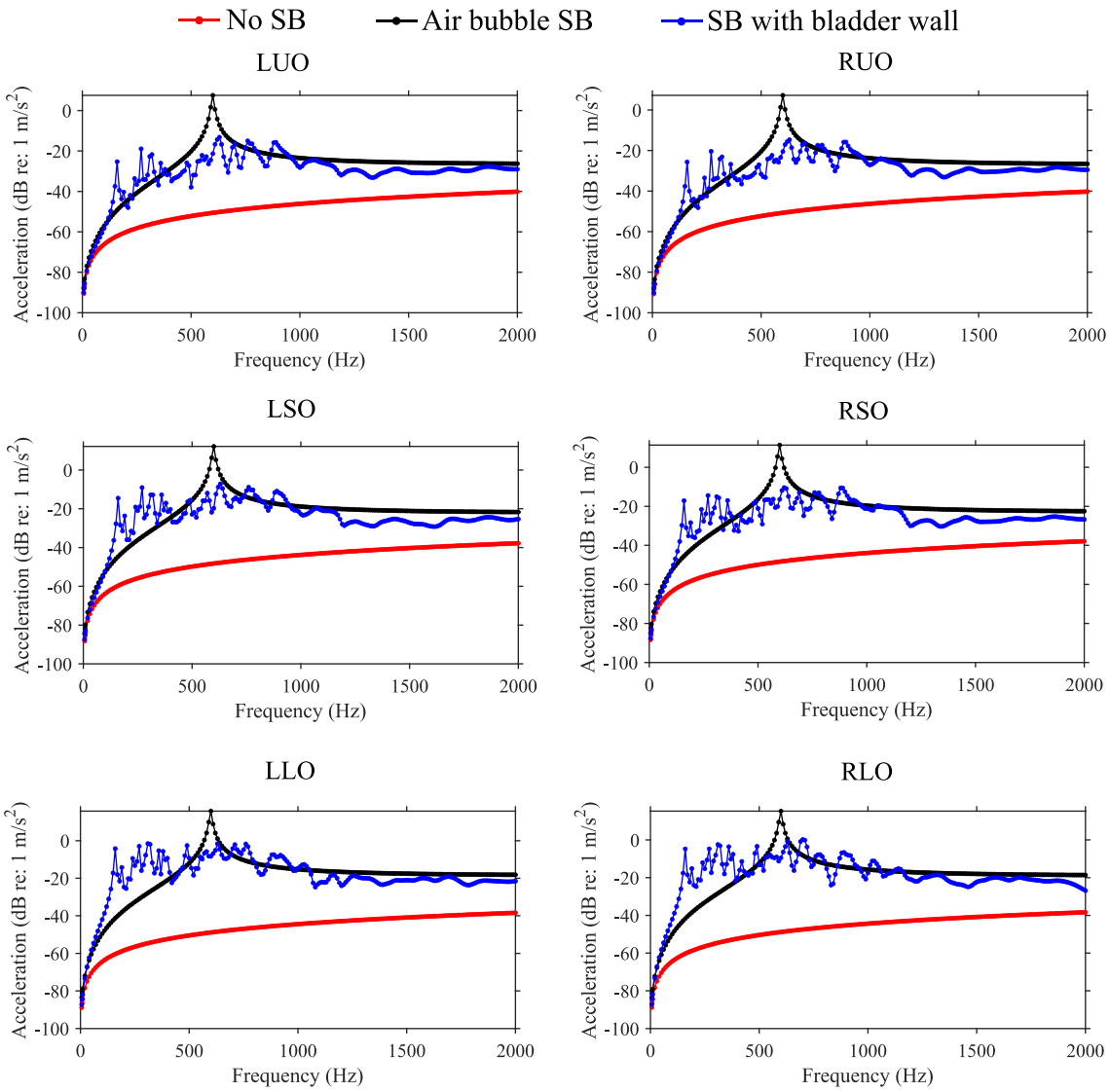

Figure S4. Acceleration amplitudes of the center of masses (COMs) of the otoliths when sounds were incident from the front of the animal (0°) for the female midshipman.

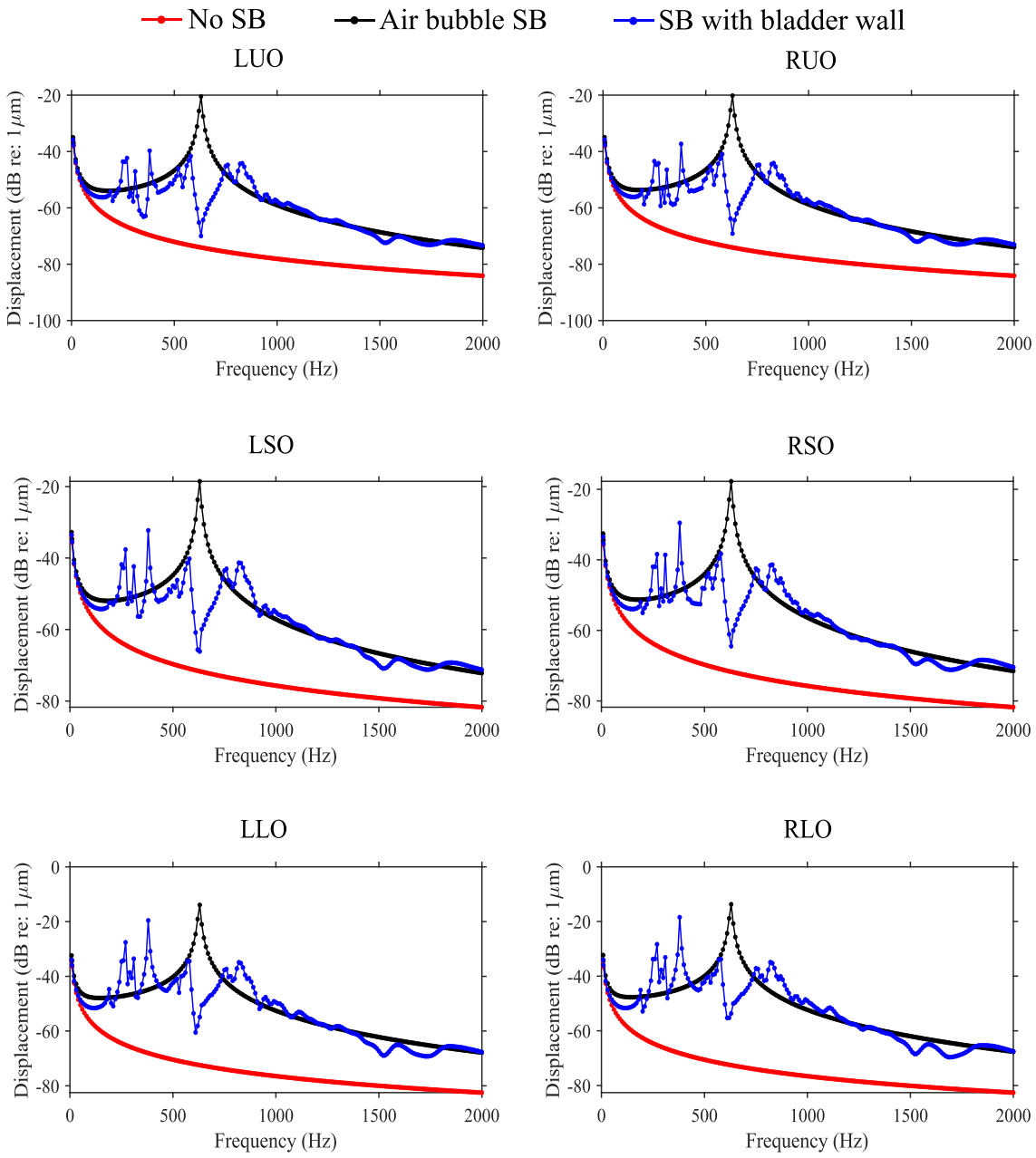

Figure S5. Displacement amplitudes of the center of masses (COMs) of the otoliths when sounds were incident from the front of the animal (0°) for the type I male midshipman.

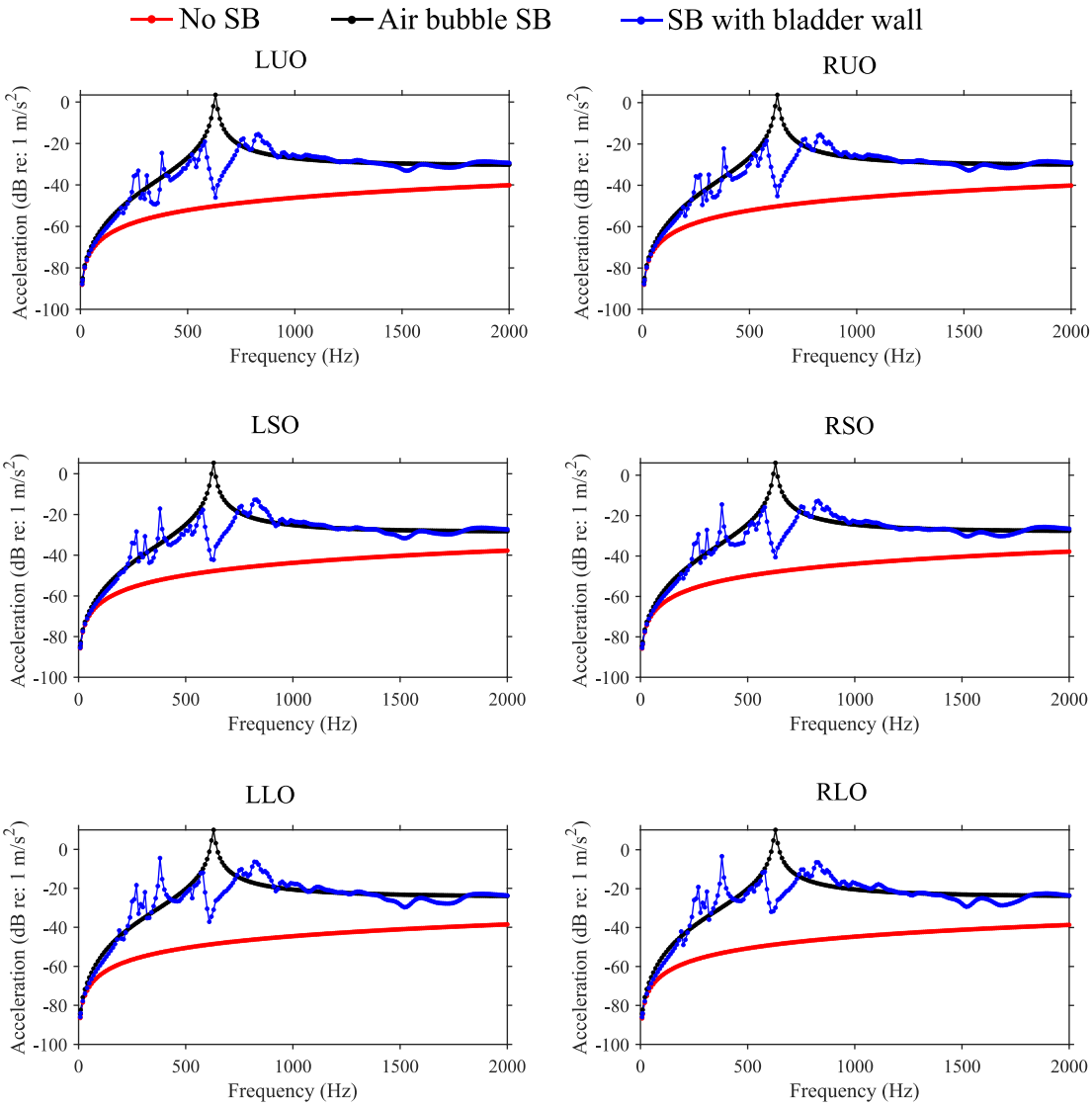

Figure S6. Acceleration amplitudes of the center of masses (COMs) of the otoliths when sounds were incident from the front of the animal (0°) for the type I male midshipman.

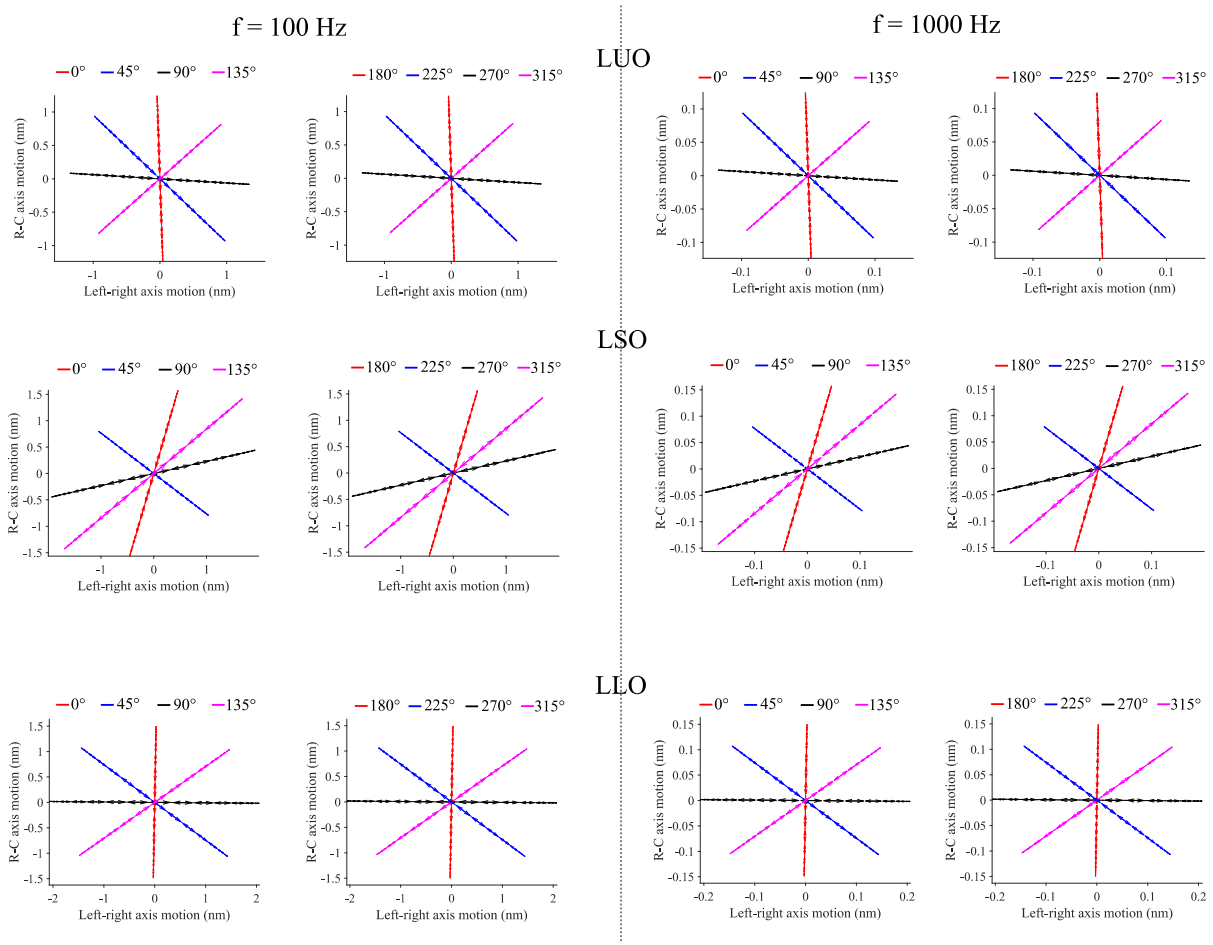

Figure S7. Projection of the motion of the COM of the left otoliths onto the horizontal plane when sounds were incident from various directions in the horizontal plane (0-315°) in the simulations without a swim bladder for the type I male midshipman for frequencies 100 and 1000 Hz.

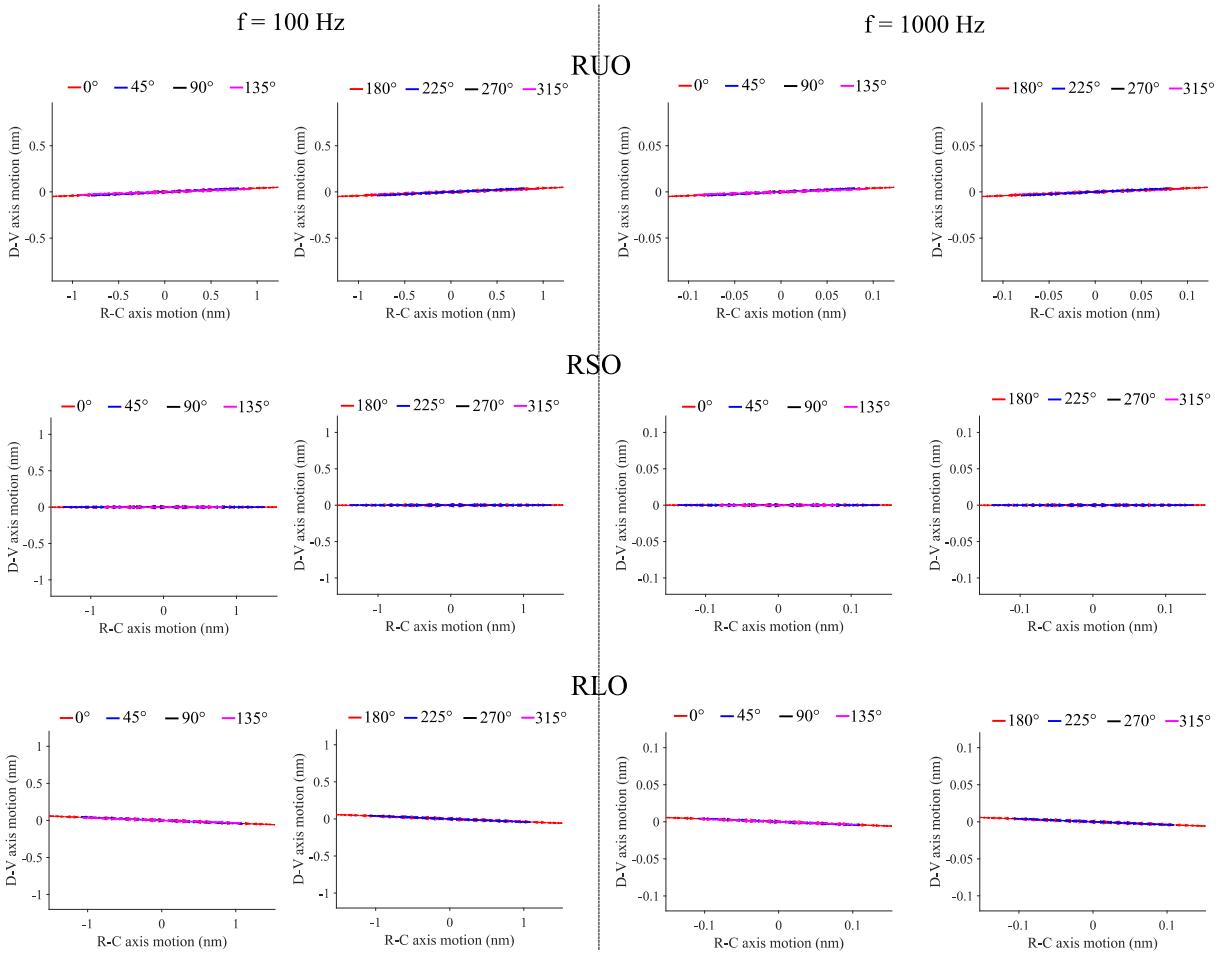

Figure S8. Projection of the motion of the COM of the right otoliths onto the midsagittal (vertical) plane when sounds were incident from various directions in the horizontal plane (0-315°) in the simulations without a swim bladder for the female midshipman for frequencies 100 and 1000 Hz.

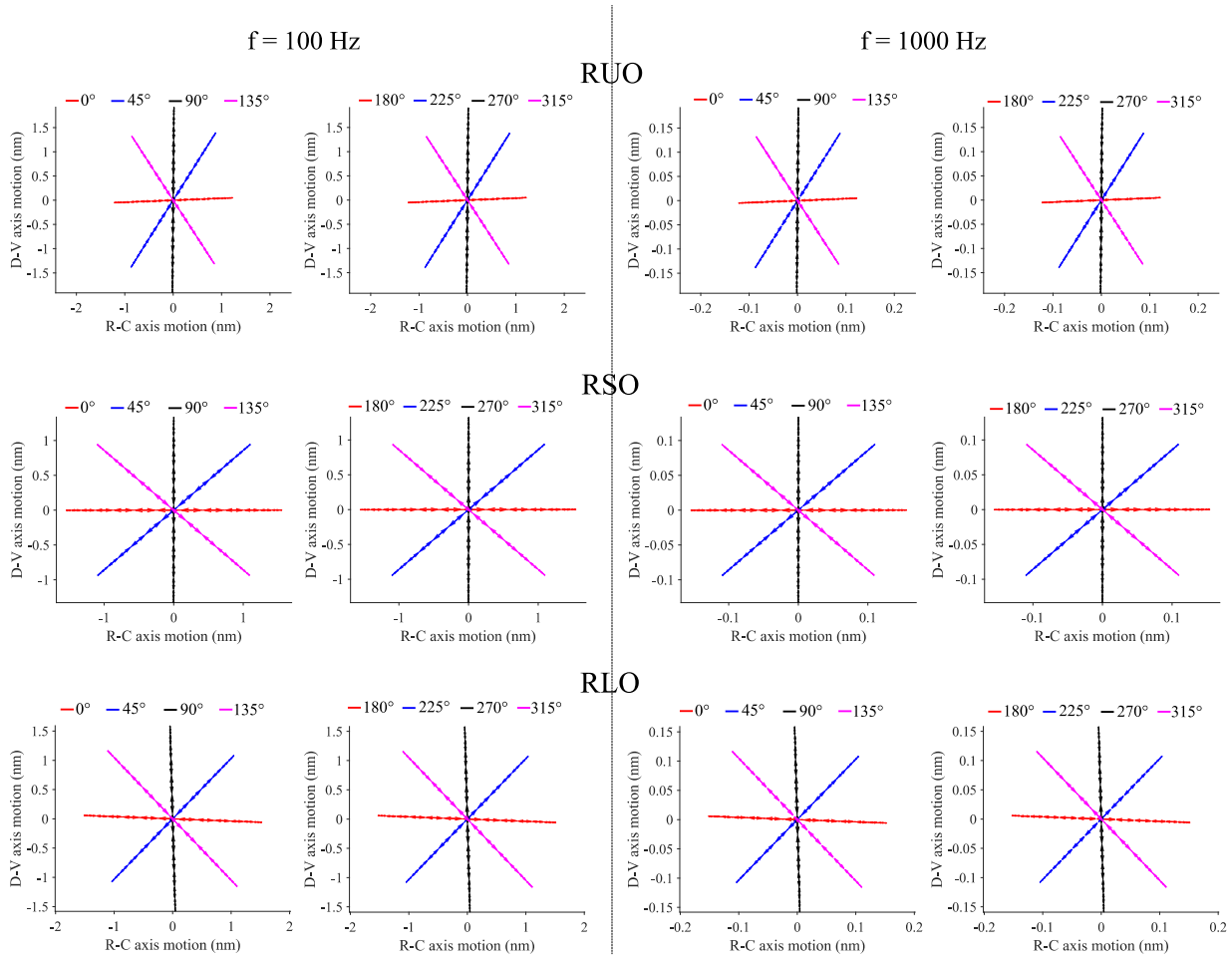

Figure S9. Projection of the motion of the COM of the right otoliths onto the vertical plane when sounds were incident from various directions in the vertical plane (0-315°) in the simulations without a swim bladder for the female midshipman for frequencies 100 and 1000 Hz.

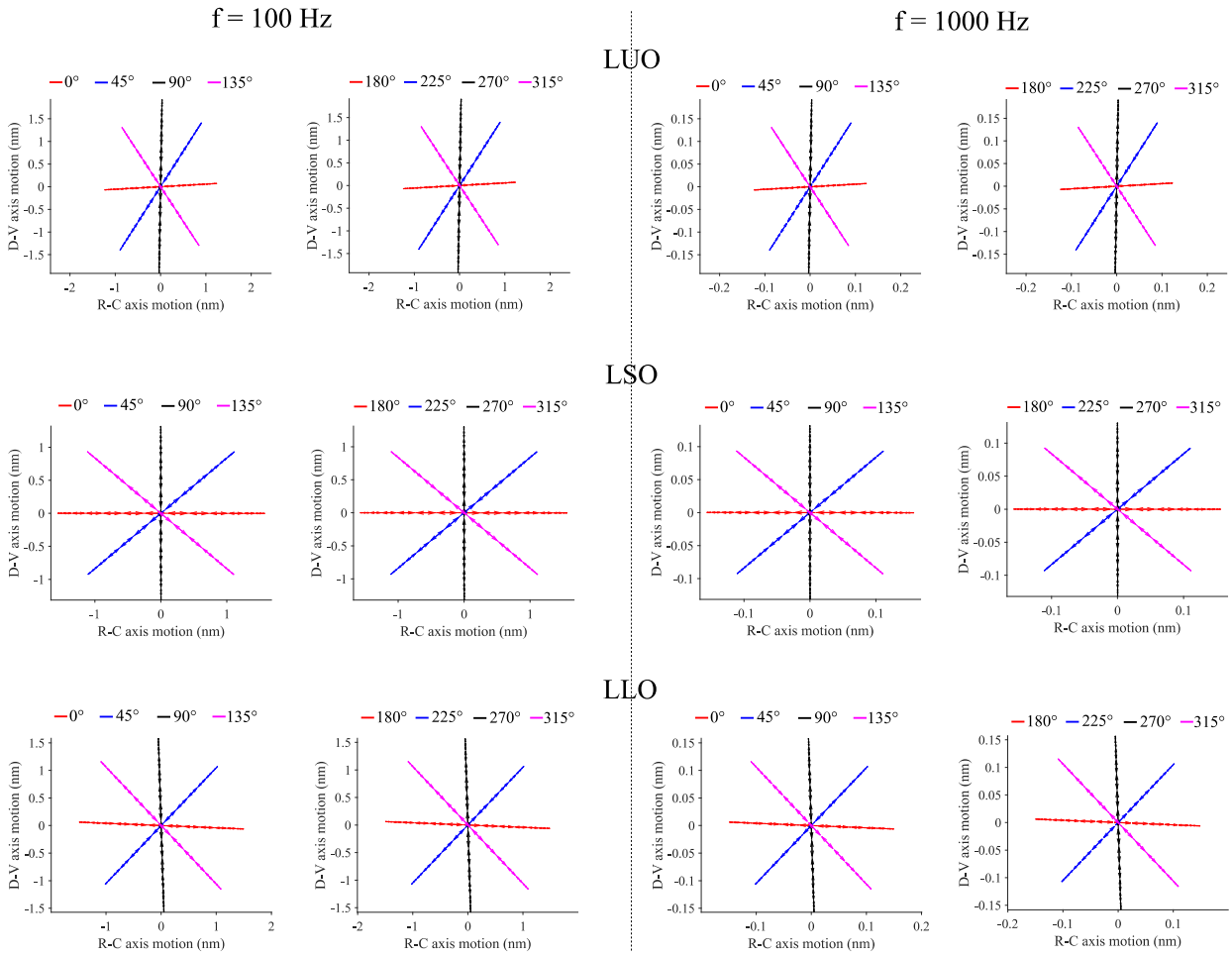

Figure S10. Projection of the motion of the COM of the left otoliths onto the vertical plane when sounds were incident from various directions in the vertical plane (0-315°) in the simulations without a swim bladder for the type I male midshipman for frequencies 100 and 1000 Hz.

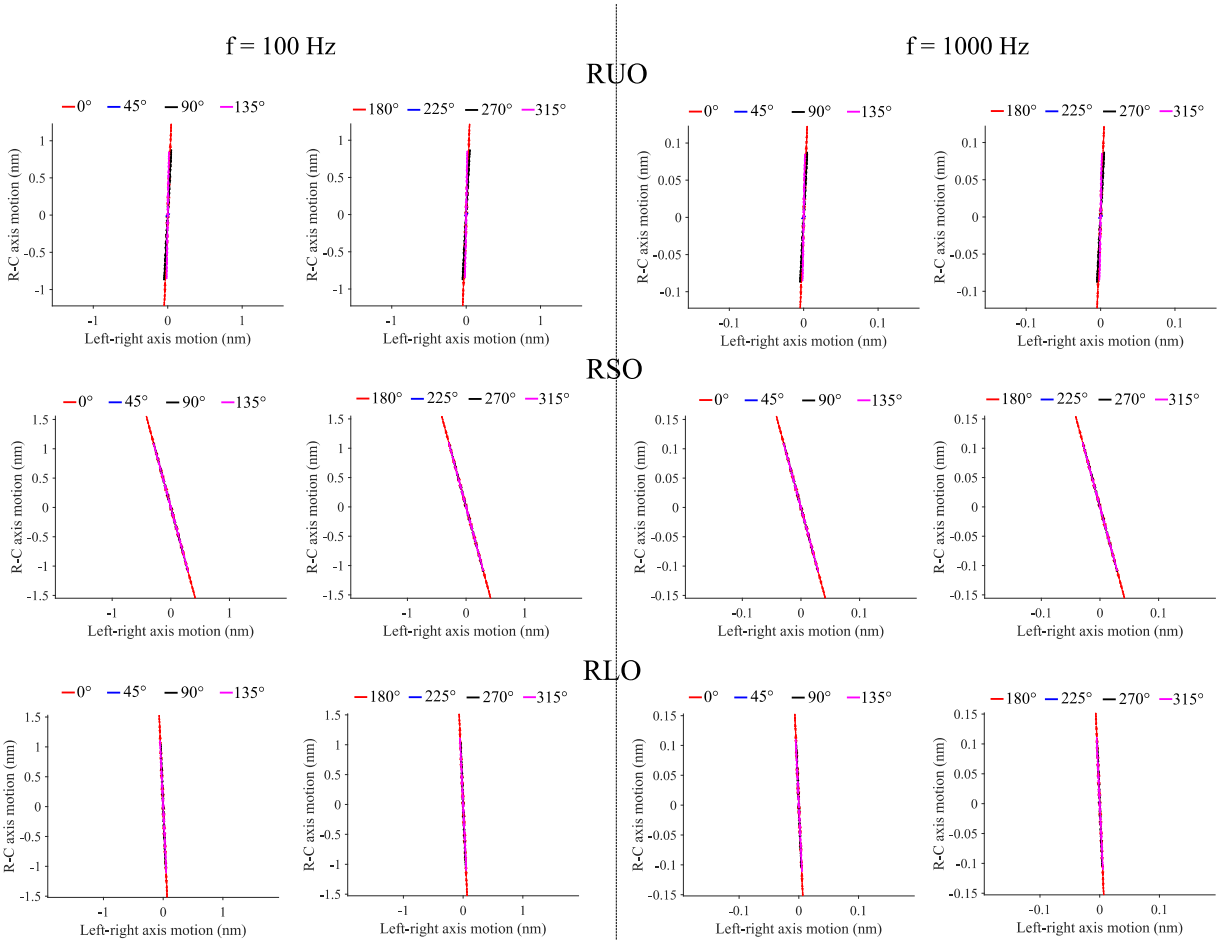

Figure S11. Projection of the motion of the COM of the right otoliths onto the horizontal plane when sounds were incident from various directions in the vertical plane (0-315°) in the simulations without a swim bladder for the female midshipman for frequencies 100 and 1000 Hz.

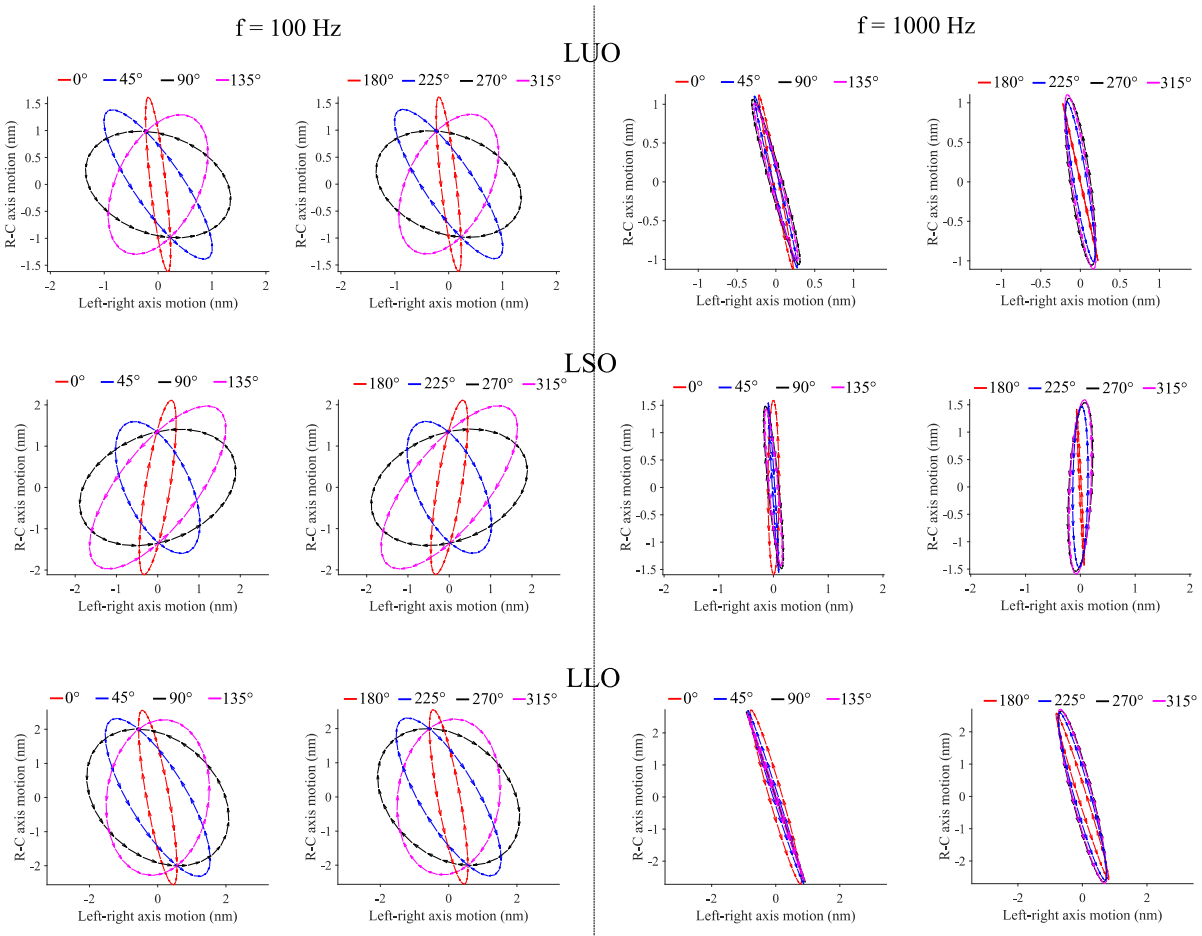

Figure S12. Projection of the motion of the COM of the left otoliths onto the horizontal plane when sounds were incident from various directions in the horizontal plane in the simulations containing a swim bladder with wall, for the type I male midshipman at frequencies 100 and 1000 Hz.

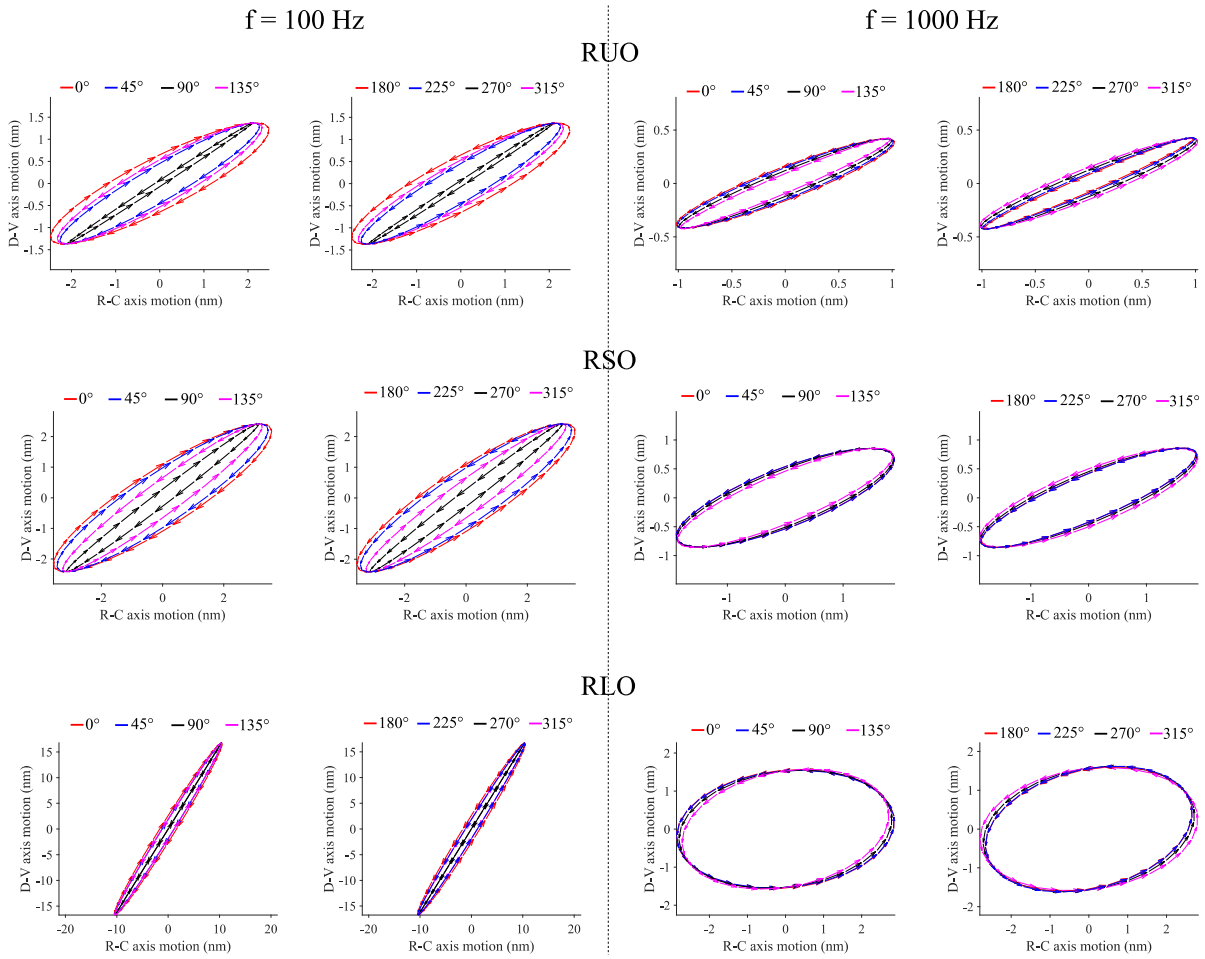

Figure S13. Projection of the motion of the COM of the right otoliths onto the vertical plane when sounds were incident from various directions in the horizontal plane in the simulations containing a swim bladder with wall, for the female midshipman at frequencies 100 and 1000 Hz.

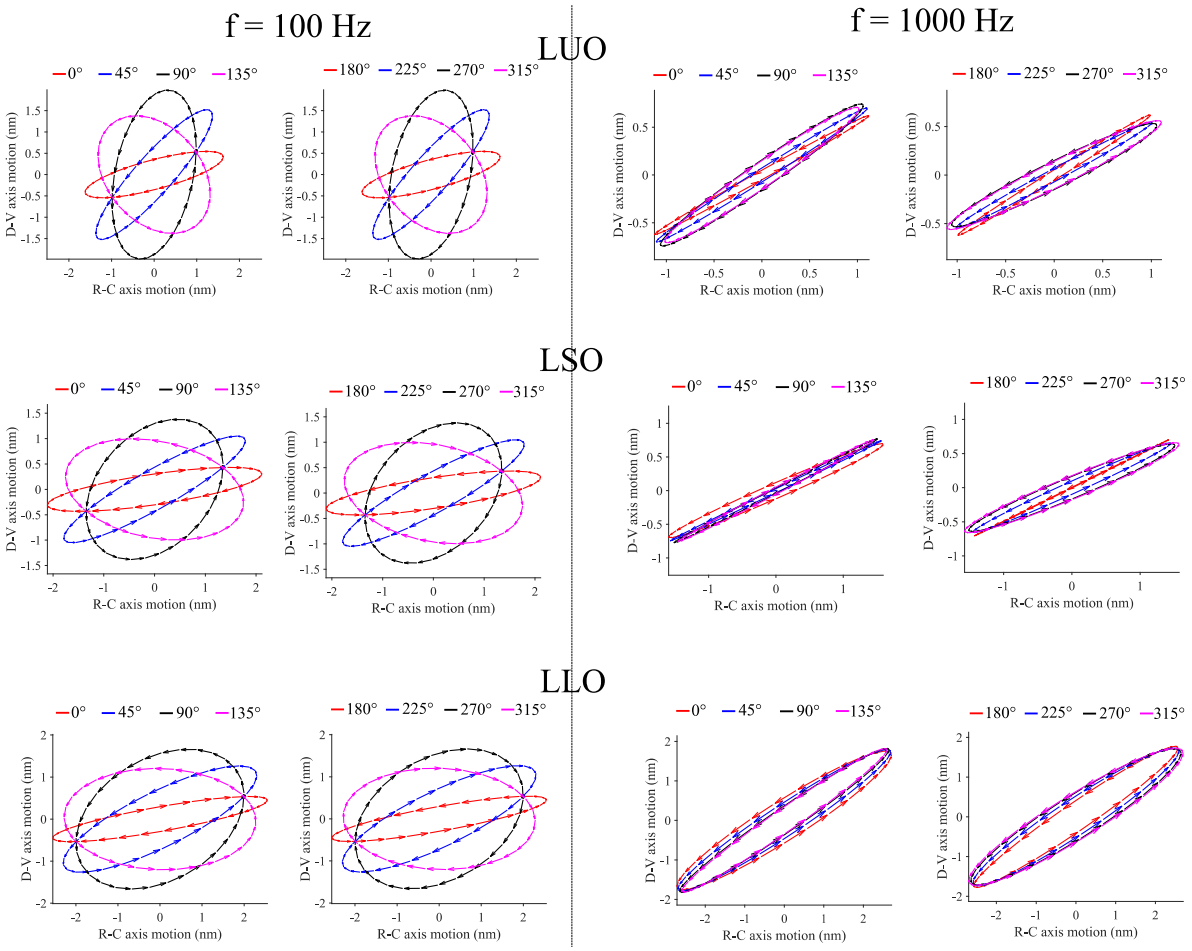

Figure S14. Projection of the motion of the COM of the left otoliths onto the vertical plane when sounds were incident from various directions in the vertical plane in the simulations containing a swim bladder with wall, for the type I male midshipman at frequencies 100 and 1000 Hz.

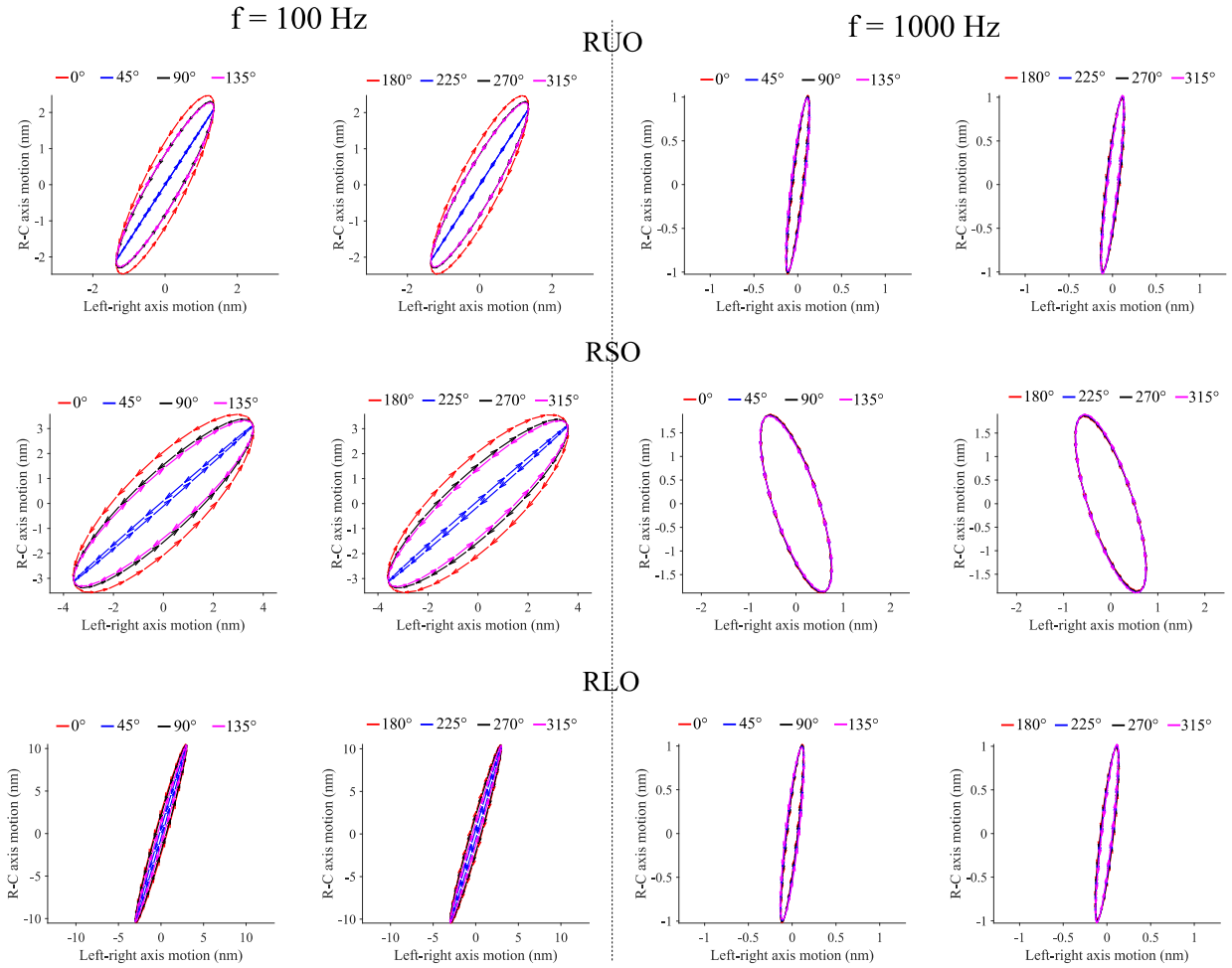

Figure S15. Projection of the motion of the COM of the right otoliths onto the horizontal plane when sounds were incident from various directions in the vertical plane in the simulations containing a swim bladder with wall, for the female midshipman at frequencies 100 and 1000 Hz.

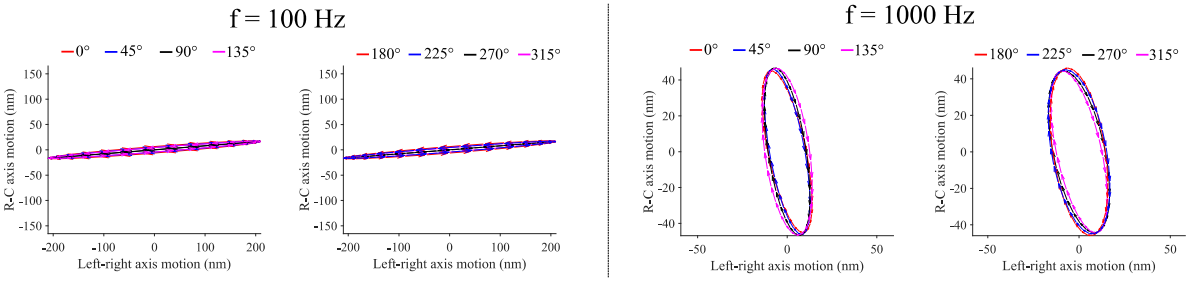

Figure S16. Projection of the motion of the tip of the right horn of the swim bladder onto the horizontal plane for sounds incident from multiple directions in the horizontal plane, at 100 and 1000 Hz, for the female midshipman.

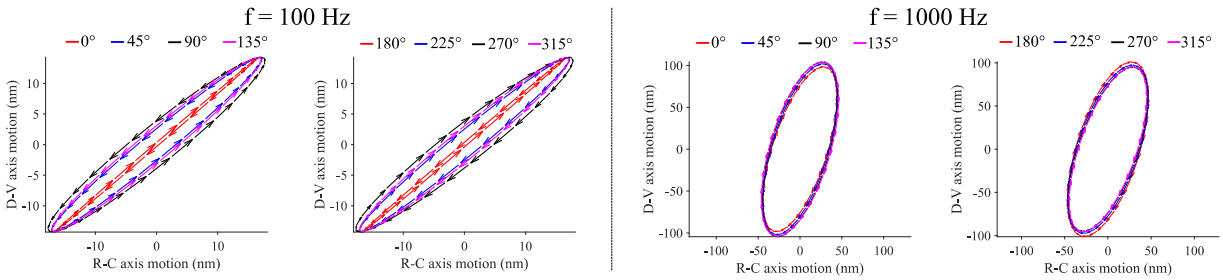

Figure S17. Projection of the motion of the tip of the right horn of the swim bladder onto the vertical plane for sounds incident from multiple directions in the horizontal plane, at 100 and 1000 Hz, for the female midshipman.

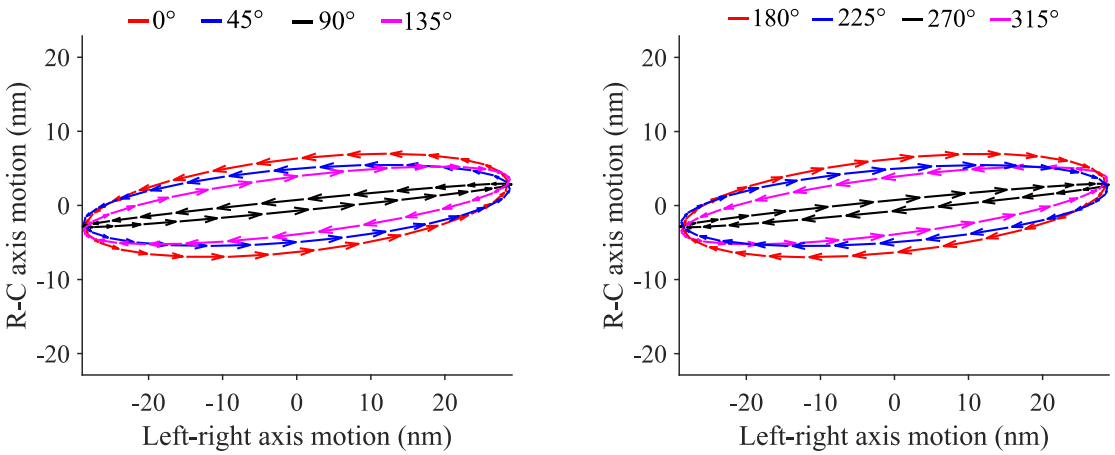

Figure S18. Projection of the motion of the tip of the left horn of the swim bladder onto the horizontal plane for sounds incident from multiple directions in the horizontal plane, at 100 Hz for the type I male midshipman.

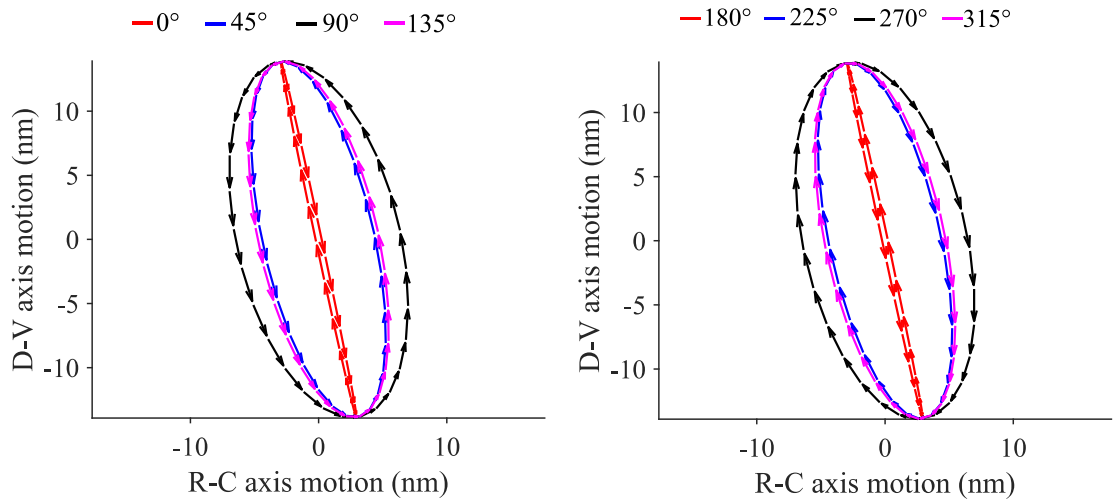

Figure S19. Projection of the motion of the tip of the left horn of the swim bladder onto the vertical plane for sounds incident from multiple directions in the horizontal plane, at 100 Hz for the type I male midshipman.

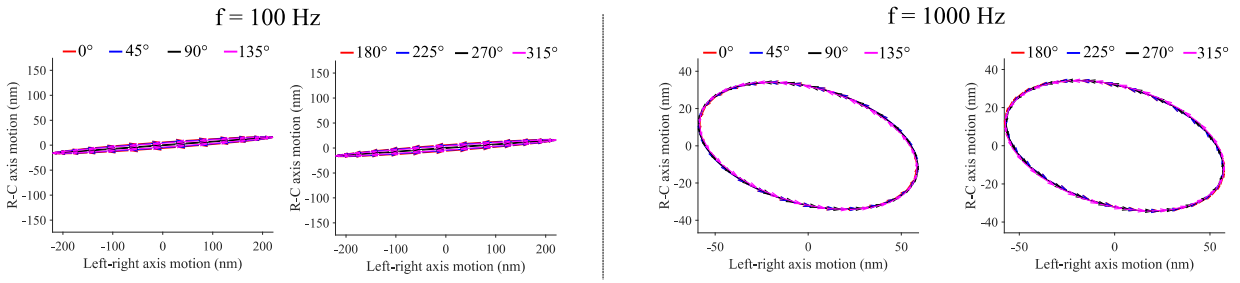

Figure S20. Projection of the motion of the tip of the right horn of the swim bladder onto the horizontal plane for sounds incident from multiple directions in the vertical plane, at 100 and 1000 Hz, for the female midshipman.

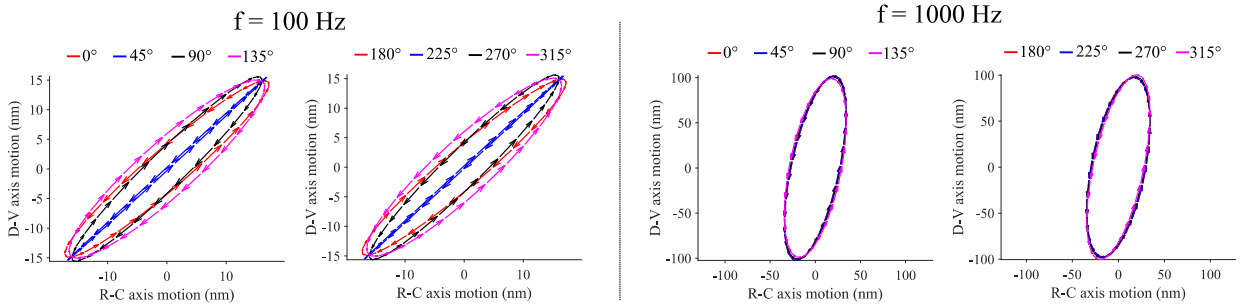

Figure S21. Projection of the motion of the tip of the right horn of the swim bladder onto the vertical plane for sounds incident from multiple directions in the vertical plane, at 100 and 1000 Hz, for the female midshipman.

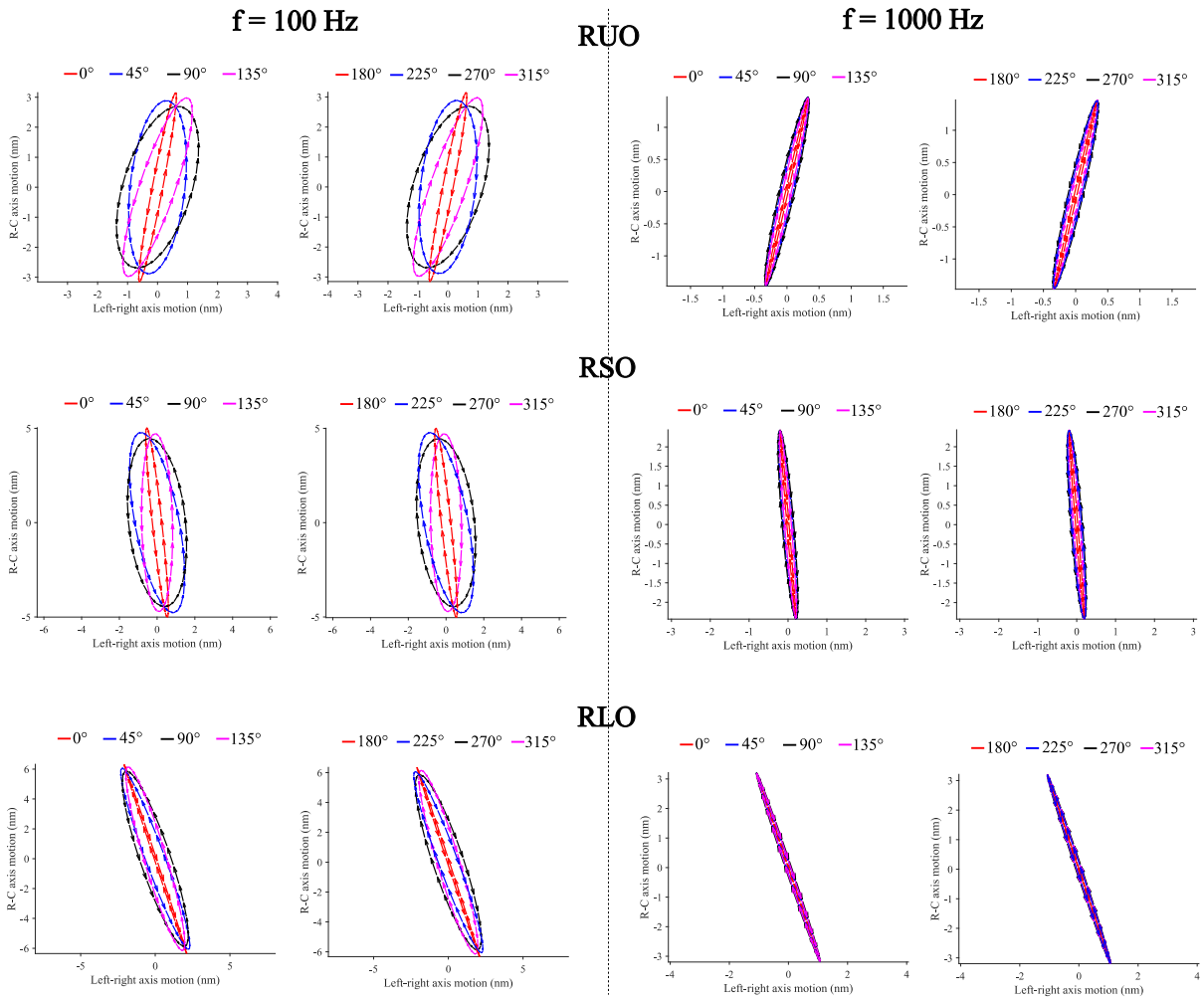

Figure S22. Projection of the motion of the COM of the right otoliths onto the horizontal plane when sounds were incident from various directions in the horizontal plane in the simulations containing an air bubble swim bladder, for the female midshipman at frequencies 100 and 1000 Hz.

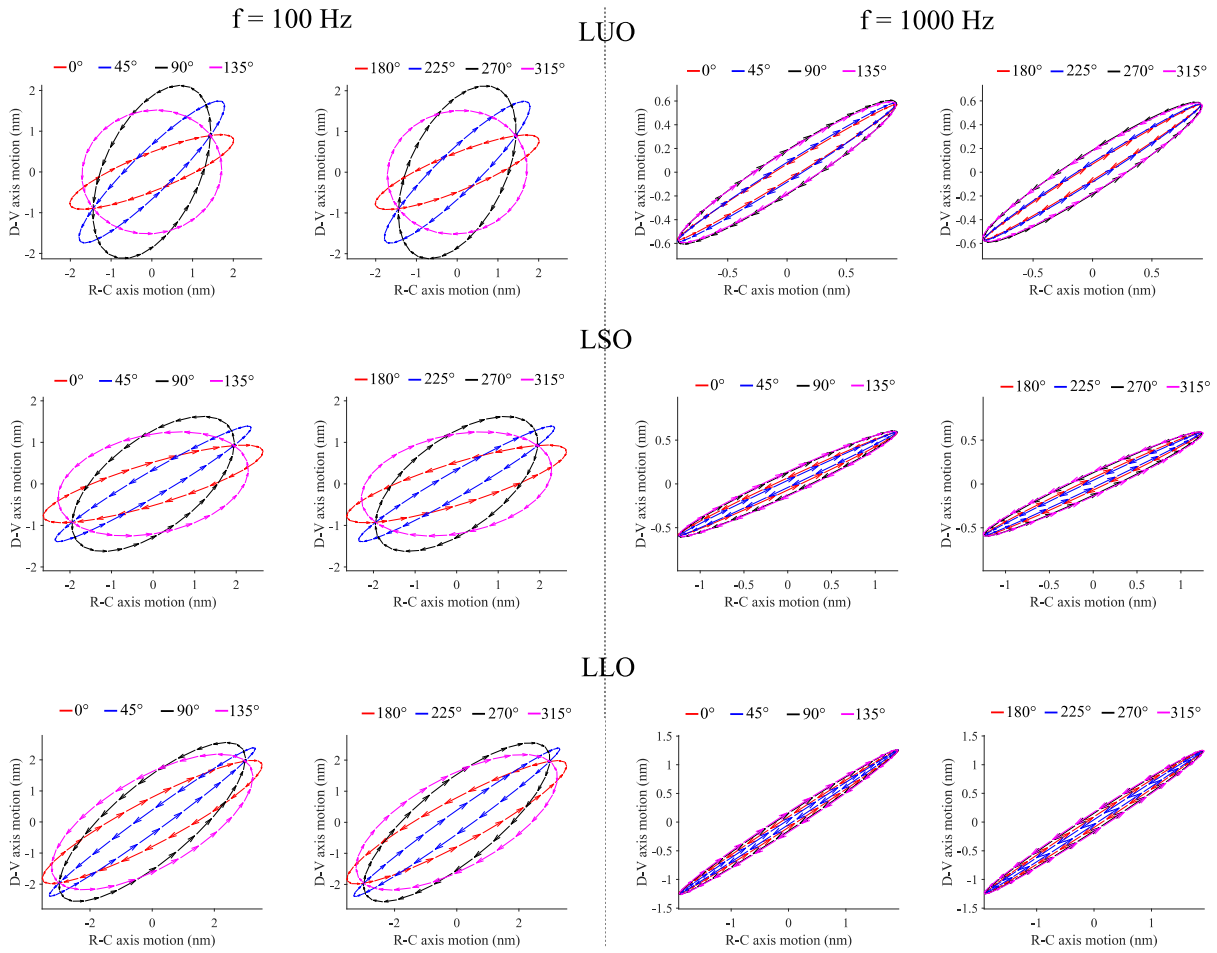

Figure S23. Projection of the motion of the COM of the left otoliths onto the vertical plane when sounds were incident from various directions in the vertical plane in the simulations containing an air bubble swim bladder, for the type I male midshipman at frequencies 100 and 1000 Hz.

Otolith	Simulation type	RC (h)°	RC (v)°	DV (h)°	DV (v)°	ML (h)°	ML (v)°
LUO	SB with wall	1.2×10^{-4}	9.2×10^{-5}	2.2×10^{-4}	3.2×10^{-4}	5.9×10^{-5}	3.8×10^{-5}
LUO	No SB	8.7×10^{-6}	1.0×10^{-6}	6.9×10^{-6}	4.3×10^{-7}	7.8×10^{-7}	1.1×10^{-6}
RUO	SB with wall	4.2×10^{-5}	7.9×10^{-5}	4.9×10^{-4}	3.7×10^{-4}	2.1×10^{-4}	1.2×10^{-4}
RUO	No SB	4.4×10^{-7}	2.8×10^{-7}	2.1×10^{-6}	4.4×10^{-6}	4.4×10^{-6}	3.1×10^{-6}
LSO	SB with wall	3.9×10^{-5}	9.5×10^{-5}	6.3×10^{-5}	1.2×10^{-4}	2.7×10^{-5}	2.2×10^{-4}
LSO	No SB	5.8×10^{-7}	3.6×10^{-6}	7.5×10^{-7}	3.8×10^{-6}	3.3×10^{-6}	4.0×10^{-6}
RSO	SB with wall	2.9×10^{-5}	6.9×10^{-5}	8.8×10^{-5}	1.3×10^{-4}	1.0×10^{-4}	2.6×10^{-4}
RSO	No SB	3.3×10^{-7}	1.7×10^{-6}	4.7×10^{-7}	5.5×10^{-7}	3.3×10^{-7}	1.6×10^{-6}
LLO	SB with wall	5.9×10^{-5}	2.1×10^{-3}	1.1×10^{-3}	1.9×10^{-3}	5.1×10^{-4}	1.3×10^{-3}
LLO	No SB	7.9×10^{-7}	4.9×10^{-6}	1.7×10^{-6}	2.0×10^{-6}	1.9×10^{-6}	4.7×10^{-6}
RLO	SB with wall	3.2×10^{-3}	5.5×10^{-4}	5.3×10^{-4}	5.7×10^{-4}	5.4×10^{-4}	5.4×10^{-4}
RLO	No SB	7.6×10^{-6}	1.4×10^{-5}	6.9×10^{-6}	3.0×10^{-6}	2.4×10^{-6}	4.9×10^{-6}

Table S1. The angles made by the rostrocaudal (RC), dorsoventral (DV), and mediolateral (ML) axes of the otoliths with the horizontal (H) and vertical (V) planes in degrees at 100 Hz when the sound was incident in the horizontal plane from the left side of the animal (90°).

Chapter 3: Natural Ambient Sounds as Sources of Biologically Relevant Information and Noise for Fishes

Published as a book chapter in the Effects of Noise on Aquatic Life, Principles and Practical Considerations
Balebail, S. and Sisneros, J. A. (2023). Natural Ambient Sounds as Sources of Biologically Relevant Information and Noise for Fishes. In The Effects of Noise on Aquatic Life : Principles and Practical Considerations (ed. Popper, A. N.), Sisneros, J.), Hawkins, A. D.), and Thomsen, F.), pp. 1–26. Cham: Springer International Publishing.

Abstract

In the field of fish bioacoustics, sounds other than conspecific communication sounds have generally been viewed as background noise interfering with the detection of communication signals. However, many fish species do not vocalize but still possess acute hearing, suggesting that fish hearing may have evolved, in part, to detect and extract information from the “ambient sounds” present in the environment. This chapter highlights some of the major sources of natural ambient sound and discusses how they function as sources of biologically relevant information. Some fishes can extract information about larval settlement sites, spawning events, food sources, and approaching predators from natural ambient sound. Instances where natural ambient sounds function as noise are also discussed. Ambient sound can mask hearing and some vocalizing fishes have been known to either produce louder vocalizations or change vocalization rates to cope with increases in ambient sound levels. Several species living in shallow water habitats vocalize at frequencies that coincide with a dip in acoustic energy in the local ambient sound spectrum. Data on the behavioral and physiological responses of fishes to natural ambient sounds remains scarce. Such information could be important for understanding how anthropogenic sounds affect the survival and reproduction of fishes.

Introduction

The International Organization for Standardization, ISO 18405:2017 document defines ambient sound as “sound that would be present in the absence of a specified activity.” “Specified activities” include the act of measuring sound, and the radiation of sound from specified sound sources. Ambient sound according to ISO is thus defined based on the perspective of a human experimenter measuring sound, where ambient sound represents the “background sound” from sources other than the one being measured.

Animals produce communication signals to convey information from one animal (sender) to another (receiver) in order to affect the behavior of the recipient (Seyfarth and Cheney 2003). A “signal” in the context of animal communication is defined as an action or behavior produced by a sender that has evolved to convey information and help the receiver make a decision, which, on average, is beneficial to both sender and receiver (Myrberg 1981; Bradbury and Vehrencamp 2011). In contrast, “cues” also provide information to a receiver, but the content has not been shaped by natural selection in order to benefit both sender and receiver (Bradbury and Vehrencamp 2011). Since it is well established that receivers detect and interpret conspecific acoustic communication signals, any sound in the environment apart from conspecific acoustic signals can be considered as ambient or background sound and a potential source of cues for an animal. In this chapter, ambient sound is thus defined from an animal’s perspective as “all the sounds impinging on the animal in a given environment apart from conspecific acoustic communication signals.”

Underwater environments are bathed in ambient sound (Hildebrand 2009; Rountree et al. 2020). Before the invention of sound-producing steamships in the early 1800s (Harris 2022), ambient sound in aquatic environments was predominantly composed of sounds generated by biotic sources such as invertebrates, fishes, and marine mammals (biophony), and abiotic sources such as wind, rainfall, and other

environmental phenomena (geophony). Despite recent increases in anthropogenic sound in many aquatic environments, natural sounds still constitute a major component of the underwater ambient sound spectrum (Hildebrand 2009; Frisk 2012).

Actinopterygian or “ray-finned” fishes are the planet’s largest and most diverse group of vertebrates (Nelson et al. 2016). At least a thousand species of ray-finned fishes (henceforth called “fishes” for brevity) have been known to actively produce sounds for communication (Looby et al. 2022), and there are likely many more vocal species. The “matched filter hypothesis” proposed by Capranica and Moffat (1983) maintains that the auditory systems of animals are tuned to detect the frequencies present in conspecific acoustic communication signals. According to this hypothesis, any sound other than that produced by a conspecific interferes with the detection of conspecific signals. However, the matched filter hypothesis does not explain why nonvocal fishes have specific tuning characteristics associated with their auditory system. The list of nonvocalizing species includes some species from families such as Cyprinidae (Jacobs and Tavolga 1967) and Mormyridae (Fletcher and Crawford 2001), which possess accessory hearing structures that improve auditory sensitivity and increase the bandwidth of hearing. Additionally, sound production is not an ancestral trait in fishes, evolving independently several times across multiple lineages (Rice et al. 2022). Therefore, since all fishes can hear (Popper et al. 2022), hearing in fishes likely evolved to detect and extract information from ambient sound in the environment.

Buckingham (1999) proposed the concept of “acoustic daylight” wherein similar to how cameras use daylight scattered from objects to form an image of the environment, ambient sound could theoretically be exploited to acoustically image the aquatic environment. Fay (2009) developed this concept in the context of fish hearing and proposed that fishes could potentially use ambient sound as acoustic daylight, extracting information about the surrounding environment. In other words, natural ambient sounds can function as “cues.” Thus, natural ambient sounds can potentially provide important behaviorally relevant information that can inform the receiver and guide a particular behavior.

In certain situations, however, natural sources of ambient sound can act as noise, masking the detection of environmental sounds important to the receiver for survival and reproduction such as mating vocalizations, sounds made by approaching predators, etc. *Here, noise is defined as any sound which interferes with the detection and interpretation of biologically relevant signals and cues important for the animal.*

This chapter highlights the major natural sources of ambient sound in the context of how such sources could provide useful information to fishes. Examples from literature on how fishes use natural ambient sounds to extract beneficial information about the environment are summarized. Cases where natural ambient sounds function as noise, interfering with the detection of relevant signals and environmental cues, are also discussed. The chapter ends with a discussion of information gaps in our understanding of how natural ambient sounds affect the physiology and behavior of fishes, and how uncovering this information could provide a more nuanced understanding of the impacts of anthropogenic sounds on fishes.

Major Sources of Natural Ambient Sounds and their Putative Biological Relevance

Natural ambient sounds can be generated by abiotic sources (geophony) and by animals (biophony). In this section, only those sources of natural ambient sound that fall within the hearing ranges of fishes will be discussed. Fishes are most sensitive to sounds below 1000 Hz, although certain fishes with hearing specializations such as ostariophysians can detect sounds up to 3 kHz (Ladich and Fay 2013), and some alosids can detect ultrasonic frequencies (30–150 kHz) (Plachta and Popper 2003). Prominent sound sources that have been omitted in the section are sounds generated by rainfall, which occur between 10–40 kHz (Scrimger et al. 1987), and sounds generated by the thermal agitation of water molecules (>50 kHz) (Hildebrand 2009). Most studies characterizing natural sources of ambient sound measure sound pressure, whereas fish ears are thought to primarily function as detectors of particle motion (Popper and

Hawkins 2018). Therefore, using sound pressure data to infer how fishes extract information from natural ambient sounds likely has limitations.

Geophony

Geophony that is within the audible range of fishes is primarily generated by: 1) weather events such as wind, 2) geological phenomena such as earthquakes, volcanoes, and release of water and smoke from hydrothermal vents, 3) sea ice, and 4) flowing and falling water (Table 1). To the best of the authors' knowledge, no data exists on the behavioral responses of fishes to geophony, and whether fishes extract information from these sound sources.

Table 1 Major sources of geophony and hypothesized biologically relevant information contained in them. See the main text for more details

Sound source		Frequency content	Hypothesized biologically relevant information contained in these sounds
1.	Wind-generated waves	~ 0.5–50 kHz (Hildebrand 2009)	Depth along the water column; and distance from the shoreline.
2.	Flowing water (rivers and brooks)	~ 10–100 Hz (Vračar and Mijić 2011; Martin and Popper 2016)	Rate of water flow; identity of different habitats such as river stretches and branch points (Velde et al. 2022).
3.	Waterfalls	< 1000 Hz (Lugli and Fine 2003)[a]	Location of jumping sites for migratory fishes such as salmon.
4.	Sea ice	~ 100–1000 Hz (Miksis-Olds et al. 2013)	–
5.	Underwater earthquakes	~ 5–35 Hz (Butler 2006)	Occurrence of earthquakes, which have been known to cause mortality in fishes.
6.	Hydrothermal vents	~ 10–250 Hz (Crone et al. 2006)	Location of hydrothermal vents.
7.	Underwater volcanoes	< ~600 Hz (Chadwick Jr. et al. 2008)	Occurrence of volcanic eruptions, which have been known to cause mortality in fishes.

[a]*The authors characterized acoustic frequencies only up to 1000 Hz;, therefore it is possible that acoustic energy is contained at frequencies >1000 Hz*

Wind-Generated Waves

Breaking waves generated at the water's surface by winds are the primary source of geophony in the oceans, with a frequency range of ~0.5–50 kHz (Hildebrand 2009). There is a strong correlation between windspeed and sound pressure levels in marine environments, even at depths of 1000–2000 m (Kurahashi and Gratta 2008). The cues used by fishes to estimate water depth are not clearly understood, although recent research suggests that hydrostatic pressure may be an important cue (Davis et al. 2021). Since wind-generated sound decays with depth (Short 2005), the presence or absence of this sound might provide fishes with a rough estimate of their vertical position along the water column. This hypothesis requires that fishes possess an internal model of how ambient sound decays with depth. Alternatively, fishes could learn to associate the loudness and spectral content of ambient sound conditions with water depth. No data currently exists, however, to support this hypothesis.

Bardyshev et al. (1973) recorded ambient sound at various distances from the shoreline and found that the ambient sound was more pulsatile closer to the shore, with large increases and decreases in the amplitude of acoustic pressure. The distribution of pressure amplitude significantly differed from a gaussian distribution up to 600 m from the shore. Beyond this distance, the distribution of pressure amplitude of ambient sound resembled that of gaussian white noise, indistinguishable from ambient

sound in the open ocean. Therefore, ambient sound from breaking waves could also potentially inform coastal fishes about their distance from the shoreline. The exact nature of how ambient sound profiles change from the shore to open ocean will depend on conditions such as the slope of the seabed, the nature of the substrate, etc.

Flowing Water (Rivers and Brooks)

Acoustic energy in rivers appears to be primarily distributed between 10–100 Hz (Vračar and Mijić 2011; Martin and Popper 2016), which falls within the range of hearing of most fishes. Vračar and Mijić (2011) found that, on average, sound pressure levels were higher in faster flowing rivers compared to two slow flowing rivers, suggesting that sound levels tend to increase with higher flow rates. Therefore, in addition to the lateral line system of fishes, which is known to sense flowing water and is important for rheotaxis (Montgomery et al. 2013), fishes might be able to obtain information about water flow rates from the loudness of the ambient sound environment.

A recent study revealed that the spectral signatures of large slow flowing rivers, small slow flowing rivers, and brooks were consistently different in sites across the Netherlands, suggesting that fishes may be able to discriminate between these habitats using spectral cues (Velde et al. 2022). The study also revealed that frequency spectra differed between river stretches and branch points, suggesting that acoustic information could potentially be used by migrating fishes to locate branch points along rivers (Velde et al. 2022). Therefore, acoustic characteristics can potentially inform fishes about different habitats in flowing water.

Waterfalls

Few studies have characterized the ambient sounds produced by waterfalls. Lugli and Fine (2003) measured low frequency sounds (0–1000 Hz) generated by waterfalls in a shallow freshwater habitat (<70 cm deep). Sound pressure levels decayed by 30 dB re 1µPa within two meters from the waterfall, suggesting that waterfalls can only be detected from close range in shallow water environments. Sounds emanating from waterfalls might be especially important for migrating fishes such as salmon, which are known to jump up waterfalls. Migrating sockeye salmon appear to have preferred locations to jump up waterfalls, which is dependent on the depth of the pool below the falls and the height of the falls (Lauritzen et al. 2005). Along with visual and hydrodynamic cues, the acoustic signature of the pool, especially the particle motion characteristics, might be important for selecting suitable locations by particle motion-sensitive salmon for jumping up waterfalls. Studies that measure the acoustic characteristics of jumping and non-jumping sites need to be carried out to determine if the ambient sound is consistently different in these two environments, which could potentially be used by migrating salmon to find suitable jumping sites.

Sea Ice

In Antarctic and Arctic waters, ambient sounds are generated by a combination of geophysical phenomenon such as thermal cracking of ice, glacial calving, and glacial waterfalls (Tegowski et al. 2011). Ambient sounds in habitats occupied by sea ice have been shown to be highly dependent on the amount of ice cover in the area, with maximum acoustic energy in the 100–1000 Hz spectral band (Miksis-Olds et al. 2013). To the best of the authors' knowledge, no studies have been conducted to determine whether sounds emanating from sea ice provide cues about relevant environmental variables such as the location of feeding and breeding sites to fishes.

Underwater Earthquakes

Earthquakes generate underwater acoustic waves called T waves, which can propagate for thousands of kilometers (Fox et al. 2001). At the seabed, T waves travel as seismoacoustic polarized interface waves (known as Ti waves). Frequencies below ~5 Hz propagate along the sediment bed and frequencies above ~5 Hz propagate as acoustic waves in the water above the seabed. The acoustic aspect of the Ti waves

contain energy primarily between 5 Hz and 35 Hz (Butler 2006), which falls within the hearing range of fishes (Sand and Karlsen 1986). Frohlich and Buskirk (1980) calculated the theoretical sound pressure levels of sounds generated by earthquakes and found that the levels are generally above the hearing thresholds of grunts (*Haernulon* species) and Atlantic cod (*Gadus morhua*). This suggests that these, and other fish species, can potentially detect underwater earthquakes. Earthquakes can cause underwater landslides, which can kill fishes and destroy habitat (Zimmerman et al. 2008). Thus, the ability to detect the sounds preceding earthquakes may potentially be adaptive to fishes, allowing them to escape the area before the earthquake strikes. More research is needed to confirm whether fishes detect and behaviorally respond to the low frequency sound waves generated by earthquakes.

Hydrothermal Vents

Hydrothermal vents produce sounds with acoustic energy primarily distributed between ~0.5 kHz and 3 kHz (Italiano et al. 2011), although majority of the energy appears to be located between ~10 Hz and 250 Hz (Crone et al. 2006). Crone et al. (2006) also found that sound pressure levels in the 0–500 Hz band measured 0.1–0.3 m from the opening of a hydrothermal vent were ~ 10–30 dB re 1µPa louder than the ambient sound in the surrounding water. The authors of this study estimated that sound pressure levels of sounds generated by vents can rise above background sound pressure levels up to ~5–15 m away from the vent opening. They suggest that hydrothermal vent sounds might function as a cue informing marine organisms about the presence of vents. Most vents are greater than 2 km deep (Baker and German 2004). Therefore, deep sea fishes may use sounds emanating from hydrothermal vents to either avoid hot fumes that are extruded from the vents or to locate prey that live close to vents. Further studies are required to explore this question.

Underwater Volcanoes

Sounds generated from underwater volcanoes are variable in nature. Some eruptions can create harmonic sounds, containing energies at integral multiples of a fundamental frequency. Other eruptions can produce more broadband sounds with acoustic energy distributed across a range of frequencies. Acoustic energy is primarily of low frequency (<~600 Hz) and explosive volcanic bursts can increase local ambient sound pressure levels by ~50 dB re 1µPa, between 10 Hz and 50 Hz (Chadwick Jr. et al. 2008). Little is known about the responses of fishes to sounds generated by volcanoes. Like earthquakes, volcanic eruptions can cause fish mortality (Caballero et al. 2023). Thus, it might be adaptive for fishes to detect sounds produced by volcanic eruptions, but such a hypothesis remains to be investigated further.

Biophony

The primary biotic sources of natural ambient sound are invertebrates such as snapping shrimp and hard-shelled invertebrates, fishes, and marine mammals (Table 2). Compared to sources of geophony, more data exists on how fishes extract biologically relevant information from biophony. However, studies characterizing the particle motion aspect of various sources of biophony are still scarce.

Table 2 Major sources of biophony, evidence for fishes extracting biologically relevant informa- tion from these sources of biophony, and additional hypothesized biologically relevant information contained in these sounds. See the main text for more details

Sound source	Frequency content	Examples of fishes extracting biologically relevant information	Additional hypothesized biologically-relevant information
1. **Invertebrates**			
a. Sound produced by snapping shrimp	~ 0.04-115 kHz (Duarte et al., 2021)	Locating coral reefs habitats (Larval fishes) (Leis et al., 2003)	-

b.	Sea urchin feeding sounds		-	Localizing reef habitats (Radford et al., 2008)
2.	**Fishes**	~ 0.01-5 kHz (Duarte et al., 2021)		
a.	Vocalizations		Location of coral reefs habitats (Larval fishes) (Tolimieri et al., 2000).	-
b.	Passive feeding sounds		Location of food (Wang et al., 2022).	-
c.	Low frequency sounds produced by struggling prey		-	Location of prey (Richard, 1968)
d.	Low frequency sounds produced by approaching predators		-	Presence of predators (Bui et al., 2013; Sand et al., 2000)
3.	**Marine mammals**	~ 0.01-340 kHz (Duarte et al., 2021)		
a.	Dolphin vocalizations		Detecting the presence of predatory dolphins (Remage-Healey et al., 2006; Luczkovich et al., 2000).	-

Invertebrates

Many invertebrate species either actively vocalize or produce sounds passively while moving or eating. Sounds generated by invertebrates encompass a wide frequency band, ranging from ~0.04 kHz to 115 kHz (Duarte et al. 2021). Snapping shrimps are usually the dominant biotic source of ambient sound in shallow tropical and sub-tropical marine environments. They produce broadband clicks with frequencies ranging primarily between 2 kHz and 20 kHz, with peak frequencies falling from 2 kHz to 5 kHz. Snapping shrimp sounds can increase local sound pressure levels by 20 dB re 1µPa, and habitats occupied by them can be as loud as 140–150 dB re 1µPa (Cato and Bell, 1992). However, since the frequencies of best hearing are usually below 1000 Hz in most fishes (Popper et al. 2019), loud sounds made by snapping shrimp are unlikely to cause hearing damage or negatively affect fish behavior. In fact, playbacks of reef sounds dominated by snapping shrimp vocalizations have been demonstrated to attract fish larvae, suggesting that snapping shrimp sounds are important cues for reef localization for larvae of coral-reef fishes (Leis et al. 2003). Grating sounds made due to the movement and feeding of hard-shelled invertebrates can also contribute to local ambient sound. Sea urchin feeding creates sounds with acoustic energy between 800 Hz and 2800 Hz, in the coastal waters of New Zealand (Radford et al. 2008). These sounds fall within the hearing range of fishes and could possibly be used by predatory fishes to locate urchins and other prey items associated with reefs. Thus, sounds produced by invertebrates could potentially be acoustic cues for locating important habitats such as coral reefs. Whether fishes use sounds from invertebrates for other purposes remains to be further investigated.

Fishes

Fish choruses are a major source of ambient sound in shallow habitats such as coral reefs (McWilliam et al. 2017), and intertidal habitats (Halliday et al. 2018). The collective ambient sound from chorusing fishes could potentially be used by hetero- specific fishes to locate habitats such as reefs and tidal estuaries. Fish vocalizations are generally major components of the playbacks of reef sounds in studies that

demonstrate the attraction of fish larvae to reef sounds (e.g., Tolimieri et al. 2004), suggesting that in coral reef environments, fish sounds can serve as important spatial cues to locate settlement sites on reefs.

Besides vocalizations, fishes also extract information about the environment from the sounds produced passively by other fishes while eating and moving. Sounds produced during feeding can inform conspecifics about the presence of food (Wang et al. 2021). Some fishes are repelled by infrasound (<20 Hz) (Sand et al. 2000; Bui et al. 2013), which is thought to be a predator avoidance response since large swimming fishes can generate infrasound (Bleckmann et al. 1991). In contrast, predatory fishes are often attracted to low frequency pulsatile sounds (Richard 1968), which are often associated with wounded or struggling prey. Thus, sounds produced passively by fishes could inform other fishes about the presence of food, predators, and prey.

Mammals

Various marine mammal groups such as cetaceans, phocids, and otariids produce underwater vocalizations in the range of 10 Hz to approximately 340 kHz depending on the species (Duarte et al. 2021). Some fishes have evolved behavioral responses to the sounds produced by predatory marine mammals, which likely reduces predation risk. Vocal activity in the Gulf toadfish (*Opsanus beta*) (Remage-Healey et al. 2006) and silver perch (Luczkovich et al. 2000) is greatly reduced when exposed to playbacks of dolphin vocalizations, but not other control sounds. Furthermore, certain members of the order Clupeiformes such as the American shad (*Alosa sapidosomma*) can detect ultrasound and at relatively high intensities can elicit an acoustic startle response by these fishes. Such a response is believed to be an antipredator adaptation to avoid echolocating odontocetes (Plachta and Popper 2003). Thus, there is evidence that fishes can obtain information about the presence of predatory mammals from their vocalizations.

Natural Ambient Sounds as Sources of Biologically Relevant Information

Few studies have been conducted on whether fishes use ambient natural sounds to extract information useful for survival and reproduction. The goldfish (*Carassius auratus*) has been shown to conduct "auditory scene analysis," which is the ability to identify and segregate the multiple sources of sound that the animal experiences at a given moment. This suggests that the goldfish and possibly other fish species may be able to identify and segregate the various sources of sound in the ambient sound spectrum and extract useful information from them. Known cases where fishes extract information about the environment from ambient sound are described in the following sections (Summarized in Table 3).

Table 3 List of examples of fishes extracting biologically relevant information from natural ambient sounds. Examples where the responses of fishes to acoustic stimuli resembling certain natural ambient sounds suggest that they have the capability to extract biologically relevant information from these natural ambient sounds have been included under "Putative examples." See the main text for more details.

Types of biologically relevant information extracted		Examples	Putative examples
1.	Location of larval settlement sites	• Larval fishes attracted to recordings of ambient reef sounds (Simpson et al. 2005, 2008; Montgomery et al. 2006). • Larval fishes attracted to sounds from specific coral reef habitats where they normally settle in but not sounds from other coral reef habitats (Radford et al. 2011). • Some larval species avoid sounds from habitats they do not	–

		generally settle in (Radford et al. 2011).	
2.	Location of spawning conspecifics	Playbacks of sounds made by chubs shaking their tails while spawning attracted conspecifics (Wang et al. 2022)	–
3.	Detection of food sources	Flower fish attracted to playbacks of worm feeding sounds (Wang et al. 2021)	• Cyprinids attracted to playbacks of sounds made while pebbles are dislodged, which may uncover hidden invertebrate prey (Holt and Johnston 2011). • Some predatory fishes attracted to low frequency pulsed sounds, thought to be produced by swimming or struggling prey (Richard 1968).
4.	Detection of predators	Some fishes reduce vocalization rates during playbacks of predatory dolphin vocalizations (Luczkovich et al. 2000; Remage-Healey et al. 2006)	• Certain fishes are repelled by infrasound (<20 Hz), thought to be generated by swimming movements of approaching predators (Sand et al. 2000). • Ultrasound evokes a startle responses in some Clupeiform fishes, which is likely an adaptation to escape predatory odontocetes (Plachta and Popper 2003).
5.	Detection of fishes possessing swim bladders	–	Goldfish (*Carassius auratus*) conditioned to detect sounds resembling scattered ambient sounds by fish swim bladders (Lewis 1994)

Location of Larval Settlement Sites

Fish larvae have been shown to be attracted to playbacks of sounds recorded from coral reefs, suggesting that fish larvae use sounds emanating from coral reefs to locate them and choose settlement sites (Montgomery et al. 2006). There is variability among taxa in the spectral components of the ambient sound spectrum preferred for settlement. Most species are preferentially attracted to the component of coral reef ambient sound spectrum primarily generated by invertebrates (>570 Hz), but other fish species demonstrate no preference for the high or low frequency components of the coral reef sound spectrum (Simpson et al. 2005, 2008).

The acoustic characteristics of different coral reef ecosystems appear to show consistent differences, which could potentially be exploited by coral fish larvae to locate preferred habitats (Radford et al. 2010). In fact, larvae of some fish species are known to demonstrate strong preferences for sounds emanating

from specific coral reef environments such as lagoons or fringing reefs, suggesting that larvae not only obtain directional information from reef sounds but also use these sounds for habitat identification (Radford et al. 2011). Parmentier et al. (2015) studied the responses of coral fish larvae of 20 fish species belonging to 10 families to ambient sound recorded from different coral reef habitats. The authors observed interspecific differences in larval attraction to playbacks of sounds recorded from the different habitats. Some species were also repulsed by sounds emanating from certain habitats. Thus, in addition to locating favorable environments, coral reef larvae also appear to be able to use ambient sound to avoid settling in specific habitats.

The acoustic environment can vary locally in a coral reef. Kennedy et al. (2010) found that the sound environment was correlated with factors such as the local density and biomass of fishes, as well as the diversity of coral and fish species. It is possible that larval fishes select different microhabitats for settlement based on their acoustic profiles, and further research on this topic is warranted.

The specific acoustic cues used to locate the sources of reef sounds remain poorly understood. Coral fish larvae could be using particle motion vectors as cues to guide them to the reef, similar to how adult female plainfin midshipman (*Porichthys notatus*) localize mating calls produced by males (Zeddies et al. 2010). In Zeddies et al. (2010), female plainfin midshipman localized a sound source ~1 m away from the animal. It has been speculated that larval fishes can localize reefs located at distances of up to 1 km from the animal (Mann et al. 2007). It is unknown if acoustic particle motion fields around coral reefs provide directional information about the location of reefs, which fish larvae could utilize to locate the reef from large distances. Alternatively, larval fishes could be climbing up intensity gradients in sound pressure, or particle motion variables (displacement, velocity, or acceleration; see Sisneros and Rogers (2016)). More research is required on the acoustic cues used by larval fishes, and how acoustic cues could be combined with other cues such as chemical cues (Atema et al. 2002) to locate reefs.

Location of Spawning Conspecifics

In several freshwater fish species, which spawn in riverbeds, both males and females are known to vigorously shake their tails while mating. This tail-shaking behavior displaces sand and gravel, and helps bury the eggs (Katano 1992b; Chuang et al. 2006). Playbacks of recorded “collision” sounds made by two species of chubs (*Opsariichthys evolans* and *Zacco platypus*) while shaking their tails during spawning, attracted more chubs of both species compared to control speakers either playing music or recorded ambient sound (Wang et al. 2022). Chubs attracted to spawning events generally tend to be satellite males or conspecifics, which cannibalize eggs (Katano 1992a, b). Thus, the presence of collision sounds in the ambient sound environment appears to provide satellite males and conspecific egg-eating chubs with information about the location of spawning pairs. Future studies should investigate if the attraction to collision sounds is present in other freshwater species which spawn in riverbeds.

Detection of Food Sources

Sounds produced during feeding can inform conspecifics about the presence of food. A few species in the family Cyprinidae are known to be attracted to playbacks of sounds that are associated with the dislodgement of pebbles during feeding in their native shallow freshwater habitat (Holt and Johnston 2011). Holt and Johnston (2011) suggest that since dislodged pebbles tend to expose hidden invertebrate prey items, the attraction of cyprinid fishes to sounds produced by pebble movement might be an adaptative or learned response for finding prey. Playbacks of sounds produced by flower fish feeding on worms attracted conspecifics (Wang et al. 2021) demonstrating that this species also obtains information about the presence of food from feeding sounds. The ability to locate food by listening to the feeding sounds made by conspecifics/heterospecifics may be present in other species and requires further investigation.

Bleckmann et al. (1991) measured the frequency content of sounds generated by the movement of five fish species: convict cichlid *Cichlasoma nigrofasciatum*, black ghost knifefish *Apteronotus albifrons*,

Mexican tetra *Astyanax fasciatus mexicanus*, striped panchax *Aplocheilus lineatus*, and rainbow trout *Salmo gairdneri*, when moving freely or startled. The frequencies of sounds produced when these fishes were tethered and struggling to escape the tether were also recorded. A fish struggling to escape from a tether resembles a naturalistic situation when a fish struggles to escape the jaws of a predator. Sounds produced by moving, tethered, and struggling fishes were primarily below 100 Hz. Predatory reef fishes such as groupers (*Epinephelus striatus*, *Mycteroperca venenosa*, and *Mycteroperca bonaci*), snappers (*Lutjanus analis*, and *Ocyurus chrysurus*), and the white margate (*Haemulon album*) have been shown to be attracted to playbacks of low frequency (25–50 Hz) pulsatile sounds (Richard 1968). The attraction of predatory reef fishes to these low frequency sounds suggests that predatory fishes can possibly detect and localize the sounds produced by swimming prey, as well as prey that are struggling to escape capture by a predator. Further studies are required to test this hypothesis.

Detection of Predators

Infrasound (<20 Hz) has been known to trigger an avoidance response in juvenile and adult salmonids, and eels (Sand et al. 2000; Bui et al. 2013). This repulsion of some fish species to infrasound has been proposed to be an adaptation to avoid predators, as approaching predators likely produce low frequency hydrodynamic sounds while swimming (Bleckmann et al. 1991). The avoidance response of species such as salmon to infrasound occur only when the fish are close to the speakers (< 2 m) (Knudsen et al. 1992), suggesting that animals only detect infrasound from sources a few body lengths away. Therefore, a sudden increase in low frequency sounds in the ambient sound environment could inform smaller prey fishes that a large animal is in close proximity to the individual.

Some vocalizing fish species appear to detect predatory dolphin vocalizations and behaviorally respond by reducing vocal activity, which presumably reduces their chances of being detected by dolphins in the natural environment (Luczkovich et al. 2000; Remage-Healey et al. 2006). Certain species of Clupeiform fishes can detect ultrasound, which is believed to be an adaptation to detect the sounds generated by predatory odontocetes during echolocation (Plachta and Popper 2003). Thus, some fishes have the ability to acquire information about the presence of predators in the environment by detecting their vocalizations in the ambient sound environment.

Detection of Fishes Possessing a Swim Bladder

Goldfish may be able to sense the presence of other individuals by detecting ambient sound scattered by the swim bladder of a nearby fish. Lewis (1994) simultaneously exposed tethered goldfish to white noise played via a speaker, as well as sound resembling scattered white noise from a fish's swim bladder, generated by a piezo- electric transducer. This experimental setup mimics a situation where another fish with a swim bladder (which scatters sound) is close to the "receiver" goldfish, while the "receiver" is experiencing white noise. Goldfish can learn to recognize the scattered white noise. Thus, the presence of ambient sound may help goldfish and possibly other fishes sense the presence of nearby fishes that possess a swim bladder, or other gas-filled chambers, especially when the fish is in a shoal of fishes that possess swim bladders. It should be noted that in the conditioning experiments carried out by Lewis (1994), the speaker relaying white noise was close to the goldfish (distance to goldfish = 36 cm) and therefore the white noise experienced by the animal was likely very different from ambient sound in a natural setting. The sound levels of ambient sound scattered by swim bladders is likely to be very low in natural environments, and it remains to be seen if goldfish and other fishes could detect the ambient sound scattered by swim bladders in natural settings.

Natural Ambient Sounds as Noise

Not all natural ambient sounds are relevant to fish survival and reproduction and such sounds are likely to be species-specific and context-specific. Below, we document cases where natural sounds have been shown to function as noise, interfering with the detection of relevant acoustic signals and cues (Table 4).

Table 4 List of examples where natural ambient sounds function as noise. Examples where the responses of fishes to nonnatural sounds suggest that increased levels of natural ambient sound could function as noise have been included under "Putative examples." Also included under the putative examples column are cases where fishes change vocal activity in responses to events, which are known to increase ambient sound levels (such as increases in wind speeds and storms). See the main text for more details

The ways in which natural ambient sounds function as noise		Examples	Putative examples
1.	Masking	• Hearing thresholds of cods (*Gadus morhua*) for pure tones increased with increased levels of natural ambient sound (Chapman and Hawkins 1973). • Auditory sensitivity to pure tones masked by playbacks of recorded ambient natural sound (Ladich 2013).	–
2.	Vocalization frequencies match "quiet windows" in the ambient sound spectrum	Peak frequency of vocalizations of several shallow water fishes lies close to ~100 Hz. This coincides with a dip in acoustic energy at ~100 Hz in the ambient sound spectra in these habitats (Lugli 2010)	–
3.	Increase in loudness of vocalizations during periods of elevated ambient sound levels	–	Blacktail shiners (*Cyprinella venusta*) increased the loudness of vocalizations of vocalizations under playbacks of white noise (Holt and Johnston 2014).
4.	Changes in vocal activity during periods of elevated ambient sound levels	–	• Brown meagre (*Sciaena umbra*) (Picciulin et al. 2012) and oyster toadfish (Luczkovich et al. 2016) increase and decrease their vocal activity respectively during increased levels of anthropogenic sound. • Pomacentrids increased calling activity during increased wind speeds, known to be correlated with ambient sound levels (Munger et al. 2022). • Calling activity of some fishes increased and others decreased during tropical storms (Locascio and Mann 2005; Boyd et al. 2021).

Masking

The presence of ambient natural sound can mask the hearing of pure tones in fishes. Chapman and Hawkins (1973) measured behavioral hearing thresholds of the cod to pure tones in the fish's natural marine environment. Hearing thresholds were dependent on the sound pressure levels of ambient sound, with thresholds increasing with increasing sound pressure levels. During the experimental period, ambient sound was primarily generated by natural sources: wind and rain. This is the only study that measured the effect of natural ambient sound on hearing in a fish's native environment.

Other studies have measured the masking effect of ambient sound on the peripheral auditory system of fishes by using the auditory evoked potential (AEP) technique. Experiments have shown that the sound levels required to generate a detectable auditory evoked potential (auditory thresholds) at the level of the peripheral auditory system for pure tones increase when recorded ambient natural sounds are simultaneously played on underwater speakers (For example, see Amoser and Ladich 2005). AEP studies on freshwater fishes have demonstrated that the physiological auditory sensitivity to pure tones is more masked (resulting in increases in auditory thresholds) in species, which possess accessory hearing structures compared to species that lack them (Ladich 2013). In contrast, the physiological auditory sensitivity (i.e., AEP thresholds) to pure tones was minimally masked in fishes that do not have hearing specializations (Vasconcelos et al. 2007; Codarin et al. 2009). Studies suggest that accessory hearing structures tend to improve physiological auditory sensitivity in fishes, especially at higher frequencies (> 1 kHz) (e.g., see Ladich 2000). Thus, it is not surprising that the generally more sensitive auditory system of fishes with accessory hearing structures appear to be more masked by increased levels of ambient sound. These results suggest that fishes with accessory hearing structures might be more susceptible to underwater noise, masking sounds important for survival (such as the sounds produced by approaching predators).

It has been pointed out that AEP techniques likely only measure the physiological auditory sensitivity of the peripheral auditory system (i.e., hair cells and auditory afferents) (Popper and Hawkins 2021). It is possible that even if sounds do not generate a detectable AEP, central processing in the brain may still allow fishes to hear these sounds. It is not known if the increased masking of the peripheral auditory system by ambient sound in fishes with accessory hearing structures translates to increased masking of hearing. More studies of hearing thresholds measured via behavioral methods under increasing levels of ambient underwater sound (such as in Chapman and Hawkins 1973) need to be performed to address this question.

While masking of pure tones by ambient sound is informative, especially for understanding the auditory physiology of the animal, it is difficult to interpret the ecological significance of these experiments. The frequency content of fish communication sounds can either be broadband, with acoustic power distributed across a large frequency range, or harmonic containing acoustic power at integral multiples of a fundamental frequency (Kaatz et al. 2017). Thus, for acoustically communicating species that use harmonic sounds as part of their communication repertoire, masking studies of pure tones by natural ambient sound could help determine how detection of conspecific communication sounds is impeded under increased levels of ambient sound. It is harder to interpret the results of masking studies for fishes, which do not communicate acoustically, or which produce more broadband communication sounds. More nuanced studies that investigate how the presence of certain kinds of environmental sounds impede the detection of sounds important for survival and reproduction (such as courtship sounds, sounds made by approaching predators, etc.) are required.

Vocalization Frequencies Match "Quiet Windows" in the Ambient Sound Spectrum

Acoustic communication in several species living in shallow water environments appear to have evolved to increase signal detectability in the presence of local ambient sound. Lugli (2010) characterized the

ambient sound spectra of the habitats occupied by nine species of goby. The habitats were classified into four categories: stony stream, spring, brackish lagoon, and rocky seashore. The peak frequency range and bandwidth of the vocalizations produced by each species coincided with the frequencies of the ambient sound spectrum that contained the least amount of energy ("quiet windows") in the fish's native habitat. This suggests that each species has evolved to maximize acoustic signal transmission in its native acoustic environment. Lugli (2010) also showed that the dominant frequencies of vocalizations produced by several fishes living in nearshore marine habitats, stony rivers and creeks, coincided with the quiet windows in the ambient sound spectra in all three habitats. The quiet window was centered around 100 Hz. Lugli (2010) hypothesized that the major reason for several shallow water fish species evolving low-frequency acoustic communication (~100 Hz) may have been to take advantage of this quiet window in ambient sound.

More studies are required to confirm if acoustic communication frequencies of shallow water species have evolved to take advantage of a quiet window in the ambient sound environment, and whether such quite windows exist in different shallow water environments. In Lugli (2010), two arbitrary spectra from two specific locations were used to demonstrate that quiet windows in nearshore marine and stony river/creek habitats occur at around 100 Hz. It remains to be seen if these quiet windows occur in other shallow water locations and if they exist near 100 Hz. Additionally, fish ears are thought to primarily function as detectors of particle motion (Popper and Hawkins 2018). The spectral content of sound pressure and particle motion can differ in aquatic environments, especially in shallow water habitats (Banner 1968; Jesus et al. 2020). Since particle motion was not measured in the study by Lugli (2010), it is unclear if the frequency spectrum of the particle motion aspect of the ambient sound environment in shallow water habitats has a dip in energy close to 100 Hz.

The overlap between the dominant frequencies of fish vocalizations and quiet windows in the ambient sound spectrum may not be a universal phenomenon. Coers et al. (2008) measured the ambient sound in the intertidal habitat of the rock-pool blenny (*Parablennius parvicornis*) and found the ambient sound spectrum to be dominated by frequencies below 250 Hz, which overlaps with the communication calls of the goby. Thus, more research is required to determine if frequencies of fish vocalizations coincide with quiet windows in local ambient sound.

Increase in Loudness of Vocalizations during Periods of Elevated Ambient Sound Levels

Vocal fish species appear to have evolved behavioral adaptations that can potentially increase the transmission and interpretability of communication signals in noisy environments. The involuntary tendency of a sender to increase vocal effort that can include increases in loudness, frequency, rate, and duration of a signal to compensate for increases in ambient sound levels is termed the Lombard effect or Lombard reflex (Summers et al. 1988). The Lombard effect has been documented in some fishes. Blacktail shiners (*Cyprinella venusta*) demonstrated an increase in the sound pressure levels of vocalizations under playbacks of white noise (Holt and Johnston 2014). Oyster toadfish (*Opsanus tau*) increased sound levels by 7 and 9 dB re 1µPa during and after passages of vessels, which temporarily increased the loudness of ambient sound (Luczkovich et al. 2016). Although fishes were exposed to non-natural sounds in these experiments (white noise and boat sounds), the fact that fishes demonstrate the Lombard effect when exposed to these sounds suggests that the ability of fish to actively increase the sound pressure levels of their signals may have evolved to increase signal transmission under increased levels of natural ambient sound. It remains to be seen whether fishes can modulate the loudness of vocalizations to improve signal transmission when the ambient sound increases in loudness due to natural causes.

Changes in Vocal Activity during Periods of Elevated Ambient Sound Levels

Data on fish vocal responses to increases in the loudness of ambient sound due to natural causes is scarce. Boyd et al. (2021) documented that during a tropical storm, underwater ambient sound levels due to abiotic sources such as wind increased at frequencies below 500 Hz. The calling rates of some fish

species increased during the storm, whereas the calling rates of other species decreased. Other environmental variables such as water level and temperature also changed during the storm, and therefore it is possible that the change in vocal activity could be driven by these other factors rather than the increase in loudness of ambient sound. Similarly, sound pressure levels of a fish chorus increased during and after a hurricane (Locascio and Mann 2005). The authors attribute the increased sound pressure levels to increased vocal activity. Munger et al. (2022) found a correlation between vocal activity of pomacentrids and wind speeds. Since ambient sound levels are known to increase with wind speed, it is possible that these fish increased vocal activity in response to increased ambient sound levels.

Fishes also appear to either increase (Picciulin et al. 2012) or reduce (Luczkovich et al. 2016) vocal activity in response to increased levels of anthropogenic sound. Thus, some fishes are capable of modulating their vocal activity to cope with increased levels of ambient sound. This increase and decrease in vocal activity has been shown in two different species, brown meagre (*Sciaena umbra*) (Picciulin et al. 2012), and oyster toadfish (Luczkovich et al. 2016), respectively. However, it is not known whether a given species can both increase or decrease their vocal activity in response to increased levels of ambient sound. Reducing vocal activity may help conserve energy for quieter periods when the probability of masking is lower. Alternatively, increasing vocal activity can likely improve signal detectability. The durations and frequencies of ambient sounds impinging on the animal may determine how fishes modify vocal activity, which needs to be investigated further.

Information Gaps on the Effect of Ambient Sounds on Fishes

This chapter summarizes the major sources of natural ambient sounds in aquatic environments and discusses how they could provide information about the environment to fishes as well as function as noise, interfering with the detection of relevant signals and cues. Existing studies likely represent a small subset of the ways in which natural ambient sounds affect fishes. Some information gaps on the biological relevance of natural ambient sounds to fishes are highlighted below.

Defining Ambient Sound from an Animal Perspective

Despite the numerous studies that characterize ambient sound, few studies have defined ambient sound from the perspective of animals. One of the few documented definitions of ambient sound from ISO 18405:2017 defines it from the perspective of a human experimenter measuring sound: any sound in the background other than the sound being quantified is considered ambient sound. However, since it is difficult to pinpoint the sounds an animal is focusing on/paying attention to in the sound environment versus the “background” sound that an animal is not focusing on, translating the ISO definition from an animal’s perspective is challenging. The only exception to this is likely conspecific communication signals, which are known to be beneficial to the sender as well as the receiver (Bradbury and Vehrencamp 2011), and therefore by definition the receiver is obligated to “pay attention” to these sounds. Therefore, in this review, all sounds impinging on an animal except conspecific communication sounds have been considered ambient sound. It is necessary to come to a consensus on a working definition of ambient sound from an animal’s perspective to limit confusion about what the term “ambient sound” entails across the bioacoustics community.

Particle Motion Content of Natural Sound Environments

Most studies that characterize ambient sound environments and the responses of fishes to ambient sound measure sound pressure and not particle motion. Particle motion is considered the primary stimulus for hearing in most fishes (Popper and Hawkins 2021). Using sound pressure to characterize sounds can still inform researchers about the temporal structure of sounds, such as, for example, the calling rates of fishes. Sound pressure data can also be used to determine the bandwidth or frequency content of sounds. However, measuring particle motion is still preferable for estimating the frequency bandwidths of ambient sounds in the context of fish hearing because the frequency content of pressure and particle motion can differ slightly in some underwater environments (For example, see Figs. 13 and

15 in Jesus et al. 2020). Hence, to better understand how fishes extract information from natural ambient sound, ambient sounds need to be characterized via particle motion (displacement, velocity, acceleration, etc.) because this is what the fish inner ear is designed to detect.

The Use of Natural Ambient Sounds as Cues

Little is known about how natural sounds function as sources of biologically relevant information, with coral fish larvae being attracted to reef sounds being the best-documented evidence of fishes using natural sounds as cues. However, there is much still to be uncovered even in this domain such as the acoustic cues used by larvae to localize reefs. To determine if a natural ambient sound source functions as a source of biologically relevant information, a correlation needs to be established between the sound and specific environments or situations. A correlation would demonstrate that the sound provides reliable information about the environment or situation, which could potentially be used by fishes. The next step would be to demonstrate a behavioral response to playbacks of these sounds, demonstrating that fishes use these sounds to guide certain behaviors. Natural sounds should be characterized as completely as possible by measuring sound pressure, particle motion (displacement, velocity, or acceleration), and other measures that define the attributes of natural sounds in a given environment such as skew, kurtosis, etc. (reviewed in detail in Wilford et al. 2021)), to determine the acoustic features of ambient sound that may provide biological relevant information about the environment. Understanding how fishes use natural ambient sounds as cues is required to predict how various sources of anthropogenic sounds such as those produced from shipping, air guns, etc., disrupt the detection of these cues and thereby disrupt behavior important for the long-term survival and reproduction of fishes.

Natural Ambient Sounds as Noise

Natural ambient sounds can also disrupt the detection of important cues and signals. Little is known about how certain natural ambient sounds can mask hearing of other biologically relevant sounds to fishes, and if fishes adjust their behavior to cope with increased levels of natural ambient sound. This information could be important for identifying anthropogenic sounds that are particularly disruptive to fishes, and the capacity of fishes to cope with anthropogenic sound.

Fish Responses to Sudden Changes in the Natural Ambient Sound Environment

Few data exist on how fish behavior is modified during periods of increased ambient sound due to natural causes such as storms or other weather-related events. Although calling activity of different fish species have been documented to change during storms (e.g., see Locascio and Mann 2005), it is difficult to rule out the effect of other variables in these studies. More studies are needed to determine if increases in natural ambient sound disrupt important behaviors such as locating mates, finding food, escaping from predators, etc.

Capacity of Fishes to Learn to Associate Ambient Sounds with Environmental Variables

It is well established that fishes can be trained to associate acoustic stimuli with positive rewards (Yan and Popper 1991) as well as aversive stimuli, such as an electric shock (Tavolga and Wodinsky 1963). The ability of fishes to associate acoustic cues with environmental variables suggests that fishes may possess the ability to learn how to extract information from natural ambient sounds that are useful for survival, such as the sounds produced by predators, sounds associated with feeding grounds, etc. More studies are required to further investigate this area of research.

Conclusion

The matched filter hypothesis by Capranica and Moffat (1983) maintains that the auditory systems of animals such as ray-finned fishes evolved to detect conspecific communication signals. This hypothesis treats any sound besides a conspecific communication sound as part of the background noise, interfering with the detection of communication sounds. This review focuses on cases where these non-

communication sounds or “ambient sounds” have been shown to provide useful biologically relevant information to fishes. Fishes are known to extract information about larval settlement sites, location of spawning conspecifics, food sources, and approaching predators, from natural ambient sounds. In some instances, however, ambient sounds can also function as noise, interfering with the detection of signals and cues, matching the predictions of Capranica and Moffat (1983). Natural ambient sounds can mask hearing, and certain vocalizing species increase their loudness or change their rate of vocalizations to cope with increases in ambient sound levels. Several species living in shallow water habitats vocalize at frequencies that coincide with a dip in acoustic energy in the local ambient sound spectrum, suggesting that these species have adapted to such environments by increasing the signal-to-noise ratio of communication sounds. The effect of natural ambient sounds on fishes remains an understudied topic. It is important to determine how ambient sounds function as cues to better understand how anthropogenic sounds could potentially disrupt these cues. Additionally, investigating whether natural ambient sounds function as noise could provide insights into the types of anthropogenic sounds that might be most disruptive to fish survival and reproduction.

References

Amoser, S. and Ladich, F. (2005). Are hearing sensitivities of freshwater fishes adapted to the ambient noise in their habitats? J. Exp. Biol. 208, 3533–3542.

Atema, J., Kingsford, M.J. and Gerlach, G. (2002). Larval reef fish could use odour for detection, retention and orientation to reefs. Mar. Ecol. Prog. Ser. 241, 151–160.

Baker, E.T. and German, C.R. (2004). On the global distribution of hydrothermal vent fields. Ocean Ridges Hydrothermal Interact Lithosphere. Oceans Geophys. Monogr. Ser. 148, 245–266.

Banner, A. (1968). Measurements of the particle velocity and pressure of the ambient noise in a shallow bay. J. Acoust. Soc. Am. 44, 1741–1742. https://doi.org/10.1121/1.1911328

Bardyshev, V.I., Kozhelapova, N.G. and Kryshnii, V.I. (1973). Study of underwater noise distributions in inland sea and coastal regions. Akust. Zh. 19, 129–132.

Bleckmann, H., Breithaupt, T., Blickhan, R. and Tautz, J. (1991). The time course and frequency content of hydrodynamic events caused by moving fish, frogs, and crustaceans. J. Comp. Physiol. A 168, 749–757. https://doi.org/10.1007/BF00224363

Boyd, A.D., Gowans, S., Mann, D.A. and Simard, P. (2021). Tropical storm Debby: soundscape and fish sound production in Tampa Bay and the Gulf of Mexico. PLoS ONE 16, e0254614. https://doi.org/10.1371/journal.pone.0254614

Bradbury, J.W. and Vehrencamp, S.L. (2011). Principles of Animal Communication. Sunderland: Sinauer Associates.

Buckingham, M.J. (1999). Acoustic daylight imaging in the ocean. Handb. Comput. Vis. Appl. 415.

Bui, S., Oppedal, F., Korsøen, Ø.J. et al. (2013). Group behavioural responses of Atlantic salmon (Salmo salar L.) to light, infrasound and sound stimuli. PLoS ONE 8, e63696.

Butler, R. (2006). Observations of polarized seismoacoustic T waves at and beneath the seafloor in the abyssal Pacific Ocean. J. Acoust. Soc. Am. 120, 3599–3606. https://doi.org/10.1121/1.2354066

Caballero, M.J., Perez-Torrado, F.J., Velázquez-Wallraf, A. et al. (2023). Fish mortality associated with volcanic eruptions in the Canary Islands. Front. Mar. Sci. 9, 999816. https://doi.org/10.3389/fmars.2022.999816

Capranica, R.R. and Moffat, A.J.M. (1983). Neurobehavioral correlates of sound communication in anurans. In Advances in Vertebrate Neuroethology (ed. J.-P. Ewert, R.R. Capranica and D.J. Ingle), pp. 701–730. Boston, MA: Springer US.

Chadwick, W.W. Jr, Cashman, K.V., Embley, R.W. et al. (2008). Direct video and hydrophone observations of submarine explosive eruptions at NW Rota-1 volcano. Mariana Arc. J. Geophys. Res. Solid Earth 113, https://doi.org/10.1029/2007JB005215

Chapman, C.J. and Hawkins, A.D. (1973). A field study of hearing in the cod, Gadus morhua L. J. Comp. Physiol. 85, 147–167. https://doi.org/10.1007/BF00696473

Chuang, L.-C., Lin, Y.-S. and Liang, S.-H. (2006). Ecomorphological comparison and habitat preference of two cyprinid fishes, Varicorhinus barbatulus and Candidia barbatus, in Hapen Creek of Northern Taiwan. Zool. Stud. 45, 114–123.

Codarin, A., Wysocki, L.E., Ladich, F. and Picciulin, M. (2009). Effects of ambient and boat noise on hearing and communication in three fish species living in a marine protected area (Miramare, Italy). Mar. Pollut. Bull. 58, 1880–1887.

Coers, A., Bouton, N., Vincourt, D. and Slabbekoorn, H. (2008). Fluctuating noise conditions may limit acoustic communication distance in the rock-pool blenny. Bioacoustics 17, 63–65. https://doi.org/10.1080/09524622.2008.9753765

Crone, T.J., Wilcock, W.S.D., Barclay, A.H. and Parsons, J.D. (2006). The sound generated by Mid-Ocean ridge black smoker hydrothermal vents. PLoS ONE 1, e133. https://doi.org/10.1371/journal.pone.0000133

Davis, V.A., Holbrook, R.I. and de Perera, T.B. (2021). Fish can use hydrostatic pressure to determine their absolute depth. Commun. Biol. 4, 1–5. https://doi.org/10.1038/s42003-021-02749-z

Duarte, C.M., Chapuis, L., Collin, S.P. et al. (2021). The soundscape of the Anthropocene Ocean. Science 371, eaba4658. https://doi.org/10.1126/science.aba4658

Fay, R. (2009). Soundscapes and the sense of hearing of fishes. Integr. Zool. 4, 26–32. https://doi.org/10.1111/j.1749-4877.2008.00132.x

Fletcher, L.B. and Crawford, J.D. (2001). Acoustic detection by sound-producing fishes (Mormyridae): the role of gas-filled tympanic bladders. J. Exp. Biol. 204, 175–183.

Fox, C.G., Matsumoto, H. and Lau, T.-K.A. (2001). Monitoring Pacific Ocean seismicity from an autonomous hydrophone array. J. Geophys. Res. Solid Earth 106, 4183–4206. https://doi.org/10.1029/2000JB900404

Frisk, G.V. (2012). Noiseonomics: the relationship between ambient noise levels in the sea and global economic trends. Sci. Rep. 2, 1–4.

Frohlich, C. and Buskirk, R.E. (1980). Can fish detect seismic waves? Geophys. Res. Lett. 7, 569–572.

Halliday, W.D., Pine, M.K., Bose, A.P. et al. (2018). The plainfin midshipman's soundscape at two sites around Vancouver Island, British Columbia. Mar. Ecol. Prog. Ser. 603, 189–200.

Harris, S.H. (2022). Robert Fulton's Demologos. Chron. Early Am. Ind. Assoc. Inc. 75, 68–70.

Hildebrand, J.A. (2009). Anthropogenic and natural sources of ambient noise in the ocean. Mar. Ecol. Prog. Ser. 395, 5–20.

Holt, D.E. and Johnston, C.E. (2011). Can you hear the dinner bell? Response of cyprinid fishes to environmental acoustic cues. Anim. Behav. 82, 529–534.

Holt, D.E. and Johnston, C.E. (2014). Evidence of the Lombard effect in fishes. Behav. Ecol. 25, 819–826.

International Organization for Standardization (2017). ISO 18405:2017. Underwater acoustics—terminology.

Italiano, F., Maugeri, R., Mastrolia, A. and Heinicke, J. (2011). SMM, a new seafloor monitoring module for real-time data transmission: an application to shallow hydrothermal vents. Procedia Earth Planet. Sci. 4, 93–98. https://doi.org/10.1016/j.proeps.2011.11.010

Jacobs, D.W. and Tavolga, W.N. (1967). Acoustic intensity limens in the goldfish. Anim. Behav. 15, 324–335. https://doi.org/10.1016/0003-3472(67)90019-X

Jesus, S.M., Xavier, F.C., Vio, R.P. et al. (2020). Particle motion measurements near a rocky shore off Cabo Frio Island. J. Acoust. Soc. Am. 147, 4009–4019. https://doi.org/10.1121/10.0001392Kaatz IM, Rice AN, Lobel PS (2017) How fishes use sound: quiet to loud and simple to complex signaling. In: reference module in life sciences. Elsevier, p B9780128096338030000

Katano, O. (1992a). Cannibalism on eggs by dark chub, Zacco temmincki (Temminck and Schlegel) (Cyprinidae). J. Fish Biol. 41, 655–661. doi:10.1111/j.1095-8649.1992.tb02692.x.

Katano, O. (1992b). Spawning tactics of paired males of the dark chub, Zacco temmincki, reflect potential fitness costs of satellites. Environ. Biol. Fish 35, 343–350.

Kennedy, E. V., Holderied, M. W., Mair, J. M., Guzman, H. M., Simpson, S. D. and Lecchini, D. (2010). Spatial patterns in reef-generated noise relate to habitats and communities: evidence from a Panamanian case study. J. Exp. Mar. Biol. Ecol. 395, 85–92.

Knudsen, F. R., Enger, P. S. and Sand, O. (1992). Awareness reactions and avoidance responses to sound in juvenile Atlantic salmon, Salmo salar L. J. Fish Biol. 40, 523–534.

Kurahashi, N. and Gratta, G. (2008). Oceanic ambient noise as a background to acoustic neutrino detection. Phys. Rev. D 78, 092001. doi:10.1103/PhysRevD.78.092001.

Ladich, F. (2000). Acoustic communication and the evolution of hearing in fishes. Philos. Trans. R. Soc. B 355, 1285–1288. doi:10.1098/rstb.2000.0685.

Ladich, F. (2013). Effects of noise on sound detection and acoustic communication in fishes. In: Brumm, H. (Ed.) Animal Communication and Noise. Springer, Berlin Heidelberg, pp. 65–90.

Ladich, F. and Fay, R. R. (2013). Auditory evoked potential audiometry in fish. Rev. Fish Biol. Fish. 23, 317–364. doi:10.1007/s11160-012-9297-z.

Lauritzen, D. V., Hertel, F. and Gordon, M. S. (2005). A kinematic examination of wild sockeye salmon jumping up natural waterfalls. J. Fish Biol. 67, 1010–1020. doi:10.1111/j.0022-1112.2005.00799.x.

Leis, J. M., Carson-Ewart, B. M., Hay, A. C. and Cato, D. H. (2003). Coral-reef sounds enable nocturnal navigation by some reef-fish larvae in some places and at some times. J. Fish Biol. 63, 724–737. doi:10.1046/j.1095-8649.2003.00182.x.

Lewis, T. N. (1994). Detection of scattered ambient noise by fish: possible passive perception of potential predators and prey from palpable pressure and particle path perturbations. PhD thesis, Georgia Institute of Technology.

Locascio, J. V. and Mann, D. A. (2005). Effects of Hurricane Charley on fish chorusing. Biol. Lett. 1, 362–365.

Looby, A., Cox, K., Bravo, S., Nielsen, K., Schram, M. and Mann, D. A. (2022). A quantitative inventory of global soniferous fish diversity. Rev. Fish Biol. Fish. 32, 581–595. doi:10.1007/s11160-022-09702-1.

Luczkovich, J. J., Daniel, H. J., Hutchinson, M., Jenkins, T., Johnson, S. E., Pullinger, R. C. and Sprague, M. W. (2000). Sounds of sex and death in the sea: bottlenose dolphin whistles suppress mating choruses of silver perch. Bioacoustics 10, 323–334. doi:10.1080/09524622.2000.9753441.

Luczkovich, J. J., Krahforst, C. S., Hoppe, H. and Sprague, M. W. (2016). Does vessel noise affect oyster toadfish calling rates? In: Popper, A. N. and Hawkins, A. D. (Eds.) The Effects of Noise on Aquatic Life II. Springer, New York, pp. 647–653.

Lugli, M. (2010). Sounds of shallow water fishes pitch within the quiet window of the habitat ambient noise. J. Comp. Physiol. A 196, 439–451. doi:10.1007/s00359-010-0528-2.

Lugli, M. and Fine, M. L. (2003). Acoustic communication in two freshwater gobies: ambient noise and short-range propagation in shallow streams. J. Acoust. Soc. Am. 114, 512–521. doi:10.1121/1.1577561.

Mann, D. A., Casper, B. M., Boyle, K. S. and Tricas, T. C. (2007). On the attraction of larval fishes to reef sounds. Mar. Ecol. Prog. Ser. 338, 307–310.

Martin, S. B. and Popper, A. N. (2016). Short- and long-term monitoring of underwater sound levels in the Hudson River (New York, USA). J. Acoust. Soc. Am. 139, 1886–1897. doi:10.1121/1.4944876.

McWilliam, J. N., McCauley, R. D., Erbe, C. and Parsons, M. J. G. (2017). Patterns of biophonic periodicity on coral reefs in the Great Barrier Reef. Sci. Rep. 7, 17459. doi:10.1038/s41598-017-15838-z.

Miksis-Olds, J. L., Stabeno, P. J., Napp, J. M., Pinchuk, A. I. and Nystuen, J. A. (2013). Ecosystem response to a temporary sea ice retreat in the Bering Sea: Winter 2009. Prog. Oceanogr. 111, 38–51. doi:10.1016/j.pocean.2012.10.010.

Montgomery, J. C., Jeffs, A., Simpson, S. D., Meekan, M. and Tindle, C. (2006). Sound as an orientation cue for the pelagic larvae of reef fishes and decapod crustaceans. In: Sims, D. W. (Ed.) Advances in Marine Biology, Vol. 51. Academic Press, pp. 143–196.

Montgomery, J., Bleckmann, H. and Coombs, S. (2013). Sensory ecology and neuroethology of the lateral line. In: Coombs, S., Bleckmann, H., Fay, R. R. and Popper, A. N. (Eds.) The Lateral Line System. Springer, New York, pp. 121–150.

Munger, J. E., Herrera, D. P., Haver, S. M., Fargione, M. J., Kotay, J. M., Bertram, J. H., Wright, T. L., Boylan, P. M. and Mann, D. A. (2022). Machine learning analysis reveals relationship between pomacentrid calls and environmental cues. Mar. Ecol. Prog. Ser. 681, 197–210. doi:10.3354/meps13912.

Myrberg, A. A. (1981). Sound communication and interception in fishes. In: Tavolga, W. N., Popper, A. N. and Fay, R. R. (Eds.) Hearing and Sound Communication in Fishes. Springer, New York, pp. 395–426.

Nelson, J. S., Grande, T. C. and Wilson, M. V. (2016). Fishes of the World. John Wiley & Sons.

Parmentier, E., Berten, L., Rigo, P., Demeulenaere, E., Ruyter, B., Vermeulen, F. and Bortz, D. M. (2015). The influence of various reef sounds on coral-fish larvae behaviour. J. Fish Biol. 86, 1507–1518.

Picciulin, M., Sebastianutto, L., Codarin, A., Ferrari, M., Ghetti, P. F., Vazzana, M., Van Parys, J. and Serafini, G. (2012). Brown meagre vocalization rate increases during repetitive boat noise exposures: a possible case of vocal compensation. J. Acoust. Soc. Am. 132, 3118–3124. doi:10.1121/1.475

Plachta, D. T. T. and Popper, A. N. (2003). Evasive responses of American shad (Alosa sapidissima) to ultrasonic stimuli. Acoust. Res. Lett. Online 4, 25–30. doi:10.1121/1.1558376.

Popper, A. N. and Hawkins, A. D. (2018). The importance of particle motion to fishes and invertebrates. J. Acoust. Soc. Am. 143, 470–488. doi:10.1121/1.5021594.

Popper, A. N. and Hawkins, A. D. (2021). Fish hearing and how it is best determined. ICES J. Mar. Sci. 78, 2325–2336. doi:10.1093/icesjms/fsab115.

Popper, A. N., Hawkins, A. D. and Sand, O. (2019). Examining the hearing abilities of fishes. J. Acoust. Soc. Am. 146, 948–955. doi:10.1121/1.5120185.

Popper, A. N., Hawkins, A. D. and Sisneros, J. A. (2022). Fish hearing “specialization” – a re-evaluation. Hear. Res. 425, 108393. doi:10.1016/j.heares.2021.108393.

Radford, C., Jeffs, A., Tindle, C. and Montgomery, J. (2008). Resonating sea urchin skeletons create coastal choruses. Mar. Ecol. Prog. Ser. 362, 37–43. doi:10.3354/meps07444.

Radford, C.A., Stanley, J.A., Tindle, C.T., Montgomery, J.C. and Jeffs, A.G., 2010. Localised coastal habitats have distinct underwater sound signatures. Marine Ecology Progress Series, 401, pp.21-29.

Radford, C. A., Stanley, J. A., Simpson, S. D. and Jeffs, A. G. (2011). Juvenile coral reef fish use sound to locate habitats. Coral Reefs 30, 295–305. doi:10.1007/s00338-010-0710-6.

Remage-Healey, L., Nowacek, D. P. and Bass, A. H. (2006). Dolphin foraging sounds suppress calling and elevate stress hormone levels in a prey species, the Gulf toadfish. J. Exp. Biol. 209, 4444–4451.

Rice, A.N., Farina, S.C., Makowski, A.J., Kaatz, I.M., Lobel, P.S., Bemis, W.E. and Bass, A.H., 2022. Evolutionary patterns in sound production across fishes. Ichthyology & Herpetology, 110(1), pp.1-12.

Richard, J. D. (1968). Fish attraction with pulsed low-frequency sound. J. Fish. Res. Board Can. 25, 1441–1452. doi:10.1139/f68-125.

Rountree, R. A., Juanes, F. and Bolgan, M. (2020). Temperate freshwater soundscapes: a cacophony of undescribed biological sounds now threatened by anthropogenic noise. PLoS One 15, e0221842. doi:10.1371/journal.pone.0221842.

Sand, O. and Karlsen, H. E. (1986). Detection of infrasound by the Atlantic cod. J. Exp. Biol. 125, 197–204. doi:10.1242/jeb.125.1.197.

Sand, O., Enger, P.S., Karlsen, H.E., Knudsen, F. and Kvernstuen, T., 2000. Avoidance responses to infrasound in downstream migrating European silver eels, Anguilla anguilla. Environmental Biology of Fishes, 57, pp.327-336.

Scrimger, J.A., Evans, D.J., McBean, G.A., Farmer, D.M. and Kerman, B.R., 1987. Underwater noise due to rain, hail, and snow. The Journal of the Acoustical Society of America, 81(1), pp.79-86.

Seyfarth, R. M. and Cheney, D. L. (2003). Signalers and receivers in animal communication. Annu. Rev. Psychol. 54, 145–173.

Short, J. R. (2005). High-frequency ambient noise and its impact on underwater tracking ranges. IEEE J. Ocean Eng. 30, 267–274.

Simpson, S.D., Meekan, M., Montgomery, J., McCauley, R. and Jeffs, A., 2005. Homeward sound. Science, 308(5719), pp.221-221.

Simpson, S.D., Meekan, M.G., Jeffs, A., Montgomery, J.C. and McCauley, R.D., 2008. Settlement-stage coral reef fish prefer the higher-frequency invertebrate-generated audible component of reef noise. Animal Behaviour, 75(6), pp.1861-1868.

Sisneros, J. A. and Rogers, P. H. (2016). Directional hearing and sound source localization in fishes. In: Sisneros, J. A. (Ed.) Fish Hearing and Bioacoustics. Springer International Publishing, Cham, pp. 121–155.

Summers, W.V., Pisoni, D.B., Bernacki, R.H., Pedlow, R.I. and Stokes, M.A., 1988. Effects of noise on speech production: Acoustic and perceptual analyses. The Journal of the Acoustical Society of America, 84(3), pp.917-928.

Tavolga, W. N. and Wodinsky, J. (1963). Auditory capacities in fishes: pure tone thresholds in nine species of marine teleosts. Bull. AMNH 126, 2.

Velde, K. te, Mairo, A., Neger, R. et al (2022). River soundscapes: Potential and vulnerability of auditory cues to migratory fish. Poster AN2022.

Tegowski, J., Deane, G. B., Lisimenka, A. and Blondel, P. (2011). Detecting and analyzing underwater ambient noise of glaciers on Svalbard as indicator of dynamic processes in the Arctic. In: Proceedings of the 4th UAM Conference. Kos, Greece, pp. 1149–1154.

Tolimieri, N., Haine, O., Jeffs, A., McCauley, R. and Montgomery, J., 2004. Directional orientation of pomacentrid larvae to ambient reef sound. Coral reefs, 23, pp.184-191.

Vasconcelos, R. O., Amorim, M. C. P. and Ladich, F. (2007). Effects of ship noise on the detectability of communication signals in the Lusitanian toadfish. J. Exp. Biol. 210, 2104–2112. doi:10.1242/jeb.004317.

Vračar, M. S. and Mijić, M. (2011). Ambient noise in large rivers (L). J. Acoust. Soc. Am. 130, 1787–1791. doi:10.1121/1.3628666.

Wang, M., Wang, Q., Ni, M., Da, W., Wang, Y., Shi, X. and Liu, G., 2021. Can feeding sound attract flower fish (Ptychobarbus kaznakovi)?. Journal of Comparative Physiology A, 207(5), pp.617-627.

Wang, Y.L., Lin, C.Y., Huang, S.P., Lee, C.Y., Tuanmu, M.N. and Wang, T.Y., 2022. Chub movement is attracted by the collision sounds associated with spawning activities. Zootaxa, 5189(1), pp.308-317.

Wilford, D.C., Miksis-Olds, J.L., Martin, S.B., Howard, D.R., Lowell, K., Lyons, A.P. and Smith, M.J., 2021. Quantitative soundscape analysis to understand multidimensional features. Frontiers in Marine Science, 8, p.672336.

Yan, H. Y. and Popper, A. N. (1991). An automated positive reward method for measuring acoustic sensitivity in fish. Behav. Res. Methods Instrum. Comput. 23, 351–356. doi:10.3758/BF03203396.

Zeddies, D.G., Fay, R.R., Alderks, P.W., Shaub, K.S. and Sisneros, J.A., 2010. Sound source localization by the plainfin midshipman fish, Porichthys notatus. The Journal of the Acoustical Society of America, 127(5), pp.3104-3113.

Zimmerman, C. E., Neal, C. A. and Haeussler, P. J. (2008). Natural hazards, fish habitat, and fishing communities in Alaska. In: American Fisheries Society Symposium, pp. 000–000.

Chapter 4: Sound-bait: A cost-effective acoustic trapping method for selective capture of fish using attractive sounds

Abstract

Marine biodiversity is threatened by various anthropogenic activities, including bycatch during commercial fishing. Methods are urgently needed to reduce bycatch. Here, we introduce Sound-bait, a low-cost acoustic trapping approach to selectively capture fish species using species-specific attractive sounds. The Sound-bait method involves creating a sound trap by placing underwater speakers inside mesh cage traps in a fish's native habitat and broadcasting attractive acoustic stimuli. Different acoustic stimuli can be broadcast on multiple traps, with the number of animals captured in each trap serving as a measure of stimulus attractiveness. We applied Sound-bait to capture the plainfin midshipman (*Porichthys notatus*) in its natural, rocky intertidal habitat. Different synthetically generated sounds resembling the mating vocalization ("hum") produced by type I male midshipman were played on the speakers to determine the sounds most effective in attracting midshipman. Preliminary experiments affirmed the importance of the fundamental frequency of the hum in luring female plainfin midshipman. Spectro-temporal alterations had minimal impact when the fundamental frequency was present, indicating its necessity and sufficiency for female attraction. Additionally, type I and type II males showed no inclination to enter traps playing hum-like stimuli. Thus, our setup allowed selective capture of female midshipman and provided insights into the frequency components of the hum most effective in attracting females. Our Sound-bait approach offers a non-invasive, cost-effective alternative for capturing fish in their natural habitats. It holds promise for reducing bycatch during commercial fishing practices. The method is adaptable for other fish species and acoustic stimuli and is potentially useful for determining the biological function of fish sounds, thereby advancing understanding of fish communication and behavior in a low-cost manner.

Introduction

Fish represent the largest and most diverse group of vertebrates in the animal kingdom (Nelson et al., 2016). They are crucial food resources for people worldwide, and the fishing industry significantly contributes to the global economy, providing livelihoods for millions. However, marine biodiversity, including several fish species, is rapidly declining in many parts of the world due to anthropogenic factors (Luypaert et al., 2020). One major contributor to this decline is the high amount of bycatch associated with commercial fishing techniques like trawling, which is estimated to be 40% of all marine catches globally (Davies et al., 2009; Kumar and Deepthi, 2006). Bycatch causes high mortality rates for endangered marine animals such as cetaceans (Read et al., 2006) and sea turtles (Finkbeiner et al., 2011). Therefore, measures are urgently needed to reduce bycatch while maintaining target fish catches.

All tested fish species can detect sound (Popper et al., 2022), and around 1,000 species are known to actively produce sounds for communication (Looby et al., 2022). Phylogenetic analysis estimates that there could be almost 22,000 sound-producing fish species worldwide (Looby et al., 2023). In many species, males produce advertisement calls to attract females for spawning (Amorim et al., 2015).

Besides conspecific vocalizations, sounds such as those from settlement site soundscapes and passive sounds during feeding and spawning are attractive to some fish species (Balebail and Sisneros, 2023). This suggests the possibility of using acoustic traps to selectively capture fish using species-specific attractive sounds.

Despite documentation of active sound production in several species, the functions of many sounds remain unknown. This gap is due to the difficulty, cost, and resources needed to capture fish and transport them to laboratories for behavioral experiments. Conducting playback studies of fish communication sounds in their natural habitats could address this issue. A number of field studies have investigated fishes' behavioral responses to acoustic stimuli, as outlined in tables VII and VIII in Mosharo and Lobel, (2023). These studies showed that many fish species are attracted to speakers playing attractive sounds in their natural habitats. These experiments have provided critical insights, such as discerning conspecific vocalizations (Myrberg & Riggio, 1985) and uncovering acoustic cues for prey localization (Myrberg et al., 1972). However, they often required expensive equipment and were labor-intensive, involving research vessels with multiple observers (e.g., Myrberg Jr et al., 1972) or trained divers (e.g., Myrberg & Riggio, 1985). Additionally, the absence of sound files and the lack of reported sound pressure levels in various studies present challenges for replication. Furthermore, utilizing techniques like videography to investigate behaviors such as phonotaxis in nocturnal fishes in the wild remains challenging.

Here, we develop “Sound-bait”, a low-cost method to selectively capture fish species using attractive sounds. Our setup was employed to assess the relative attractiveness of distinct synthetic mate-call-like stimuli to plainfin midshipman fish (*Porichthys notatus*) within its natural environment. Underwater speakers with long cables, positioned inside modified shrimp traps, were used to relay synthetically generated acoustic stimuli mimicking the mating "hums" produced by type I male midshipman (Balebail & Sisneros, 2022; McKibben & Bass, 1998). The quantity of fishes captured in each acoustic trap served as an indicator of the relative attractiveness of the various hum-like stimuli to midshipman. Detailed protocols for setting up the acoustic traps, calibrating the speakers, and the code used for sound generation are provided. While our initial focus was on finding the attractive components of mate calls, the adaptability of our experimental setup renders it suitable for use as a tool to selectively capture fishes as well as for exploring whether different sounds are attractive to fishes in shallow water environments - especially advantageous in low-light conditions when direct observation of animal behavior becomes challenging.

Methods

Study organism and test problem: perception of mating calls in the plainfin midshipman (*Porichthys notatus*)

Plainfin midshipman breed in rocky intertidal habitats throughout the West Coast of North America from late April - September (Eschmeyer and Herald, 1983; Sisneros et al., 2009). During the first half of the

breeding season, type I or “singing” males construct nests under rocks, emitting long-duration nocturnal advertisement calls, referred to as "hums," to attract females. Females likely use hums for locating nests (Zeddies et al., 2010), depositing their eggs on the nest roof after engaging in courtship rituals with the type I male (Brantley and Bass, 1994). Type I males provide parental care until the larvae hatch and depart the nest (DeMartini, 1988). Type II or “sneaker males” do not produce hums or construct nests, engaging in sneak spawning (Brantley and Bass, 1994).

Hums, the longest uninterrupted vocalizations in the animal kingdom, exhibit durations ranging from minutes to hours (Balebail and Sisneros, 2022). These vocalizations possess a highly periodic temporal structure and periodicity in the frequency domain, with the fundamental frequency (f_0) ranging from ~70-120 Hz, contingent upon the water temperature (Brantley and Bass, 1994) and body condition (Balebail and Sisneros, 2022) (Figure 1a,b). While previous research has established the sufficiency of f_0 to attract females (McKibben and Bass, 1998), the significance of the hum waveform's temporal shape (Figure 1a), and frequency domain periodicity (Figure 1b) in hum recognition remains ambiguous. To address these gaps, preliminary acoustic playback experiments were conducted using our experimental assay, aiming to elucidate the importance of the fundamental frequency, as well as the spectro-temporal structure in hum recognition and attraction.

Acoustic stimuli

For a detailed description of acoustic stimulus generation and the experimental procedure, see the Supplementary Experimental Protocol. Using custom MATLAB code (MathWorks, Natick, MA, USA), synthetic versions of three stimuli were crafted: a natural hum ("hum"), a hum with reduced energy at the fundamental frequency (f_0) relative to higher harmonics ("diminished f_0 hum"), and a hum-like buzz with energy at f_0 but distinct spectro-temporal structure compared to a natural hum (Figure 1c-h). Given the established correlation between the fundamental frequencies (f_0) of hums and temperature (Brantley and Bass, 1994), we systematically adjusted the f_0 and harmonics (where applicable) of the acoustic stimuli in direct proportion to temperature variations.

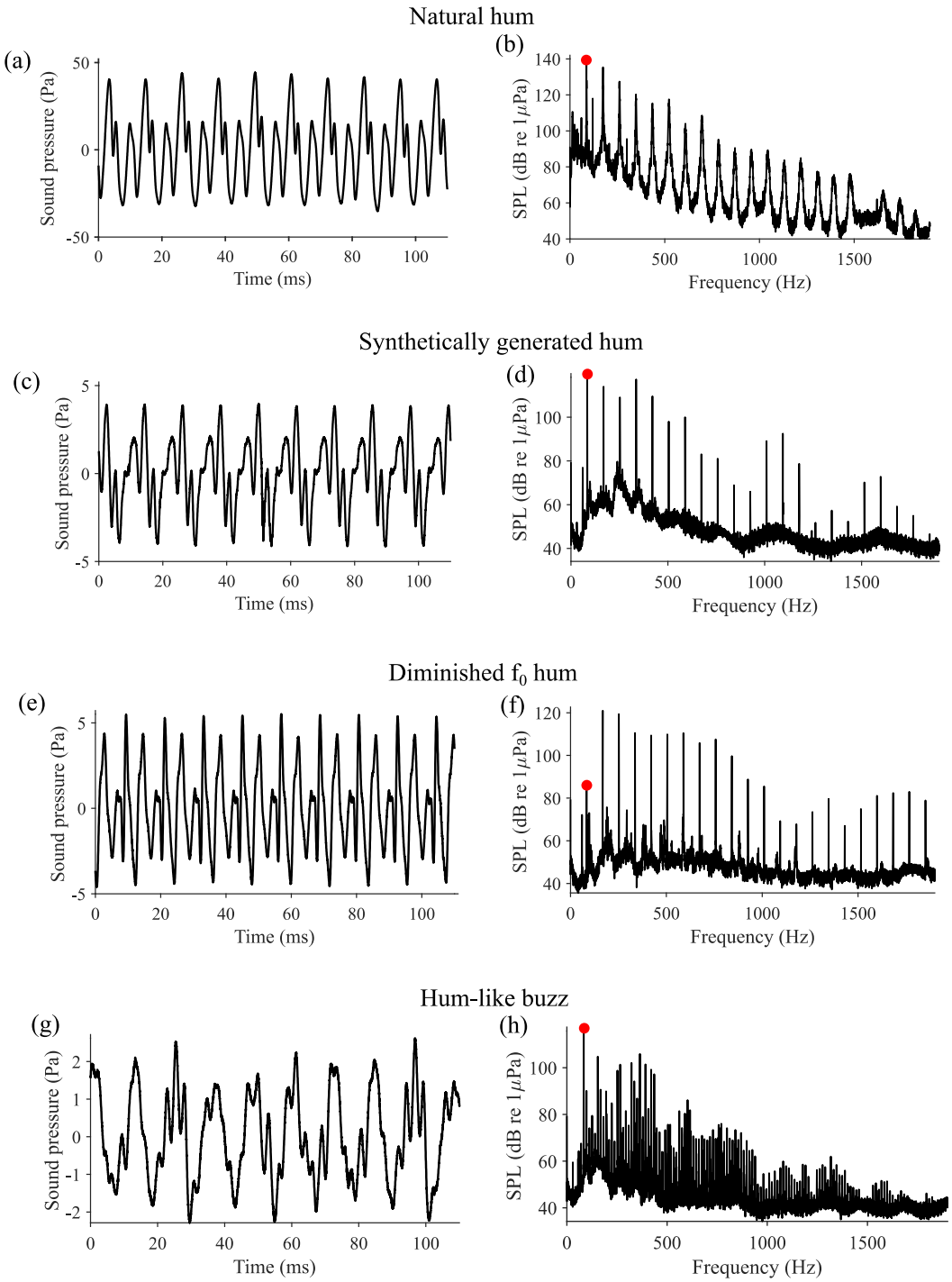

Figure 1. Temporal waveform and power spectra of a representative natural hum (a, b) and the acoustic stimuli employed in the Sound-bait acoustic trapping experiments (c-h). The power spectra were generated using the Welch method with a Hanning window of size 441000 and a 50% segment overlap. The fundamental frequency (f_0) is marked by a red dot.

Experimental setup

The main components employed in the experiments are listed in Table 1. Experiments were conducted in the rocky intertidal breeding grounds of the plainfin midshipman at Seal Rock, Brinnon, WA (Figure 2a). The experiments included four sets of acoustic-trapping experiments: 1) hum vs silent control; 2) diminished f_0 hum vs silent control; 3) hum vs hum-like buzz; and 4) hum vs hum-like buzz vs silent control. Experiments 1-3 were in 2021, and experiment 4 in 2022 (Table S1).

The experimental layout is illustrated in Figure 2b-d. For experiments 1-3, two octagonal shrimp traps (Dimensions: 61 cm × 61 cm × 21.6 cm; Seattle Marine and Fishing Supply Co., Seattle, WA, USA) were strategically positioned roughly parallel to the shoreline, 41 m offshore from the high tide line. Each trap featured four funnel-shaped openings, and an underwater speaker (Lubell AQ339, Clark Synthesis, Littleton, CO, USA) was suspended from the top center via bungee cords, approximately 10-12 cm above the ground. Trap positions were fine-tuned to ensure that the centers of the two speakers were 2 m apart. An HTI-96-mini hydrophone (Sensitivity: -164.2 dB re: 1 V/µPa; Frequency response: 2 Hz - 30kHz) (High Tech Inc., Long Beach, MS, USA) was positioned equidistant (1 m away) from each speaker. Nests within approximately 3 m of each trap were cleared to minimize the chances of females visiting nearby type I male nests instead of entering the acoustic traps. A 2.4 m tall wooden stick was secured to the ground slightly offshore from the two traps.

The layout for experiment 4 resembled experiments 1-3 with two exceptions: speaker traps were positioned 4 m apart, and a third trap positioned between the two traps with a speaker-like object served as a silent control. Additionally, the three traps were covered with fine wire mesh and flaps made from wire mesh were sewn onto trap openings, acting as one-way trap doors to prevent fish escape.

The hydrophone connected to an oscilloscope (TDS 1002, Tektronix, Beaverton, OR, USA), and each speaker linked to an amplifier (Bosch Plena PLE-1P120-US, Bosch Security Systems Inc., Fairport, NY, USA). Acoustic stimuli were relayed via mp3 players (RUIZU, Shenzen, China). Five-minute sound files corresponding to temperatures from 10-25˚C in 0.5˚C increments (anticipated water temperature range at the experimental site), for each stimulus type were stored in the mp3 players. The electronic equipment was powered by a gasoline-fueled generator (Sportsman 4,000/3,500-Watt, Buffalo Corporation, Missouri, USA). The experimental setup was typically assembled between approximately 9:30 am - 3 pm, during the lowest low tides for site accessibility.

Component function	Device used	Device model
Power source for all electronic equipment	Gasoline powered generator	Sportsman 4,000/3,500-Watt
Acoustic stimuli playback	Underwater speakers	Lubell AQ339 with 61 m long electric cables, Clark Synthesis
Audio input	Mp3 players	RUIZU
Audio signal amplification	Audio amplifiers	Bosch Plena PLE-1P120-US, Bosch Security Systems Inc.

Trapping fish attracted to acoustic stimuli	Octagonal shrimp trap	Seattle Marine and Fishing Supply Co.
Detecting acoustic stimuli	Hydrophone	HTI-96-mini with 61 m long electric cable, High Tech Inc.
Recording playback sounds	Audio recorder	Zoom H2 digital recorder
Real time sound visualization	Oscilloscope	TDS 1002, Tektronix
Measuring water temperature near traps	Data logger	HOBO Pendant MX Water Temperature Data Logger

Table 1. Overview of the key components comprising the experimental setup utilized in the Sound-bait acoustic trapping experiments.

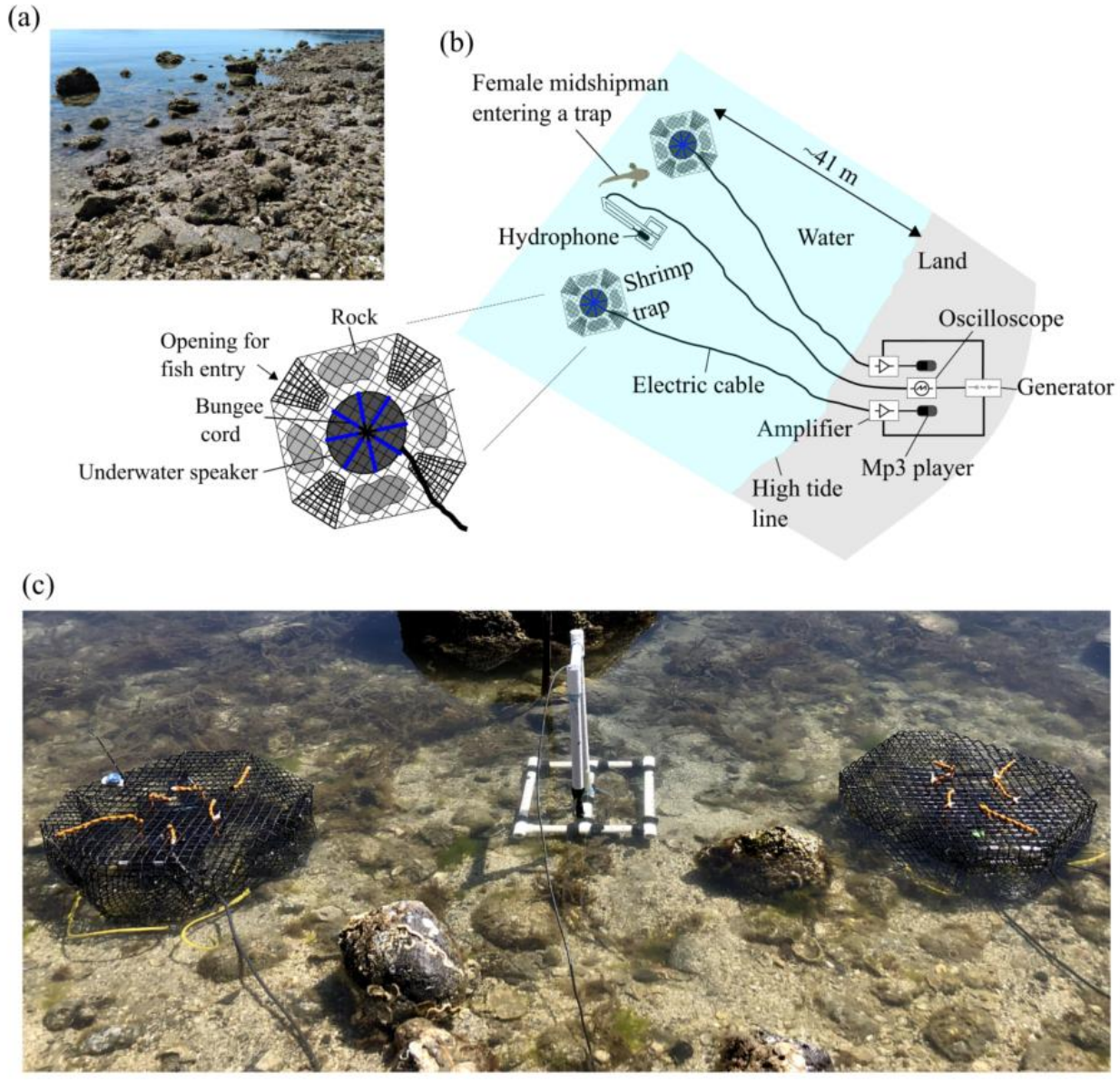

Figure 2. (a) Rocky intertidal breeding habitat of the plainfin midshipman at Seal Rock, Brinnon, WA, USA. (b) Illustration of the experimental setup, featuring a close-up of the shrimp trap containing the

underwater speaker used to relay acoustic stimuli. (c) Photograph capturing the experimental setup as the tide began to submerge the traps and the hydrophone.

Experimental procedure

Acoustic playbacks ran from 9 pm to 6 am, with all stimuli (Apart from the silent control) consistently played at 127.2 dB re 1µPa, 1 m away. Water temperature was measured every 3 hours to the nearest 0.1˚C by casting a data logger (HOBO Pendant MX Water Temperature Data Logger, Bourne, MA) towards the fish traps' location using a fishing rod. The sound file corresponding to the nearest 0.5˚C interval in the mp3 player (See section 2.3) was played as a loop on the speakers. Each night constituted a single trial for one of the four experiments (1-4). During late morning low tides, captured fish were sexed, and the numbers of females, type I males, and type II males in each trap was recorded. Mass and standard length of each fish was also measured. In experiments 1-3, speaker positions were randomized, and in experiment 4, speaker positions were interchanged between the right and left traps, with the silent control trap between them.

Results

Attraction of female and male plainfin midshipman to different hum-like stimuli

In the hum vs silent control experiment, the trap emitting the synthetically generated hum captured a significantly higher number of females overnight compared to the silent trap, demonstrating the attractiveness of the synthetically generated hum to females (Wilcoxon signed-rank test, $n = 8$ nights, $p < 0.01$; Figure 3a). Contrastingly, in the diminished f_0 hum vs silent control experiment, the difference in the number of females captured overnight in the trap emitting the diminished f_0 hum and the silent trap was not significant (Wilcoxon signed-rank test, $n = 7$, $p > 0.05$; Figure 3b), suggesting that reducing energy in the fundamental frequency relative to higher harmonics diminished the hum's attractiveness to females.

In the hum vs hum-like buzz experiment, the difference between the number of females captured overnight in the two traps was not significant (Wilcoxon signed-rank test, $n = 6$, $p > 0.05$; Figure 3c). However, in the hum vs hum-like buzz vs silent experiment, the type of stimulus (hum, hum-like buzz, or silent) significantly affected the number of females captured overnight in each trap (Friedman test, $n = 8$, $p < 0.01$). More females were captured overnight in the traps emitting the hum and the hum-like buzz compared to the silent trap (Conover post hoc test: $p < 0.05$ for both comparisons; Figure 3d). Importantly, there was no difference in the number of females captured overnight in traps emitting the hum and the hum-like buzz stimuli (Conover post hoc test: $p > 0.05$; Figure 3d), indicating that sounds containing the same fundamental frequency as the hum but differing drastically in spectro-temporal structure are as attractive to females as a hum.

Across all four experiments, the different types of acoustic stimuli—hum, hum-like buzz, mistuned harmonic hum, or silent—had no discernible effect on the number of type I or type II males captured

overnight in the traps (Wilcoxon signed-rank test for experiments 1-3, Friedman test and Conover post hoc test for experiment 4; Figure S1).

For each experiment conducted, the presence of type I or type II males in a trap did not influence the number of females. Spearman's rank correlation coefficients (r_s) between the number of females and type I males captured in the trap broadcasting each type of stimulus in each experiment were computed, and none of the correlation coefficients were significantly different from 0 (Table S2). Moreover, for the experiments conducted in 2022, there was no correlation between the number of type II males and females captured in any of the three traps (traps emitting the hum, hum-like buzz, or silent stimuli) (Table S3).

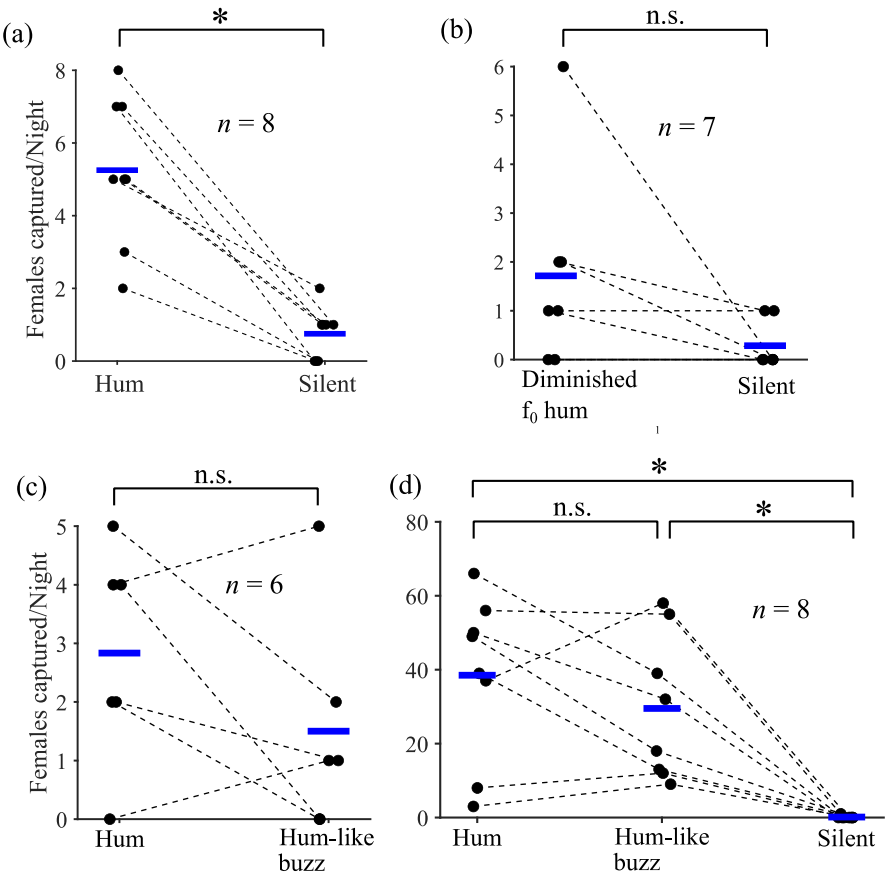

Figure 3. Overnight capture counts of females in the four Sound-bait acoustic trapping experiments: (a) Hum vs silent, (b) Diminished f_0 hum vs silent, (c) Hum vs hum-like buzz, and (d) Hum vs hum-like buzz vs silent. Refer to the text for information on the statistical tests employed for comparing the number of captured females in each trap.

Temporal Trends in the Sizes of Captured Females and Males Over the Course of the Breeding Season

Experiments 1-3 were conducted intermittently over 47 days during the spring tides between May and July 2021. The size of captured females and type I males exhibited a decreasing trend over the breeding

season. Specifically, the standard length and mass of captured females and type I males showed a negative correlation with the number of days after 5/11/2021, the date of commencement of acoustic trapping experiments (r_s = -0.45 to -0.51, n = 96 for females, and 59 for type I males, p < 0.001 for all 4 correlations; Figure 4).

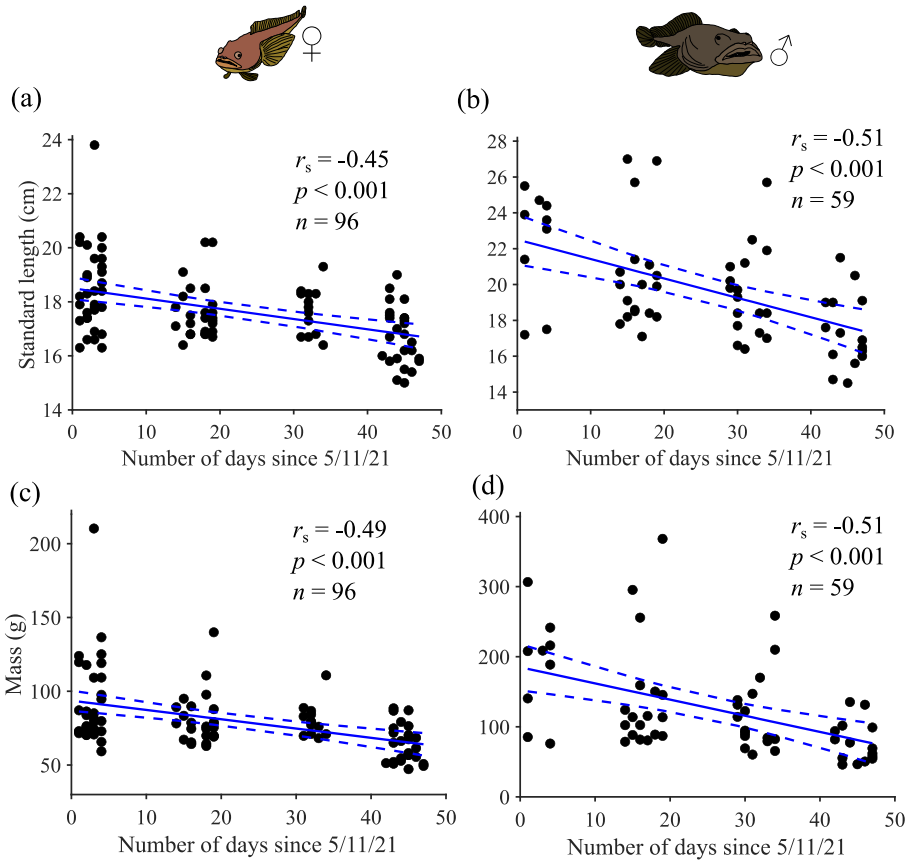

Figure 4. Temporal trends in the standard length and mass of captured females and type I males throughout the breeding season in the Sound-bait acoustic trapping experiments conducted in 2021 (experiments 1-3, detailed in the text). r_s = Spearman's rank correlation coefficient. The plots include best fit lines with corresponding 95% confidence interval bands.

Discussion

In this study, we introduced "Sound-bait," an experimental assay designed to attract fish using sound and investigate whether fish sounds are attractive to conspecifics. We explored the response of a nocturnal, acoustically communicating fish to mating vocalizations ("hums") within its natural environment. Our results align with previous tank experiments, highlighting the pivotal role of the fundamental frequency in the attractiveness of the hum to females (McKibben and Bass, 1998; Zeddies et al., 2010). Although higher harmonic frequencies may facilitate long-range hum detection (Bass and Clark, 2003), our results suggest that the fundamental frequency is necessary for females' final entry into a type I male's nest. The

equal attractiveness of the hum and hum-like buzz to females, despite distinct spectro-temporal structures, underscores the sufficiency of the fundamental frequency to attract females. Additionally, our experiments indicate that type I and type II males are unlikely to be drawn to hums and do not appear to locate nests of calling type I males by listening to hums. Consequently, our Sound-bait setup not only validates the lab-documented behavioral preferences of female midshipman to specific acoustic stimuli in natural settings but also sheds new light on the behavioral responses of male midshipman to the mating calls of other males.

While we played sounds resembling the mating hums of the plainfin midshipman, our setup can be readily adapted to capture other fish species using sounds known to attract them. Numerous past studies have demonstrated that various fish species can be attracted by playing different types of sounds in the wild (Reviewed in Mosharo and Lobel, 2023). However, many of these studies did not report the parameters required to replicate the findings, such as the equipment used and the procedures for ensuring specific sound pressure levels. We have provided a detailed description of the methodology and code used to set up our acoustic trapping experiments, enabling others to implement our methodology to capture their target species. Given the significant bycatch issue with traditional fishing methods, our methodology could potentially allow commercial fishers to conduct pilot studies to determine which sounds are attractive to their respective fish species before adapting the method to work smoothly with commercial fishing techniques like trawling. The Sound-bait method will likely be most effective in capturing sonic species like the Atlantic cod (Rowe and Hutchings, 2006), but could also be effective for non-sonic fish species by identifying other attractive sounds, such as passive sounds produced while swimming or foraging.

Approximately 22,000 fish species are estimated to actively produce sounds, making our assay a potentially valuable tool to investigate the attractiveness of sounds across various fish species and contribute to addressing the existing knowledge gap (Looby et al., 2023). The nocturnal nature of many sonic species (McCauley and Cato, 2016) makes our acoustic-trapping assay particularly advantageous for studying the function of fish sounds, given the challenges associated with nighttime videography. Many fish species that do not vocalize still possess acute hearing. Our experimental assay can also be used to explore if fish are attracted to non-conspecific communication sounds, such as feeding sounds known to be attractive to some fish species (Wang et al., 2021). Furthermore, our experimental setup holds promise for investigating the role of sounds produced by other small aquatic taxa, including invertebrates like crabs and snapping shrimps (Au and Banks, 1998; Flood et al., 2019).

Capturing, transporting, housing, and rearing fish in a laboratory setting can incur substantial expenses, particularly due to the need for spacious aquaria to accommodate the fish, along with the necessity for precise control over factors such as salinity, aeration, and mineral content of the water. Additionally, captive fish may exhibit variations in behavioral responses to acoustic stimuli compared to their wild counterparts (Meager et al., 2011). In contrast, our setup offers a non-invasive and cost-effective means to investigate the function of vocalizations in wild fish. The total expenditure for conducting our acoustic

trapping experiments during the summers of 2021 and 2022 amounted to less than $7,000, making the study of nocturnal, shallow-water fish species particularly accessible.

The hum produced by type I male plainfin midshipman is a periodic signal in the frequency domain, containing acoustic energy at integral multiples of a fundamental frequency, forming a multi-harmonic complex. Fay's (2005) experiments showed that goldfish (*Carassius auratus*) conditioned to multi-harmonic complexes missing the fundamental could generalize this stimulus to one containing the fundamental frequency. This suggests that goldfish can perceive the periodicity of a harmonic complex even without the fundamental frequency. In contrast, our experiments using the Sound-bait method showed a decrease in the number of females captured when acoustic energy at the fundamental frequency of the hum was reduced. Thus, we found no evidence of female midshipman perceiving the periodicity of hums in the absence of the fundamental frequency. More experiments are required to test if female midshipman can perceive the frequency periodicity of hums.

The marked increase in the number of females captured in 2022, as seen in Figure 3d compared to Figures 3a-c, is likely due to improvements in trap design, such as the addition of netting and trap doors, which likely reduced escape rates. While a higher female population in 2022 cannot be ruled out, trap modifications offer a more probable explanation. No type II males were captured in 2021, but a few were captured in 2022. This is likely due to their smaller size compared to females, which may have allowed them to escape through the mesh before the addition of netting. The number of type II males captured did not differ significantly between silent traps and those playing hum or hum-like buzz stimuli (Fig. S1e), suggesting that type II males may not rely on phonotaxis to locate the nests of type I males.

The sizes of captured females and type I males decreased over the course of the breeding season. This suggests that larger females mature and arrive earlier in the breeding season. For type I males, two possibilities exist: larger males arrive earlier, or they secure prime nesting sites, and smaller, nestless males enter traps later in the season. Consequently, our setup holds promise for monitoring the structure of fish populations, offering a potentially less ecologically damaging alternative to traditional techniques such as trawling for luring and capturing fish for research or monitoring purposes.

References

Amorim, M. C. P., Vasconcelos, R. O. and Fonseca, P. J. (2015). Fish Sounds and Mate Choice. In Sound Communication in Fishes (ed. Ladich, F.), pp. 1–33. Vienna: Springer Vienna.

Au, W. W. and Banks, K. (1998). The acoustics of the snapping shrimp Synalpheus parneomeris in Kaneohe Bay. The Journal of the Acoustical Society of America 103, 41–47.

Balebail, S. and Sisneros, J. A. (2022). Long duration advertisement calls of nesting male plainfin midshipman fish are honest indicators of size and condition. Journal of Experimental Biology 225, jeb243889.

Balebail, S. and Sisneros, J. A. (2023). Natural Ambient Sounds as Sources of Biologically Relevant Information and Noise for Fishes. In The Effects of Noise on Aquatic Life : Principles and Practical Considerations (ed. Popper, A. N.), Sisneros, J.), Hawkins, A. D.), and Thomsen, F.), pp. 1–26. Cham: Springer International Publishing.

Bass, A. H. and Clark, C. W. (2003). The Physical Acoustics of Underwater Sound Communication. In Acoustic Communication (ed. Simmons, A. M.), Fay, R. R.), and Popper, A. N.), pp. 15–64. New York: Springer-Verlag.

Brantley, R. K. and Bass, A. H. (1994). Alternative male spawning tactics and acoustic signals in the plainfin midshipman fish Porichthys notatus Girard (Teleostei, Batrachoididae). Ethology 96, 213–232.

Davies, R. W. D., Cripps, S. J., Nickson, A. and Porter, G. (2009). Defining and estimating global marine fisheries bycatch. Marine Policy 33, 661–672.

DeMartini, E. E. (1988). Spawning success of the male plainfin midshipman. I. Influences of male body size and area of spawning site. Journal of Experimental Marine Biology and Ecology 121, 177–192.

Eschmeyer, W. N. and Herald, E. S. (1983). A field guide to Pacific coast fishes: North America. Houghton Mifflin Harcourt.

Fay, R.R., 2005. Perception of pitch by goldfish. Hearing research, 205(1-2), pp.7-20.

Feng, N. Y. and Bass, A. H. (2016). “Singing” Fish Rely on Circadian Rhythm and Melatonin for the Timing of Nocturnal Courtship Vocalization. Current Biology 26, 2681–2689.

Finkbeiner, E. M., Wallace, B. P., Moore, J. E., Lewison, R. L., Crowder, L. B. and Read, A. J. (2011). Cumulative estimates of sea turtle bycatch and mortality in USA fisheries between 1990 and 2007. Biological Conservation 144, 2719–2727.

Flood, A. S., Goeritz, M. L. and Radford, C. A. (2019). Sound production and associated behaviours in the New Zealand paddle crab Ovalipes catharus. Marine Biology 166, 1–14.

Kumar, A. B. and Deepthi, G. R. (2006). Trawling and by-catch: Implications on marine ecosystem. Current Science 90, 922–931.

Looby, A., Cox, K., Bravo, S., Rountree, R., Juanes, F., Reynolds, L. K. and Martin, C. W. (2022). A quantitative inventory of global soniferous fish diversity. Rev Fish Biol Fisheries 32, 581–595.

Looby, A., Erbe, C., Bravo, S., Cox, K., Davies, H. L., Di Iorio, L., Jézéquel, Y., Juanes, F., Martin, C. W. and Mooney, T. A. (2023). Global inventory of species categorized by known underwater sonifery. Scientific Data 10, 892.

Luypaert, T., Hagan, J. G., McCarthy, M. L. and Poti, M. (2020). Status of marine biodiversity in the Anthropocene. In YOUMARES 9-The oceans: Our research, Our future: proceedings of the 2018 conference for YOUng MArine RESearcher in oldenburg, Germany, pp. 57–82. Springer International Publishing.

McCauley, R. D. and Cato, D. H. (2016). Evening choruses in the Perth Canyon and their potential link with Myctophidae fishes. The Journal of the Acoustical Society of America 140, 2384–2398.

McKibben, J. R. and Bass, A. H. (1998). Behavioral assessment of acoustic parameters relevant to signal recognition and preference in a vocal fish. The Journal of the Acoustical Society of America 104, 3520–3533.

Meager, J. J., Rodewald, P., Domenici, P., Fernö, A., Järvi, T., Skjæraasen, J. E. and Sverdrup, G. K. (2011). Behavioural responses of hatchery-reared and wild cod Gadus morhua to mechano-acoustic predator signals. Journal of Fish Biology 78, 1437–1450.

Mosharo, K. K. and Lobel, P. S. (2023). A comparison of underwater speakers for fish playback studies. The Journal of the Acoustical Society of America 154, 2365–2382.

Nelson, J. S., Grande, T. C. and Wilson, M. V. (2016). Fishes of the World. John Wiley & Sons.

Popper, A. N., Hawkins, A. D. and Sisneros, J. A. (2022). Fish hearing “specialization” – a re-evaluation. Hearing Research 425, 108393.

Read, A. J., Drinker, P. and Northridge, S. (2006). Bycatch of Marine Mammals in U.S. and Global Fisheries. Conservation Biology 20, 163–169.

Rowe, S. and Hutchings, J. A. (2006). Sound Production by Atlantic Cod during Spawning. Trans Am Fish Soc 135, 529–538.

Sisneros, J. A., Alderks, P. W., Leon, K. and Sniffen, B. (2009). Morphometric changes associated with the reproductive cycle and behaviour of the intertidal-nesting, male plainfin midshipman Porichthys notatus. Journal of Fish Biology 74, 18–36.

Wang, M., Wang, Q., Ni, M., Da, W., Wang, Y., Shi, X. and Liu, G. (2021). Can feeding sound attract flower fish (Ptychobarbus kaznakovi)? J Comp Physiol A 207, 617–627.

Zeddies, D. G., Fay, R. R., Alderks, P. W., Shaub, K. S. and Sisneros, J. A. (2010). Sound source localization by the plainfin midshipman fish, Porichthys notatus. J. Acoust. Soc. Am. 127, 11.

Supplementary material

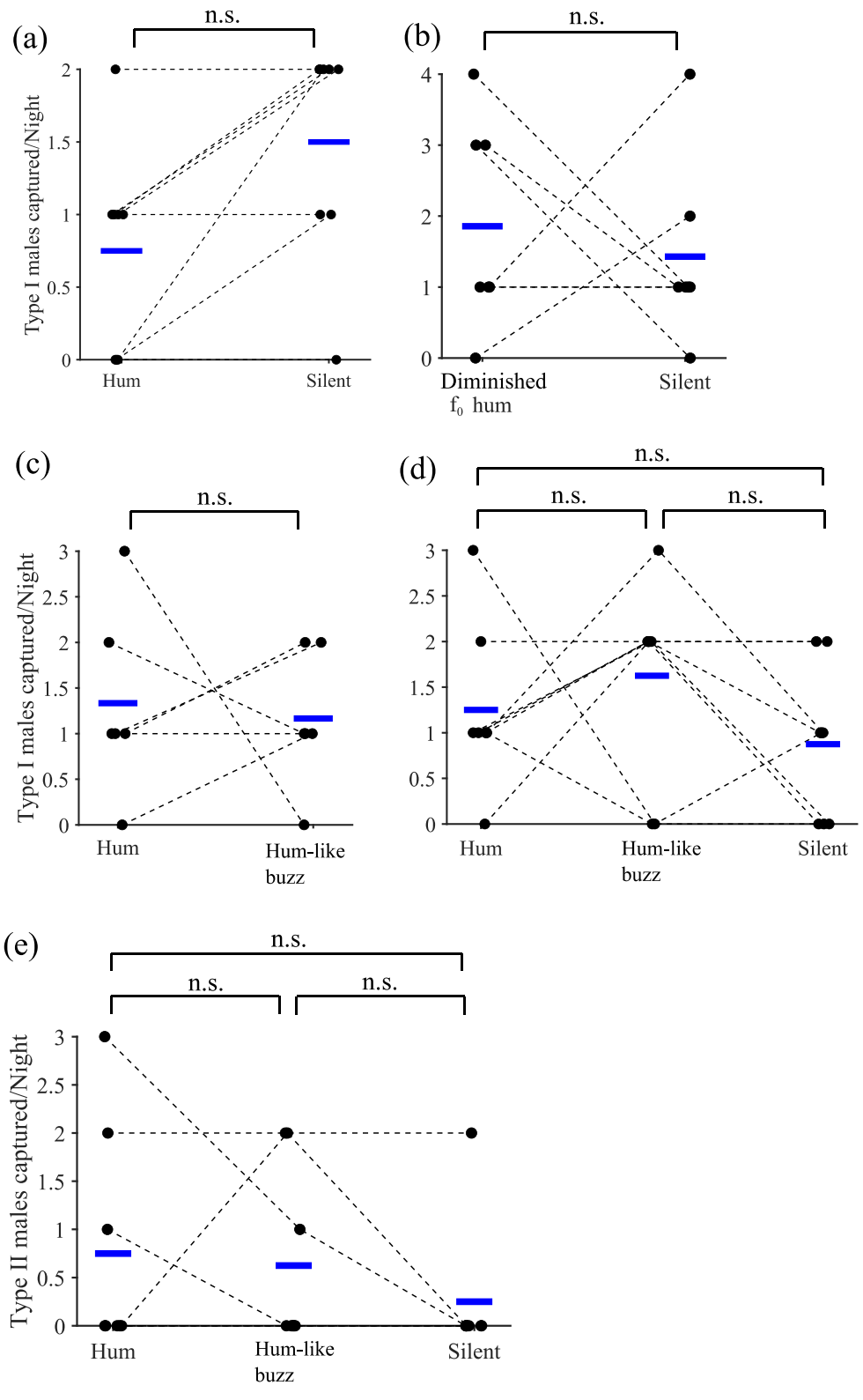

Figure S1. Number of type I males and type II captured overnight in the Sound-bait acoustic trapping experiments. No significant differences were observed in the number of type I males captured in traps

emitting different acoustic stimuli for (a) Hum vs silent control (n = 8), (b) Diminished f_0 hum vs silent control (n = 7), and (c) Hum vs hum-like buzz (n = 6) experiments, as determined by the Wilcoxon signed-rank test (p > 0.05 for a-c). Similarly, the Friedman test revealed no significant differences in the number of type I (d) and type II (e) males captured in traps broadcasting different acoustic stimuli (hum, hum-like buzz, or silent) for the hum vs hum-like buzz vs silent control experiments (p > 0.05 for d and e).

Date	Experiment conducted
5/12/2021 - 5/13/2021	Hum vs silent
5/13/2021 - 5/14/2021	Hum vs silent
5/14/2021 - 5/15/2021	Hum vs silent
5/15/2021 - 5/16/2021	Hum vs silent
5/25/2021 - 5/26/2021	Hum vs silent
5/26/2021 - 5/27/2021	Hum vs silent
5/27/2021 - 5/28/2021	Diminished f_0 hum vs silent
5/28/2021 - 5/29/2021	Diminished f_0 hum vs silent
5/29/2021 - 5/30/2021	Hum vs silent
6/9/2021 - 6/10/2021	Diminished f_0 hum vs silent
6/10/2021 - 6/11/2021	Diminished f_0 hum vs silent
6/11/2021 - 6/12/2021	Diminished f_0 hum vs silent
6/12/2021 - 6/13/2021	Hum vs silent
6/13/2021 - 6/14/2021	Diminished f_0 hum vs silent
6/14/2021 - 6/15/2021	Diminished f_0 hum vs silent
6/22/2021 - 6/23/2021	Hum vs hum-like buzz
6/23/2021 - 6/24/2021	Hum vs hum-like buzz
6/24/2021 - 6/25/2021	Hum vs hum-like buzz
6/25/2021 - 6/26/2021	Hum vs hum-like buzz
6/26/2021 - 6/27/2021	Hum vs hum-like buzz
6/27/2021 - 6/28/2021	Hum vs hum-like buzz
5/17/2022 - 5/18/2022	Hum vs hum-like buzz vs silent
5/19/2022 - 5/20/2022	Hum vs hum-like buzz vs silent
5/20/2022 - 5/21/2022	Hum vs hum-like buzz vs silent
5/29/2022 - 5/30/2022	Hum vs hum-like buzz vs silent
5/30/2022 - 5/31/2022	Hum vs hum-like buzz vs silent
5/31/2022 - 6/01/2022	Hum vs hum-like buzz vs silent
6/01/2022 - 6/02/2022	Hum vs hum-like buzz vs silent

6/02/2022 - 6/03/2022	Hum vs hum-like buzz vs silent

TABLE S1. Dates of the Sound-bait acoustic trapping experiments conducted in 2021 and 2022.

Experiment	Hum trap	Diminished f_0 hum trap	Hum-like buzz trap	Silent trap
Hum vs silent	r_s=−0.09; p=0.83; n=8	-	-	r_s=−0.63; p=0.10; n=8
Diminished f_0 hum vs silent	-	r_s=0.02; p=0.97; n=7	-	r_s=−0.17; p=0.71; n=7
Hum vs hum-like buzz	r_s=−0.44; p=0.39; n=6	-	r_s=0.61; p=0.20; n=6	-
Hum vs hum-like buzz vs silent	r_s=0.49; p=0.22; n=8	-	r_s=0.01; p=0.97; n=8	r_s=0.09; p=0.84; n=8

TABLE S2. Spearman's rank correlation coefficients (r_s) illustrating the relationship between the number of females and type I males captured in traps emitting various stimuli across each experiment. The correlation coefficients exhibited no significant deviation from 0, as determined by a t-test with a significance level (α) set at 0.05.

Experiment	Hum trap	Diminished f_0 hum trap	Hum-like buzz trap	Silent trap
Hum vs hum-like buzz vs silent	r_s=0.68; p=0.06; n=8	-	r_s=-0.17; p= 0.70; n=8	r_s=-0.14; p=0.74; n=8

TABLE S3. Spearman's rank correlation coefficients (r_s) depicting the association between the number of females and type II males captured in traps emitting various stimuli during the hum vs. hum-like buzz vs. silent control experiment. The correlation coefficients demonstrated no statistically significant deviation from 0, as determined by a t-test with a significance level (α) set at 0.05.

Procedure for conducting the "Sound-bait" Assay to investigate hum attraction in the plainfin midshipman (*Porichthys notatus*) fish

Experimental setup

- Experiments were conducted in the rocky intertidal habitat at Seal Rock, Brinnon, WA (Figure 2a) between May-July 2021, and May-June 2022. Four sets of acoustic trapping experiments were

conducted: 1) hum vs silent control; 2) diminished f_0 hum vs silent control; 3) hum vs hum-like buzz; and 4) hum vs hum-like buzz vs silent control. Experiments 1-3 were conducted in 2021, and experiment 4 was conducted in 2022 (Table S1).

- Experiments were conducted during the spring tides on days when the lowest low tide levels fell below -30 cm, providing approximately 1-2 hours of access to the rocky intertidal habitat on foot.
- Refer to figure 2b for an overview of the experimental setup. In experiments 1-3, we deployed two octagonal shrimp traps (Dimensions: 61 cm × 61 cm × 21.6 cm) obtained from Seattle Marine and Fishing Supply Co., Seattle, WA, USA. These traps were situated roughly parallel to the shoreline, positioned 41 m offshore from the high tide line and featured four funnel-shaped openings. The average mesh size of the traps was 2.54 × 2.54 cm.
- An underwater speaker (Lubell AQ339, Clark Synthesis, Littleton, CO, USA) was suspended from the top center of each trap using bungee cords, maintaining a height of approximately 10-12 cm above ground. The positions of the traps were adjusted to ensure that the centers of the two speakers were 2 m apart from each other. Rocks were strategically placed inside and, at times, on top of each trap to anchor them and prevent displacement caused by waves or undersea currents.
- An HTI-96-mini hydrophone (Sensitivity: -164.2 dB re: 1 V/µPa; Frequency response: 2 Hz - 30kHz) from High Tech Inc., Long Beach, MS, was precisely positioned between the two speakers, maintaining a distance of 1 m from each. A custom stand constructed with PVC pipes and fittings (The Home Depot Inc., USA) (Figure S2) held the hydrophone at a height of 10 cm above the ground, and stones were placed at its base to prevent displacement due to water currents.

Figure S2. Support stand for the hydrophone constructed from PVC pipes and fittings. The stand is designed with holes in the PVC pipes to enable water entry, facilitating sinking. The hydrophone is suspended from the pipe at the far left.

- Nests within approximately 3 m of each trap were manually cleared of any resident plainfin midshipman. This involved handpicking the residents and gently releasing them into the water nearby, minimizing the likelihood of approaching females visiting nearby type I male nests instead of entering our acoustic traps.
- A wooden stick was staked to the ground slightly offshore from the two traps, reaching a height of 240 cm above the seabed. Submersion of this stick by the tide was a necessary prerequisite to speaker calibration (See Experimental Procedure).

- The setup for experiment 4 mirrored the previous ones, but the two traps containing the speakers were positioned such that the centers of the two speakers were 4 m apart. The hydrophone was precisely located between the two speakers, 2 m away from each. A third trap with two glued plastic discs (resembling an underwater speaker) suspended from bungee cords was positioned roughly in between the two traps, close to the hydrophone, but positioned closer to the shore. All three traps were covered with fine netting material to minimize the chances of small fish escaping, and flaps made from netting material were sewn onto the trap openings, functioning as one-way trap doors (Figure S3).

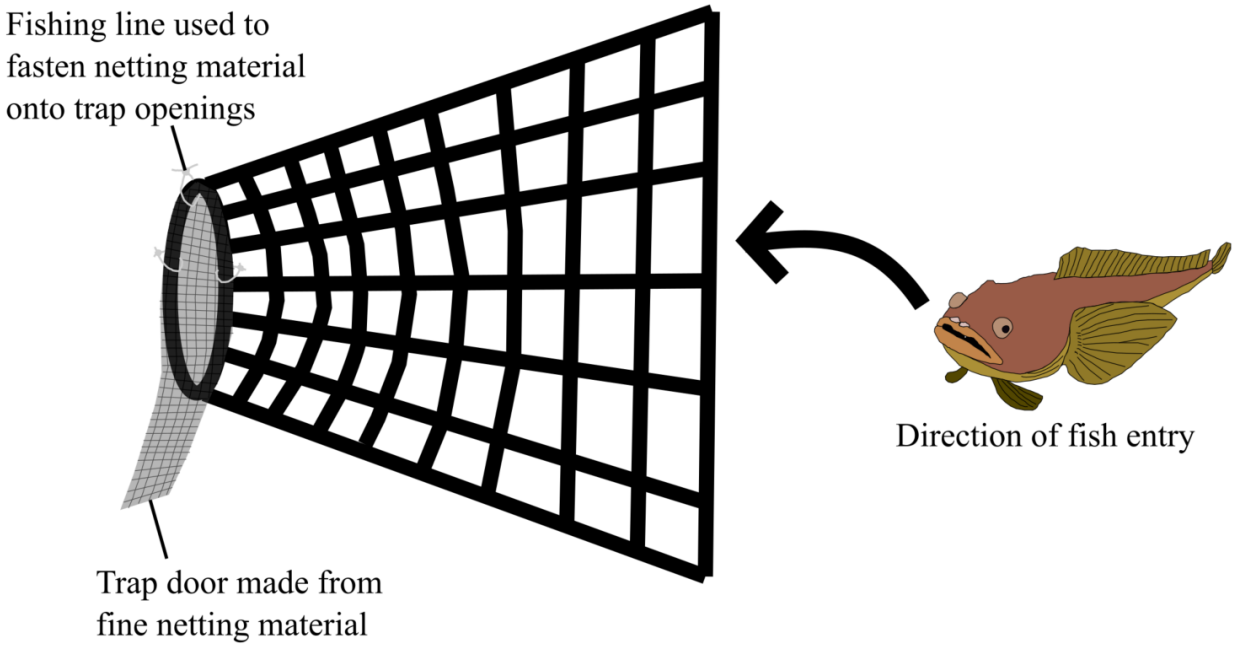

Figure S3. Netting material on the trap openings functioning as one-way trap doors.

- The hydrophone was connected to an oscilloscope (TDS 1002, Tektronix, Beaverton, OR, USA), and each speaker was linked to an amplifier (Bosch Plena PLE-1P120-US, Bosch Security Systems Inc., Fairport, NY, USA). Acoustic stimuli were delivered to the speakers via mp3 players (RUIZU, Shenzen, China). All electronic equipment was powered by a generator (Sportsman 4,000/3,500-Watt, Buffalo Corporation, Missouri, USA) running on gasoline.
- The experimental setup was generally arranged between approximately 9:30 am - 3 pm, aligning with the lowest low tides and ensuring accessibility to the experimental site on foot.

Experimental procedure

- The fundamental frequencies (f_0) of hums exhibit a linear relationship with temperature (Brantley and Bass, 1994). Consequently, the f_0 and harmonics of the acoustic stimuli were linearly adjusted based on temperature (see the section on Generation of Acoustic Stimuli). Custom MATLAB code was utilized to create 5-minute sound files for temperatures ranging from 10 to 25˚C (the anticipated water temperature range at the experimental site) in 0.5˚C increments for each stimulus type. These sound files were stored in the mp3 players used to deliver acoustic stimuli to the underwater speakers.

- The underwater speakers were calibrated to a root mean squared (rms) sound pressure level (SPL) of 127 dB re. 1µPa, 1 m away from the source. This SPL has been proven effective in attracting female plainfin midshipman in previous studies (Zeddies et al., 2010).

- Calibration of the speakers took place in the evenings between approximately 3-8 pm, after the water depth exceeded 2.4 m (following complete submersion of the wooden stick placed near the hum traps).

- Calibration of the speakers was based on the following equation:

$$RL\ (dB\ re.\ 1\mu Pa) = 20 \log10\ (V_{rms}\ in\ V) - S \quad (1)$$

where RL is the received sound pressure level of the speaker at the hydrophone, V_{rms} is the rms voltage of the hydrophone signal measured on the oscilloscope, and S is the hydrophone sensitivity (-164.2 dB re: 1 V/µPa). Solving for equation 1 revealed that a V_{rms} of 13.8 mV corresponds to a received level of 127 dB re. 1µPa at the hydrophone. In practice, the speaker was turned on, and the amplifier output control knob was adjusted until the cycle rms voltage on the oscilloscope approached 13.8 mV. The cycle rms voltage was variable because the acoustic stimuli were not pure sine waves. Given the variable nature of the cycle rms voltage due to the non-pure sine wave characteristics of the acoustic stimuli, five measurements of cycle rms were taken within a minute, and the voltage values were averaged. If the average cycle rms value fell within the range of 13.6-14 mV, the speaker was deemed calibrated.

- For experiment 4, with the hydrophone positioned 2 m away from the speakers, we assumed spherical spreading of sounds, with the pressure amplitude decaying as a function of 1/d, where d is the distance from the sound source. Consequently, the amplifier output control knob was adjusted until the cycle rms voltage on the oscilloscope read 6.9 mV, corresponding to an SPL of 121 dB re. 1µPa at the hydrophone (And based on our assumption, 127 dB re. 1µPa, 1 m away from the speaker).

- Sound files corresponding to a temperature of 13˚C were used for calibration. A 1-5 minute recording of the acoustic stimuli was made on a recorder (Zoom H2 digital recorder, Zoom, Hauppauge, NY) at a sampling frequency of 44.1 kHz and bit depth of 16. The hydrophone-sound recorder combination was calibrated using a pistonphone (Type 42AC, G.R.A.S. Sound & Vibration, Holte, Denmark).

- Plainfin midshipman predominantly vocalize nocturnally (Feng and Bass, 2016). To mimic natural conditions, acoustic playbacks commenced at 9 pm and continued until 6 am.
- A few minutes before 9 pm, the water temperature was measured by using a fish rod to cast a data logger (HOBO Pendant MX Water Temperature Data Logger, Bourne, MA) from the shoreline towards the location of the fish traps. Water temperature was measured to the nearest 0.1˚C, and the sound file corresponding to nearest 0.5˚C in the mp3 player was played as a loop on the speakers. Temperature measurements were taken every 3 hours, and acoustic stimuli were adjusted accordingly.
- Each night of the experiment constituted a single trial for one of the experiments (1-4).
- During course of the experiments, water depth was ~4 m at the fish traps (Measured by SB and LR). Before beginning the playbacks, 5-120-minute recordings of ambient sound were taken to later assess ambient sound conditions (Figure S4)

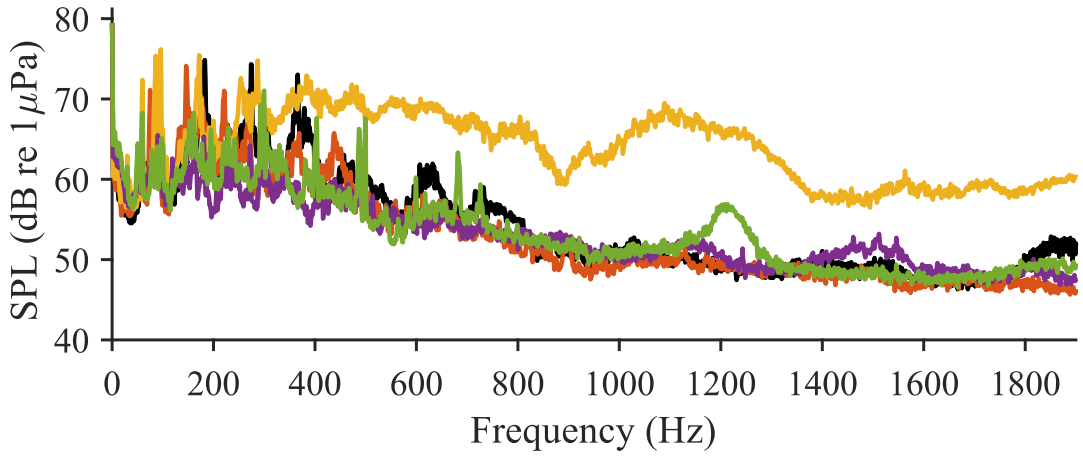

Figure S4. Ambient sound conditions. Power spectra of 5 recordings of ambient sound (Sampling frequency of recording= 44100 Hz, Window size= 44100, Hanning window with 50% segment overlap), taken ~1-5 minutes before 9 pm, when the speakers broadcasting acoustic stimuli for the acoustic playback experiments were turned on. Each recording is 1 minute in duration.

- During the late morning low tides, captured fish were extracted from each trap when the traps became accessible by foot. The fish were sexed, and the number of females, type I males, and type II males in each trap were counted. The mass of each captured fish was measured to the nearest 0.1 g using a kitchen balance, and standard length was measured to the nearest 0.1 cm using a ruler.
- In experiments 1-2, the positions of the speaker broadcasting the acoustic stimulus or being silent were randomized (Either left or right as viewed from the shore). In experiment 3, the positions of the

speaker playing either the hum or hum-like buzz were randomized in the same manner. In experiment 4, the positions of the speaker playing the hum or hum-like buzz were interchanged between the right and left trap (as viewed from the shore), and the trap in between the two traps contained the speaker-like object and served as the silent control trap in the experiment.

Generation of acoustic stimuli

- In a prior study conducted by SB and JAS, hums produced by 22 type I males were recorded in a laboratory setting (Balebail and Sisneros, 2022). From this dataset, 1-minute clips of seven representative hums produced by seven type I males with the best body condition (Fulton's K) were selected, and their Fourier transforms were computed and plotted in MATLAB. Up to 20 harmonics were visually identified from the power spectra (Fig S5).

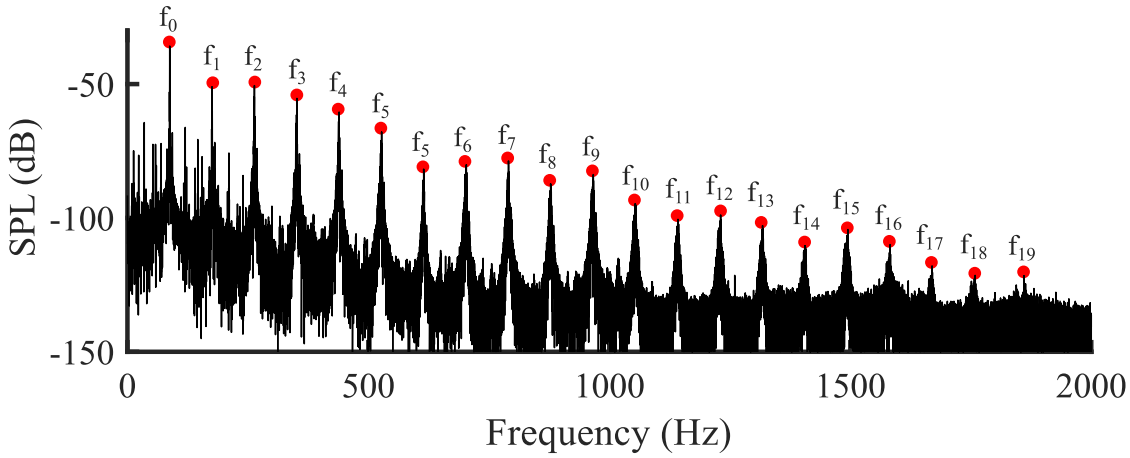

Figure S5. Power spectrum (Sampling frequency of recording= 44100 Hz, Window size= 2647170), of a 1-minute segment of a representative hum produced by one of the type I males with the best body condition in Balebail and Sisneros, (2022). 20 harmonics ($f_0 – f_{19}$) are present in this hum. The amplitude (rms) of each i^{th} harmonic relative to the fundamental (f_0) was computed by computing the amplitude of the i^{th} harmonic as 10^[(SPL of f_i)/20], and then proceeding to divide the computed amplitude of the i^{th} harmonic by the amplitude of f_0= 10^[(SPL of f_0)/20].

- The amplitudes of each harmonic relative to the fundamental were extracted and averaged across the 7 hums (Table S4).

Amplitude relative to f_0

	1	2	3	4	5	6	7	Mean amplitude
f_0	1.0000	1.0000	1.0000	1.0000	1.0000	1.0000	1.0000	1.0000

f_1	0.2600	0.1758	0.2089	0.1396	0.2427	1.1091	1.0116	0.4497
f_2	0.1202	0.1841	0.1189	0.0692	0.2239	0.1479	0.1799	0.1491
f_3	0.0944	0.1059	0.0295	0.0112	0.1429	0.0977	0.1365	0.0883
f_4	0.0484	0.0589	0.0355	0.0229	0.0871	0.0282	0.0631	0.0492
f_5	0.0214	0.0251	0.0158	0.0145	0.0170	0.0106	0.0309	0.0193
f_6	0.0042	0.0051	0.0068	0.0078	0.0172	0.0106	0.0172	0.0098
f_7	0.0086	0.0062	0.0055	0.0072	0.0046	0.0020	0.0016	0.0051
f_8	0.0032	0.0072	0.0021	0.0011	0.0069	0.0041	0.0083	0.0047
f_9	0.0012	0.0027	0.0034	0.0032	0.0044	0.0013	0.0021	0.0026
f_{10}	0.0034	0.0040	0.0019	0.0022	0.0019	0.0007	0.0035	0.0025
f_{11}	0.0002	0.0011	0.0003	0.0015	0.0012	0.0005	0.0008	0.0008
f_{12}	0.0003	0.0006	0.0003	0.0003	0.0003	0.0003	0.0004	0.0004
f_{13}	0.0002	0.0007	0.0003	0.0002	0.0006	0.0004	0.0005	0.0004
f_{14}	0.0000	0.0004	0.0003	0.0002	0.0004	0.0002	0.0003	0.0003
f_{15}	0.0000	0.0002	0.0003	0.0002	0.0003	0.0002	0.0002	0.0002
f_{16}	0.0000	0.0004	0.0002	0.0000	0.0001	0.0000	0.0001	0.0002
f_{17}	0.0000	0.0002	0.0000	0.0000	0.0001	0.0000	0.0002	0.0002
f_{18}	0.0000	0.0001	0.0000	0.0000	0.0001	0.0000	0.0000	0.0001
f_{19}	0.0000	0.0001	0.0000	0.0000	0.0001	0.0000	0.0000	0.0001

Table S4. Ratio of the amplitude (rms) of each harmonic relative to the fundamental frequency (f_0). Columns numbered from 1 to 7 represent the amplitude of each harmonic relative to f_0 for 7 representative hums recorded from 7 different type I males with the best body condition in Balebail & Sisneros (2022). The amplitude of each harmonic relative to f_0, averaged over 7 hums is computed in the extreme right column, and these relative amplitudes were used to construct synthetic hums (See Methods).

- Synthetic hums were then generated using custom MATLAB code implementing the following equation, using the amplitudes of each harmonic averaged across 7 hums:

$$h(t) = \sum_{i=1}^{20} A_i \sin(2\pi \times i \times f_0 \times t) \quad (2)$$

Here, i represents harmonic number, A_i represents the amplitude of the i^{th} harmonic relative to the amplitude of f_0 averaged over 7 hums, and t represents time.

- The diminished f_0 hum stimulus was initially intended to be a hum completely missing energy in the fundamental frequency. Therefore, the equation to create the diminished f_0 hum stimulus was almost identical to equation 2, but the amplitude of f_0 (A_0) was set to 0 in equation 2.

- The hum-like buzz stimulus was initially intended to be a “mistuned harmonic hum stimulus”, containing the same fundamental frequency as a hum, but with all the higher harmonic frequencies shifted randomly. For experiment 3, the equation to generate the hum-like buzz stimulus was as follows:

$$h(t) = A_0 \sin(2\pi \times f_0 \times t) + \sum_{i=2}^{20} A_i \sin(2\pi \times i \times (f_0 \pm \frac{f_0}{3}) \times t) \quad (3)$$

Here, $f_0/3$ was either added to or subtracted to each higher harmonic (f_1 and beyond). For experiment 4, equation 3 was modified in the sense that uniform random numbers between $f_0/10$ and $f_0/3$ were generated and either added or subtracted to each harmonic with equal probability.

- We assumed that f_0 changes linearly with temperature, with the same slope (m= 4.54) as observed in calling type I males in Brantley & Bass (1994) (Equation 3):

$$f_0 \text{ (in Hz)} = 4.54 \times T \text{ (in } ^\circ\text{C)} + 40 \quad (4)$$

Calls from the 7 reference type I males taken from Balebail & Sisneros (2022) were recorded in a tank maintained within a narrow temperature range (13.9 $\pm$ 0.3˚C). The average f_0 at that temperature was 88.2 Hz. f_0 of the hum for any temperature was linearly adjusted using the slope in equation 4, and the mean value of f_0 at 13.9 C (88.2 Hz).

- Acoustic stimuli were generated at temperature intervals of 0.5˚C ranging from 10-25˚C. They were converted to sound files (.wav) using custom MATLAB code. The root mean squared (rms) amplitudes of all sound signals were equalized to 0.786 using custom MATLAB code to ensure that the input signals to the underwater speakers at all temperatures between 10-25˚C had the same rms amplitude. Each sound file was 5 minutes in duration.

- During the experiments, we were unaware that the MATLAB function "audiowrite," used for creating audio files, clipped the peak amplitude of the acoustic signals between -1 to 1. Consequently, this led to the input signals to the speakers differing from our intended ones (Figure S6). Nevertheless, the resulting output stimuli from the underwater speakers (Figure 1 in the main article) still allowed us to draw important inferences about hum perception in female plainfin midshipman. In the folder titled

"MATLAB scripts," the codes for creating synthetic acoustic stimuli (Hum, diminished f0 hum, and hum-like buzz) have been modified to eliminate the clipping effect of audiowrite. This modification ensures that researchers implementing the code have better control over the acoustic features of the stimuli.

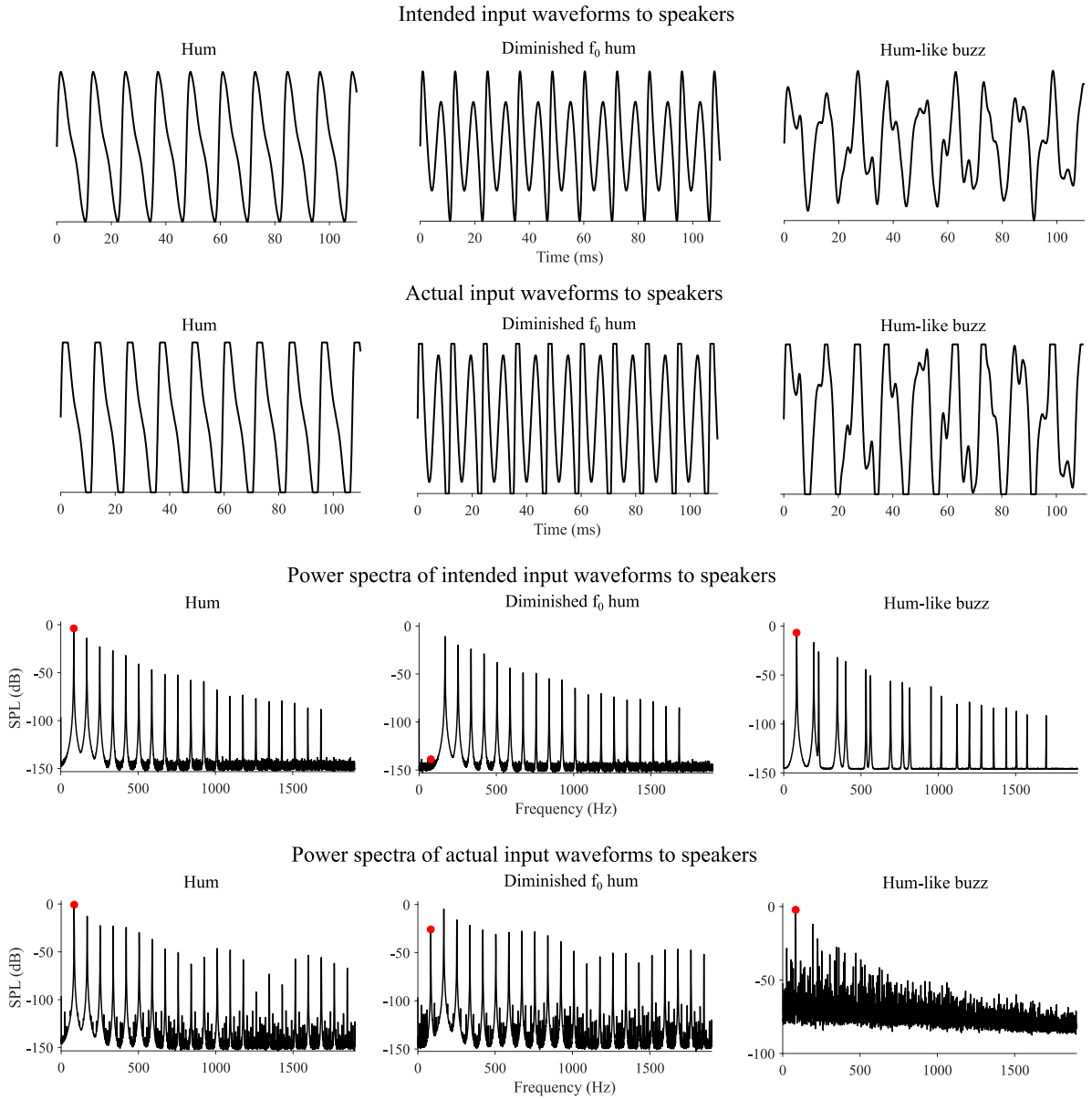

Figure S6. Representative waveforms and power spectra comparing the intended input acoustic signals to the underwater speakers with the actual acoustic signals sent to the speakers. The MATLAB code used for generating the sound files inadvertently clipped the amplitude of the input signals between -1 and 1 for all three acoustic stimuli (Hum, diminished f_0 hum, and hum-like buzz).

- The mean SPL of f_0 for the diminished f_0 stimulus ranged from 84.4 to 99.1 dB re. 1μPa, 1 m away from the source and the SPL of f_0 was lower than that of f_1 by 20-39.2 dB re. 1μPa.

Analysis:

- Wilcoxon signed-rank tests were employed for pairwise comparisons of the number of females in each of the two traps in experiments 1-3. In experiment 4, a Friedman test was utilized to compare the number of females captured overnight in the three traps. Conover post hoc tests, with Bonferroni corrections, were then conducted to examine pairwise differences in the number of animals captured. The identical analysis procedure was applied to compare the numbers of type I and type II males in the traps for experiments 1-4.

- To investigate whether the presence of type I males influenced the number of females captured in each trap, Spearman's rank correlation coefficients (r_s) between the number of females and type I males captured in the trap broadcasting each type of stimulus were computed for each experiment. In experiment 4, where type II males were also captured, Spearman's rank correlation coefficients (r_s) between the number of females and type II males captured in the trap broadcasting each type of stimulus (hum, hum-like buzz, or silent stimuli) were also calculated.

- Experiments 1-3 were conducted in 2021 over a span of 47 days. Spearman's rank correlation coefficients (r_s) were computed between variables measuring body size (mass and standard length) and the time of the season (calculated as the number of days since the first day of conducting experiments) to assess potential changes in the size of animals captured in the traps over the course of the season. For all instances where Spearman's rank correlation coefficients (r_s) were calculated, a t-test was employed to determine if r_s significantly differed from zero ($\alpha = 0.05$) (Zar, 1972).

References for supplementary

Balebail, S., and Sisneros, J. A. (2022). Long duration advertisement calls of nesting male plainfin midshipman fish are honest indicators of size and condition. Journal of Experimental Biology, 225(8), jeb243889. https://doi.org/10.1242/jeb.243889

Brantley, R. K., and Bass, A. H. (1994). Alternative male spawning tactics and acoustic signals in the plainfin midshipman fish Porichthys notatus Girard (Teleostei, Batrachoididae). Ethology, 96(3), 213–232.

Feng, N. Y., and Bass, A. H. (2016). "Singing" Fish Rely on Circadian Rhythm and Melatonin for the Timing of Nocturnal Courtship Vocalization. Current Biology, 26(19), 2681–2689. https://doi.org/10.1016/j.cub.2016.07.079

Zar, J. H. (1972). Significance Testing of the Spearman Rank Correlation Coefficient. Journal of the American Statistical Association, 67(339), 578–580. https://doi.org/10.2307/2284441